DENOGRAD: DEEP GRADIENT DENOISING FRAMEWORK FOR ENHANCING THE PERFORMANCE OF INTERPRETABLE AI MODELS

A PREPRINT

J. Javier Alonso-Ramos ^{1,2}, Ignacio Aguilera-Martos ^{1,2}, Andrés Herrera-Poyatos ³, Francisco Herrera ^{1,2}

¹Department of Computer Science and Artificial Intelligence, University of Granada, Granada, Spain.

²Andalusian Institute of Data Science and Computational Intelligence (DaSCI), University of Granada, Spain.

Emails: {jjalonso, nacheteam, adreshp}@ugr.es, herrera@decsai.urg.es

November 14, 2025

ABSTRACT

The performance of Machine Learning (ML) models, particularly those operating within the Interpretable Artificial Intelligence (Interpretable AI) framework, is significantly affected by the presence of noise in both training and production data. Denoising has therefore become a critical preprocessing step, typically categorized into instance removal and instance correction techniques. However, existing correction approaches often degrade performance or oversimplify the problem by altering the original data distribution. This leads to unrealistic scenarios and biased models, which is particularly problematic in contexts where interpretable AI models are employed, as their interpretability depends on the fidelity of the underlying data patterns. In this paper, we argue that defining noise independently of the solution may be ineffective, as its nature can vary significantly across tasks and datasets. Using a task-specific high quality solution as a reference can provide a more precise and adaptable noise definition. To this end, we propose DenoGrad, a novel Gradient-based instance Denoiser framework that leverages gradients from an accurate Deep Learning (DL) model trained on the target data – regardless of the specific task – to detect and adjust noisy samples. Unlike conventional approaches, DenoGrad dynamically corrects noisy instances, preserving problem's data distribution, and improving AI models robustness. DenoGrad is validated on both tabular and time series datasets under various noise settings against the state-of-the-art. DenoGrad outperforms existing denoising strategies, enhancing the performance of interpretable IA models while standing out as the only high quality approach that preserves the original data distribution.

Keywords Noise · Denoise · Gaussian · Gradient · Deep Learning · Interpretable AI

1 Introduction

The performance of ML models, especially within the Interpretable AI framework, is directly influenced by the level of noise present in training and production data [1]. Ensuring the quality of the data by applying denoising techniques as a preprocesing step is a standard practice. This process has become crucial, and there are many state-of-the-art alternatives to achieve it, generally falling into two main categories: methods that detect and remove noisy instances and those that correct them [2, 3].

In Interpretable AI, the impact of noise extends beyond performance metrics. Since Interpretable AI aims to interpret model decisions, noisy data may result in misleading explanations or obscure the true decision boundaries. Consequently, ensuring data quality becomes even more critical in scenarios where transparency and trust in the model are required [4]. Although numerous denoising strategies have been proposed, their integration within the Interpretable AI framework remains a challenge, particularly because noise can distort not only predictions, but also the interpretability of learned patterns [5].

Recent approaches to instance correction often present two major limitations. First, they may degrade the performance fo the model by introducing overcorrections that suppress relevant but atypical patterns [6]. Second, some techniques inadvertently alter the original data distribution [7], simplifying the learning task to the extent that the model no longer reflects the underlying complexity of the real-world problem. This results in Interpretable AI models which explanations are less representative or useful in practice. These limitations highlight a gap in current methodologies, where noise reduction is achieved at the expense of either fidelity or generalization.

One of the key challenges lies in the definition of noise itself. Most denoising techniques rely on fixed assumptions or heuristics about what constitutes a noisy instance. However, these assumptions are highly problem-dependent. What is considered noise in one dataset may carry valuable information in another. The boundary between noise and signal is often diffuse, making it difficult to design a universal correction strategy [8]. We argue that instead of defining noise a priori, it may be more effective to have a solution based on a Deep Learning (DL) model for the problem and let it guide the identification of noise.

In this paper, we present **DenoGrad**, a **Grad**ient-based **Deno**iser framework using DL tailored to a specific problem. Rather than relying on predefined rules, DenoGrad leverages the behavior of a well-trained model to detect and correct noisy instances. By analyzing the gradients associated with each instance, our approach identifies data points that are misaligned with the model's learned representation. This allows us to perform noise correction in a context-aware manner, preserving the intrinsic complexity of the task and enhancing both model performance and interpretability.

The validation of DenoGrad is conducted on both tabular and time series problems, using a diverse set of real-world and synthetic datasets. For each type of task, we evaluate the method on five real datasets and two synthetic benchmarks, covering a broad range of scenarios. DenoGrad is compared against seven state-of-the-art denoising techniques, and its performance is assessed using multiple Interpretable AI models (five for static tabular data and six for time series). Evaluation metrics include the coefficient of determination (R²) to measure predictive performance, the Kullback–Leibler divergence to assess the preservation of the original data distribution, and the average change in pairwise correlations to quantify alterations in the structural relationships among variables. This multifaceted evaluation allows us to analyze both the effectiveness and the integrity of the denoising process across different learning contexts.

The rest of the text is structured as follows: in Section 2, we review the background of Interpretable AI models, denoising methods, and deep learning, including references to the Interpretable AI models and denoisers used in our analysis. In Section 3, we explain the theoretical foundations of our approach. Section 4 presents the experimental setup, including metrics and datasets. In Section 5, we report and analyze the results. Finally, Section 6 summarizes the key takeaways from our study. Additionally, two appendices are included: the first, Appendix A, presents the code of one of the functions used to generate synthetic data in the development, and the second, Appendix B, contains an extensive collection of plots showing some metrics obtained during experimentation.

2 Background: Interpretable AI, Denoising and Deep Learning

Noise in data analysis refers to errors, inconsistencies, or corruptions within datasets that can adversely affect the performance of Artificial Intelligence (AI) models [9]. This noise may manifest itself, in tabular datasets, as class label noise, where training instances are incorrectly labeled [10], or as attribute noise, involving inaccuracies or irregularities in feature values [11]. Its presence can degrade the accuracy of the model, increase its complexity, and prolong training time [9]. Moreover, noise can manifest in different forms depending on the data modality; for instance, as pixel distortions in images or semantic inconsistencies in text.

The degree to which noise affects the learning process depends on several factors, including class imbalance [12], the magnitude of deviation from the original values [13], and the specific algorithm employed [9]. Moreover, as data volumes increase, traditional noise handling methods face scalability challenges, prompting the need for new techniques better suited to big data environments [14].

Depending on the data source and the nature of its distribution, noise can be classified into different types. *Random* (or stochastic) noise refers to unpredictable variations introduced by uncontrolled factors during data generation or measurement processes [15, 16, 17]. *Systematic noise*, on the other hand, consists of non-random deviations arising from consistent errors, such as sensor biases or human misconceptions [18]. Finally, *Laplacian noise* typically present in non-Gaussian contexts, is notable for its use in differential privacy mechanisms and as impulsive noise in wireless communication systems [19].

Besides the already mentioned noise types based on their distribution, numerous additional noise types can be identified depending on the specific characteristic under consideration, including *impulsive noise*, *outliers*, and *missing values*, among others. However, in this work, we focus specifically on Gaussian noise because it is one of the most extensively studied types of noise in the literature, which is modeled as a random variable following a normal distribution. This

type of noise is common in natural processes and measurement systems due to the central limit theorem [20], which states that the sum of many independent sources of error tends to follow a normal distribution. In practice, Gaussian noise is typically assumed to have zero mean and constant variance. Although these assumptions do not always hold, it is precisely this type of noise that our denoising method is designed to address.

The impact of noise, particularly Gaussian noise, can vary significantly depending on the data structure. In tabular datasets, it generally has a localized effect that affects individual attributes. In such cases, noise can obscure the useful signal, especially if its variance is comparable to that of the original feature values [1, 21]. In contrast, time-series-data noise exhibits a more complex behavior due to the temporal dimension. Since observations are temporally correlated, noise affects not just individual points but may distort temporal dependencies (e.g. trends or seasonality), making them harder to detect. Furthermore, when noise accumulates or propagates over time (as in autoregressive models), it can become amplified, more severely impacting model stability [22].

In summary, noise introduces uncertainty and distortion into the data and its characterization and mitigation are essential for building robust models. Understanding the type of noise present enables the design of more effective strategies for data cleaning, modeling, and evaluation in scientific data analysis.

Building upon this understanding, it is important to recognize that noise is an inherent characteristic of data in real-world problems. It can emanate from a variety of sources, including sensor imprecision, adverse conditions, external interventions in the measured system, or human errors. Although a certain amount of noise can be beneficial for AI models [23], excessive noise has the potential to entirely hinder their ability to fit data [24]. At low noise levels, models can generalize more effectively, reducing the risk of overfitting and enhancing performance on unseen data. Conversely, when noise levels are high, the inherent properties of the data and the original relationships between variables may be distorted or lost, preventing the model from accurately representing the system's true behavior.

Moreover, the extent to which noise impacts model performance is closely tied to the model architecture. Noise levels that are detrimental to one type of model may fall within an optimal range for another. Although this sensitivity varies between models, a general trend can be observed: deep learning architectures tend to be more resilient to noise than traditional ML models [25], especially those within the domain of Interpretable AI [26].

2.1 Interpretable Artificial Intelligence Models

Interpretable AI aims to bridge the gap between predictive performance and human interpretability, allowing stakeholders to understand, trust, and effectively interact with ML systems. In domains such as healthcare, finance, and environmental modeling, where transparency and accountability are essential, leveraging inherently interpretable models provides an effective balance between accuracy and explainability [27, 28]. This subsection presents several classical and widely used Interpretable AI models, highlighting their mechanisms and interpretability advantages.

- Ridge Regression: Ridge regression, introduced by Hoerl and Kennard [29], enhances linear regression by incorporating L2 regularization, which penalizes large coefficient magnitudes. By adding a term proportional to the squared L2 norm of the coefficients to the loss function, ridge regression addresses issues of multicollinearity and overfitting. This regularization encourages simpler models with coefficients that are shrunk but not entirely eliminated, thereby preserving a degree of interpretability while improving generalization.
- Partial Least Squares (PLS): PLS regression, formalized by Wold et al. [30], is a supervised dimensionality reduction technique that simultaneously projects predictor and response variables into a new latent space. Unlike Principal Component Analysis (PCA), which is unsupervised, PLS maximizes the covariance between transformed inputs and outputs. This allows the model to retain interpretability while effectively handling multicollinearity and high-dimensional data common in chemometrics and genomics.
- **Decision Tree:** Decision trees are hierarchical rule-based models that recursively partition the input space based on feature thresholds to minimize impurity measures such as the Gini index or entropy [31]. Each path from root to leaf represents a decision rule, making the model inherently interpretable. Decision trees are particularly favored in domains that require transparent decision logic, although they are prone to overfitting unless pruned or regularized.
- Support Vector Regression Machines (SVR): Support Vector Regression (SVR) extends the principles of Support Vector Machines (SVM) to regression tasks, as introduced by Vapnik [32]. Rather than separating classes with a maximal margin hyperplane, SVR seeks to find a function that deviates from the actual target values by no more than a specified margin *ϵ*, while maintaining model flatness. The use of kernel functions, such as the polynomial or radial basis function (RBF) kernels, enables SVR to capture nonlinear relationships by implicitly mapping the input data into higher-dimensional feature spaces. Although SVR models are less

interpretable than linear regression, insights can still be obtained by analyzing the support vectors and the sensitivity of the model to input features.

- **k-Nearest Neighbors** (**kNN**): The kNN algorithm [33] is a non-parametric, instance-based method that makes predictions based on the majority label (classification) or average response (regression) among the *k* closest training samples, according to a distance metric like Euclidean distance. Its simplicity and reliance on local neighborhoods make it intuitively interpretable, though it can become less effective in high-dimensional settings due to the curse of dimensionality.
- ARIMA (AutoRegressive Integrated Moving Average): ARIMA, popularized by Box and Jenkins [34], is a statistical model designed for univariate time series forecasting. It integrates autoregressive (AR) terms, differencing (I) to ensure stationarity, and moving average (MA) components to account for autocorrelation in residuals. The model's parameters and structure provide clear interpretability, with coefficients directly relating to temporal dependencies and seasonality.

The effectiveness of explainable models is highly dependent on the quality of the input data. In the presence of noisy, corrupted, or high-variance observations, these models – despite their transparency – can yield unstable or misleading explanations [35, 36]. This poses a critical challenge when deploying Interpretable AI in real-world settings where data is often noisy due to measurement errors, sensor drift, or environmental variability. As a result, improving data quality through denoising becomes a crucial step to ensure both predictive accuracy and the reliability of model interpretability.

2.2 Denoising

The term "denoising" refers to the process of identifying and removing unwanted noise or random fluctuations from data to enhance its quality and reliability for subsequent analysis. The objective of denoising is to recover the latent clean-data representation by suppressing or filtering out extraneous components while preserving relevant structural or statistical information [37]. This procedure is fundamental in various domains, including signal processing, image analysis, and time series forecasting, where it enables more accurate inference, improved pattern recognition, and robust predictive modeling [38, 39, 40, 41].

To address the challenges posed by noise in data, several strategies have been proposed, which can be broadly classified into three main categories. The first includes *data cleaning techniques*, which aim to detect and eliminate instances containing noisy features or incorrect labels [42]. The second approach encompasses *data modification methods*, which seek to transform noisy data into a less corrupted version, improving data quality while preserving its informative content [43]. The third consists of *noise-robust algorithms*, which are designed to perform well even in the presence of noise, maintaining stable performance across varying data conditions [12, 44]. The method proposed in this study aligns with the second category as it focuses on modifying the input data to produce a cleaner and more informative representation.

However, these strategies present certain risks. Notably, aggressively removing noise may cause AI models to overfit the training set, thereby impairing their generalization ability on unseen data. Conversely, applying inappropriate denoising techniques may distort the data or eliminate important intrinsic relationships – such as variable correlations or distributional patterns – ultimately degrading the representativeness and utility of the dataset.

Furthermore, many denoising methods in the literature have been developed with classification tasks in mind and therefore focus on detecting noisy labels and removing their corresponding instances rather than correcting them [45]. While this approach may be suitable when there are no temporal dependencies among features or when large datasets are available, it becomes inadequate in contexts where data is limited or temporally correlated. In such cases, discarding instances is not viable, and correction-based denoising strategies become essential.

A selection of seven different methods, representing the latest state-of-the-art approaches, have been chosen for comparison with DenoGrad. These methods are as follows:

• Denoising Autoencoder (DAE) [46]: This approach uses artificial neural networks (ANNs) to learn how to map noisy inputs to clean outputs via an encoder–decoder architecture. During training, if the original, unnoisy data is available, artificial noise is added to the input data and the model learns to reconstruct the original signal. This enables it to develop robust feature representations. If only noisy data is available, the DAE learns to reconstruct the noisy data, but training stops before the model fully converges, leaving the remaining fit as the noisy part of the data.

Advantages: Adaptable to various data types; capable of learning complex nonlinear features.

Disadvantages: Requires a large amount of data to generalize well; performance may degrade if the noise in real data differs significantly from that seen during training.

Recommended scenarios: Effective for images, biomedical signals, and time-series data with complex noise. *Limitations:* Not ideal for small datasets or when the noise type is entirely unknown or highly variable.

• Empirical Mode Decomposition (EMD) [47]: A nonlinear, non-stationary technique that decomposes a signal into intrinsic mode functions (IMFs), each representing different oscillation scales. Noise can be attenuated by discarding high-frequency IMFs associated with artifacts.

Advantages: Makes no prior assumptions about the signal; suitable for non-stationary data.

Disadvantages: Susceptible to edge artifacts; sensitive to noise type; number of IMFs can be difficult to control.

Recommended scenarios: Biomedical, geophysical, and financial signal analysis.

Limitations: Performs poorly on highly periodic signals or rigidly structured data.

• Kalman Filter (KF) [48]: A recursive algorithm that estimates the latent state of a dynamic system from noisy observations, minimizing the variance of the estimation error. Particularly suited to linear systems with white Gaussian noise.

Advantages: Highly efficient computationally; provides optimal estimation under ideal conditions; updates in real time.

Disadvantages: Assumes linearity and Gaussian noise; performance degrades under non-ideal assumptions.

Recommended scenarios: Object tracking, navigation, real-time time-series processing.

Limitations: Not suitable for highly nonlinear systems without adaptations.

• Moving Average (MA) [49]: A simple statistical technique that smooths a signal by replacing each point with the average of its neighbors. This attenuates short-term fluctuations, revealing long-term trends.

Advantages: Easy to implement; low computational cost.

Disadvantages: Can distort sharp peaks and introduce lag; cannot differentiate between noise and legitimate high-frequency signals.

Recommended scenarios: Financial data, process control, real-time sensor signals.

Limitations: Ineffective for signals with fast transitions or significant high-frequency structure.

• **Principal Component Analysis (PCA) [50]:** A dimensionality reduction method that projects data onto new axes aligned with directions of maximum variance. By retaining only the principal components, noise associated with minor variations can be suppressed.

Advantages: Useful for redundancy removal and dimensionality reduction; can improve downstream model performance.

Disadvantages: Assumes linearity; relevant information may be lost if components are poorly selected.

Recommended scenarios: Multivariate data preprocessing, compression, exploratory analysis.

Limitations: Ineffective with nonlinear relationships or structured noise.

• Denoising Residual Network (DN-ResNet) [51]: An ANN variant with residual (skip) connections that enables the model to learn the noise signal and subtract it from the input. This architecture supports the preservation of structural information. As is the case with DAEs, when clean (noise-free) data is unavailable, the model must be trained using noisy data to reconstruct that same noisy input. The training process is intentionally stopped before full convergence to prevent the model from completely fitting the noise. The residual difference between the input and the partially fitted output is then assumed to approximate the noise component.

Advantages: Effective in modeling complex noise; mitigates vanishing gradients; preserves fine details.

Disadvantages: High computational cost and data requirements; prone to overfitting without proper regularization.

Recommended scenarios: Image, audio, and physiological signal denoising where detail preservation is crucial. *Limitations:* Low interpretability; expensive to train when clean references are unavailable.

• Wavelet Transform Decomposition (WTD) [52]: Analyzes signals at multiple scales and resolutions using wavelet functions, decomposing the signal into frequency-specific components. Noise is suppressed by thresholding high-frequency coefficients. The thresholding strategy follows Donoho's universal threshold [53], which estimates the noise level based on the median absolute deviation of detail coefficients. This adaptive approach enables effective denoising even without prior knowledge of the noise magnitude.

Advantages: Good localization in both time and frequency domains; suitable for non-stationary signals.

Disadvantages: Requires careful selection of wavelet basis and decomposition levels; poor configuration may introduce artifacts.

Recommended scenarios: Biomedical signal processing, image analysis and audio compression.

Limitations: Sensitive to parameter selection; less effective if noise is not concentrated in high-frequency bands.

As demonstrated, there is a considerable degree of intricacy in these methodologies, which enables their categorization. Low-complexity methods, including MA, KF, and EMD, employ straightforward mathematical approaches that require minimal computation. These methods are used primarily to eliminate basic and predictable noise in the data. Medium-complexity methods, such as PCA and WTD, involve more sophisticated techniques that aim to decompose the data into its fundamental components or scales. These methods are particularly effective in environments characterized by moderate or structured noise, as they enable more precise and controlled removal of noise. High-complexity methods, exemplified by DAE and DN-ResNet, depend on deep learning models that are capable of learning advanced representations of the data. These methods have been shown to be highly effective in the removal of noise in complex signals through nonlinear and adaptive techniques. DenoGrad falls within this latter category, as it is founded on the premise of deep learning gradients.

Despite the diversity and maturity of existing denoising algorithms, several critical limitations remain unaddressed. Traditional low – and medium – complexity methods often struggle with nonstationary or highly structured noise, and their performance typically degrades in the absence of strong assumptions about signal properties or noise characteristics. High-complexity, learning-based methods, particularly those that rely on clean reference data such as DAEs and DN-ResNets, offer powerful solutions but require extensive clean datasets, which are often unavailable in real-world scenarios. Moreover, these models usually need to be trained specifically for the denoising task, demanding significant computational resources and making them less practical for dynamic or resource-constrained environments. Importantly, current approaches rarely leverage the representational power of already trained models, leaving a gap in methods that can exploit the internal knowledge of networks that have learned from noisy data. This opens up an opportunity to develop more generalizable, lightweight, and adaptive denoising strategies that do not rely on clean targets or model retraining and can instead work by harnessing the existing structure and gradients of trained neural networks as we have done with our proposal, DenoGrad.

Given that DenoGrad is grounded in DL principles, developing a comprehensive understanding of the relationship between DL and noise is crucial to fully appreciate its potential and limitations.

2.3 Deep Learning and its Interaction with Noise

DL is a subfield of ML that employs Artificial Neural Networks (ANNs) [54, 55] to address complex prediction and classification tasks. These networks, inspired by the architecture of the human nervous system, are composed of basic computational units called artificial neurons, organized into interconnected layers.

Each neuron computes a linear combination of its inputs, applies a nonlinear activation function, and transmits the result to the neurons in subsequent layers. This layered architecture allows ANNs to transform data representations progressively, capturing increasingly abstract patterns as information flows through the network.

The process of learning in an ANN entails the adjustment of its internal parameters, namely the weights that govern the strength of the connections between neurons. The objective of this adjustment is to minimize the discrepancy between the model's predictions and the actual values. This discrepancy is quantified by a loss function, which serves as the objective to be optimized during training.

Mathematically, the cost function L minimized by the network is expressed as an expectation over the data distribution as shown in Equation (1):

$$E[L(\theta)] = E[\ell(f_{\theta}(x), y)] \tag{1}$$

where ℓ is the loss function (e.g., mean squared error), $f_{\theta}(x)$ is the network's output for parameters θ , and y is the target variable. In practice, given that the true distribution is unknown, we instead work with an empirical approximation over a finite dataset $\{(x_i, y_i)\}_{i=1}^N$, as defined in Equation (2). This is the empirical loss function, which is simply the average loss over all samples in the dataset:

$$L(\theta) = \frac{1}{N} \sum_{i=1}^{N} \ell(f_{\theta}(x_i), y_i)$$
 (2)

The optimisation of the loss function is achieved through gradient-based algorithms, with stochastic gradient descent (SGD) [56] being the most widely used. The central component of this process is the computation of gradients: vectors of partial derivatives of the loss function with respect to each network parameter.

From a geometric perspective, the gradient points in the direction of the steepest increase of the loss function. Consequently, to mitigate the loss, the model's parameters undergo an update in the opposite direction (scaling the gradients by a factor called *learning rate*), a process referred to as gradient descent. The gradients are efficiently computed using the backpropagation algorithm, which applies the chain rule of differential calculus to propagate the error from the output layer back through the network [57]. This mechanism enables the model to assess how each weight contributes to the overall error, thereby facilitating informed parameter updates.

The efficiency of backpropagation has been instrumental in enabling the training of deep architectures. However, the magnitude of the gradients also plays a critical role. Extremely large gradients may lead to gradient explosion [58], resulting in unstable updates, while very small gradients can cause the vanishing gradient problem [59], where parameters cease to update effectively – particularly in deep networks. To mitigate these issues, a variety of techniques have been proposed, including weight normalisation, alternative activation functions (such as ReLU [60]), and architectural innovations like residual connections [61], which preserve gradient flow across layers.

It has been demonstrated that, given the manner in which this optimization of the loss function process is carried out, in the event that the data under consideration contains zero-mean Gaussian noise during the training phase, such noise will not result in the introduction of a systematic bias into the loss function. In contrast, the incorporation of random variability may impact convergence stability without compromising the fundamental direction of learning [62]. This finding underscores the robustness of gradient-based learning in the presence of stochastic perturbations.

In simpler terms, when the noise in the data follows a Gaussian distribution, it ensures that if one noisy data point pushes the gradient in one direction, there will likely be another noisy point pulling it in the opposite direction. As a result, these effects tend to cancel each other out, keeping the gradient aligned with the true underlying pattern in the data.

In consideration of the foregoing discourse, the employment of noise reduction methods based on ANNs is a particularly advantageous strategy in data processing tasks, owing to their flexibility and their capacity to incorporate adaptive learning into the preprocessing stage. In contrast to conventional methodologies, which predominantly depend on statistical transformations or predetermined rules, ANN-based approaches have the capacity to learn to identify and differentiate meaningful patterns from noise directly from the data. This capacity is instrumental in facilitating data-driven preprocessing systems.

This learning-guided approach offers several key advantages. Firstly, it is evident that neural networks are capable of capturing nonlinear and contextual structures that classical methods often fail to adequately model, particularly in domains such as image data, time series, or tabular data with complex correlations. Secondly, the utilisation of supervised training enables the model to selectively preserve the meaningful features of the signal while minimising distortions caused by noise. This is an essential capability in tasks where fine-grained details are critical to the performance of downstream systems.

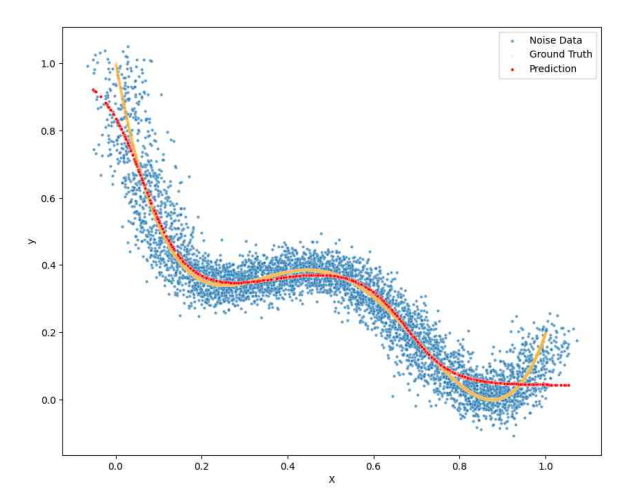
3 DenoGrad: a Gradient-based Denoiser Framework Using Deep Learning

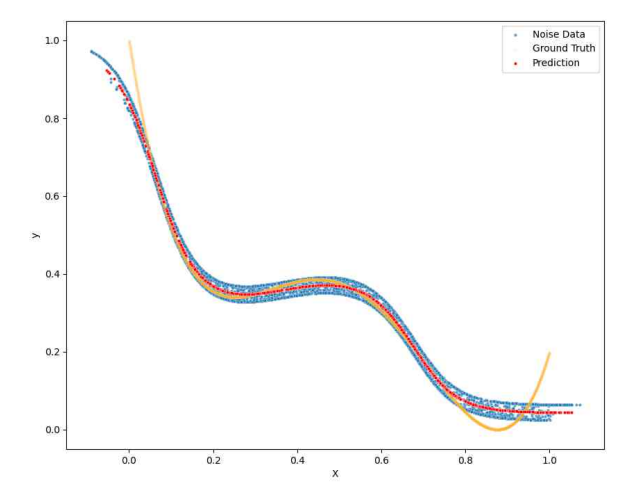
We named our proposal "DenoGrad" as it is a denoiser based on the gradients of an DL model. DenoGrad is classified as a framework because it is not limited to a specific model, but rather defines a method capable of incorporating any DL architecture as its backbone for denoising. To achieve effective noise reduction, it is important that the selected DL model provides a sufficiently good fit to the noisy data. However, a perfect fit is neither expected nor required, as this is generally unattainable in the presence of noise.

This concept is illustrated through a simple 2D example shown in Figure 1, where an DL model trained on noisy data achieves a coefficient of determination (R^2) of 0.8988. This indicates that the model captures most of the underlying signal, which is sufficient to enable effective denoising.

A key advantage of this framework lies in its model-agnostic nature, which makes it inherently compatible with ongoing advancements in deep learning: as more powerful DL architectures emerge, the performance of our denoising approach is expected to improve accordingly without requiring changes to the core methodology.

In contrast to other complex deep learning-based methods (which require training a new model from scratch on noisy data), our approach is capable of leveraging an DL model that has already been deployed in production, thereby significantly reducing computational overhead and integration effort due to the model-agnostic nature. It is important to note that the DL model could be designed to perform the same task as the Interpretable AI models, or alternatively, a





- (a) The plot presents a 2D example in which a sufficiently well-fitted DL model (in red) is shown alongside the noisy data points (in blue) and the ground truth function (in orange).
- (b) The plot presents the results of applying DenoGrad to the noisy data (in blue), using the previously fitted DL model (in red), alongside the ground truth function (in orange).

Figure 1: 2D noisy data before and after applying DenoGrad.

different one. However, it is crucial that the input features of the DL model encompass all the input features of the Interpretable AI models, as these are the ones to be denoised.

Even in scenarios where no such model has been previously deployed and one must be trained from scratch, the proposed framework can leverage an DL model tailored to the original predictive task. Consequently, the resulting model not only serves the denoising purpose but also remains fully operational for subsequent prediction tasks. This dual functionality enables the model to act as a baseline or reference point to evaluate the performance of subsequent Interpretable AI models. In contrast, many alternative denoising approaches require the training of an DL model dedicated solely to noise removal. These models typically become obsolete once the denoising step is completed, offering no added utility beyond that point.

Another key feature of DenoGrad is its efficiency, as it simultaneously denoises all input features. This is similar to other deep learning-based denoising methods, but contrary to classical methods that reduce noise feature by feature.

The framework developed for this experimentation is publicly available on GitHub ¹, allowing unrestricted study, use, and extension by the research and professional community. This ensures reproducibility of the results, facilitates comparison with future proposals, and promotes the open development of noise reduction and explainability techniques for both tabular and time series data.

3.1 DenoGrad: How it Works

DenoGrad is a simple, gradient-based denoising framework. Its appeal lies in its originality and ease of implementation, supported by robust mathematical underpinnings. Despite its simplicity, DenoGrad is effective across a variety of datasets and noise conditions.

The core idea of DenoGrad is to take advantage of a trained DL model to guide the denoising process. Importantly, this network is not specifically trained for denoising, but for any predictive task on the same dataset. The denoising effect is applied exclusively to the DL model's input variables, that is, the features and the targets.

The first step involves training an DL model on the dataset that requires denoising. While the network does not need to perform the exact same task planned for downstream stages (such as Interpretable AI or benchmarking), it is essential that the model is sufficiently well-fitted to the data. The objective is not the task itself, but rather to learn a reliable mapping between inputs and outputs that captures the data's underlying structure.

Once training is complete, the entire dataset designated for denoising is passed through the network to obtain predictions. These predictions are compared to the targets to compute the error (loss) for each data instance. This step is conceptually identical to a standard forward pass during training.

¹https://github.com/ari-dasci/S-noise-gradient

Unlike in regular training, where gradients are computed with respect to the DL model parameters, DenoGrad computes the gradients of the loss with respect to the inputs themselves. This is achieved by backpropagation, using the same loss function that was employed during training. Formally, the gradients are expressed as shown in Equation (3) where x and y represent the input features and the targets, respectively; f(x) is the output of the DL model; and $\mathcal L$ is the loss function.

$$\nabla_{x,y} \mathcal{L}(f(x), y) \tag{3}$$

The final step consists of updating the input data by subtracting the computed gradients, scaled by a predefined noise reduction rate μ , from the original input tensors. This process shifts the inputs toward regions in the input space that the network has learned as less noisy or more consistent with the learned data distribution. The update expression is given by Equation (4).

$$(x', y') = (x, y) - \nabla_{x, y} \mathcal{L}(f(x) - y) \cdot \mu, \tag{4}$$

This transformation effectively reduces the noise in the inputs without requiring any changes to the DL model itself. The denoised data can then be used for subsequent analysis, including interpretability studies or evaluation tasks.

To control the execution time and the extent of the denoising and avoid excessive corrections that might degrade the data or cause overfitting, two stopping criteria are established: a maximum number of denoising epochs and an error threshold.

The first criterion, the maximum number of epochs, ensures that the denoising process is computationally bounded by limiting the total number of update iterations. This helps make the denoising process practical for large datasets or real-time applications.

The second criterion, the error threshold, imposes a limit on how much deviation is acceptable for each instance. Once this threshold is met or surpassed, no further updates are applied to that instance. This strategy enables the preservation of a certain level of noise in the dataset, which may be desirable to improve model generalization and reduce overfitting, as discussed in Section 2 and in [23]. The effect of this threshold is illustrated in Figure 1(b), where the blue points (denoised data) do not perfectly aligning with the red points (original clean data), maintaining a buffer on both sides that corresponds to the threshold value.

The iterative denoising process of inference, error computation, gradient extraction, and update is repeated until either the maximum number of epochs is reached or none of the remaining instances exceed the error threshold. To facilitate a clearer understanding of the process, the pseudocode provided in Algorithm 1 offers a step-by-step representation of the DenoGrad framework.

3.2 DenoGrad: Time-Series Scenario

It is necessary to make a distinction according to the type of problem we face, as the behavior of our framework DenoGrad slightly differs depending on whether the task involves tabular inference or time series forecasting. In the case of tabular data, the input features (X) and the target variable (y) are independent entities, such that $y \notin X$. The model learns to map X to y through the learned function, and the gradient-based denoising process focuses on correcting inconsistencies within X that lead to deviations in the output space.

However, in the context of time series forecasting, the situation changes fundamentally. Here, the target variable at a future time step is inherently part of the historical data used as input. Therefore, the target variable is embedded in the input structure, i.e., $y \in X$. This configuration introduces an additional layer of complexity, as the model's gradients with respect to the input now include contributions from both the attributes and the target variable itself. As a result, two distinct gradient sources emerge for y: one derived from its role as an input feature and another from its role as the prediction target. To prevent redundancy and ensure consistent noise correction, DenoGrad overrides the gradient computation for the target variable and restricts noise reduction exclusively to the gradients with respect to X. This guarantees that denoising focuses on improving the signal quality of the input window without inadvertently modifying the predictive target.

It is also important to emphasize the limitations that arise when applying our noise reduction strategy to recurrent neural network (RNN) architectures, which are among the most widely used models for time-series analysis. Notable examples include Long Short-Term Memory (LSTM) networks [63]—and their more recent variant, the Extended-LSTM (xLSTM) [64]—as well as Gated Recurrent Units (GRU) [57]. Although these architectures were designed to mitigate the vanishing gradient problem that affects classical RNNs [65], they remain more prone to this issue

Algorithm 1 DenoGrad for Static Tabular Data

```
1: Input: Noisy data (X_{noisy}, y_{noisy}), trained DL model, loss function, noise threshold, noise reduction rate \eta, max
 2: Output: Denoised data (X, y)
 3: Train DL_model on (X_{noisy}, y_{noisy})
 4: Freeze parameters of DL_model
 5: X, y \leftarrow copy \ of(X_{noisy}, y_{noisy})
 6: epoch \leftarrow 0
 \textit{7: still\_noisy} \leftarrow True
 8: while epoch < max\_epochs and still\_noisy do
 9:
         Enable gradients for X and y
10:
         y_{pred} \leftarrow \mathtt{DL\_model}(X)
         loss \leftarrow \texttt{loss\_function}(y_{pred}, y)
11:
12:
         Backpropagate loss to compute gradients w.r.t. X and y
13:
         error \leftarrow |y_{pred} - y|
         is\_noisy \leftarrow (error > noise\_threshold)
14:
15:
         still\_noisy \leftarrow any(is\_noisy)
16:
         grad_X \leftarrow \nabla_X
         grad_y \leftarrow \nabla_y
17:
         total\_grad \leftarrow \texttt{concatenate}(grad_X, grad_y)
18:
19:
         norm \leftarrow \texttt{L2\_norm}(total\_grad)
20:
         grad_X \leftarrow grad_X/norm
         grad_y \leftarrow grad_y / norm
21:
22:
          X \leftarrow X - \eta \cdot grad_X \cdot is\_noisy
23:
         y \leftarrow y - \eta \cdot grad_y \cdot is\_noisy
24:
         epoch \leftarrow epoch + 1
25: end while
26: return (X, y)
```

than feedforward neural networks (FNNs) [66]. Consequently, when DenoGrad is applied to RNN-based models, the convergence of the noise reduction process tends to be slower due to the diminished gradient flow across time steps. Nonetheless, while the convergence speed is affected, the overall denoising efficacy remains comparable to that achieved with feedforward models, provided that sufficient iterations are allowed.

Finally, as in the tabular data scenario, a pseudocode representation for the time series adaptation of DenoGrad is included in Algorithm 2 to provide a clearer understanding of the specific modifications required to handle temporal dependencies and gradient management in sequential data.

4 Experimental Set-up

We conducted a series of experiments to evaluate the effectiveness of our denoising framework, DenoGrad. Our study focuses on tabular and time-series problems, using five real-world datasets and two synthetic ones for each category. To demonstrate the strong performance of DenoGrad, we compared it against seven state-of-the-art denoising methods, which were introduced in Section 2.2.

4.1 Train-Test Scenarios in Different Denoising Stages

A performance evaluation of five Interpretable AI models is conducted both before and after the application of the denoising process. In scenarios involving time series, the ARIMA model is also included in the analysis. When working with synthetic datasets, it is additionally necessary to evaluate the model performance on the original, noise-free version of the dataset. To ensure a comprehensive assessment, we executed the full combination of training and testing configurations, considering all possible stages of the denoising process (i.e., noisy, denoised, and original in the case of synthetic data). The following describes the insights provided by each combination of training and testing conditions, as well as their practical utility:

Algorithm 2 DenoGrad for Time Series Data

```
1: Input: Noisy data (X_{noisy}, y_{noisy}) with windowing mechanism, trained DL model, loss function, noise threshold,
     noise reduction rate \eta, max epochs
 2: Output: Denoised data (X_{denoised}, y_{denoised})
 3: if model is recurrent (e.g., RNN) then
         Set model to training mode
 5: else
 6:
         Freeze model weights
 7: end if
 8: epoch \leftarrow 0
 9: still\ noisy \leftarrow True
10: while epoch < max\_epochs and still\_noisy do
         still\_noisy \leftarrow False
11:
12:
         for all (X_{batch}, y_{batch}) in DataLoader(X_{noisy}, y_{noisy}) do
13:
             Enable gradients for X_{batch}
14:
             y_{pred} \leftarrow \mathtt{model}(X_{batch})
             loss \leftarrow loss\_function(y_{pred}, y_{batch})
15:
             Backpropagate loss to compute gradients w.r.t. X_{batch}
16:
17:
             error \leftarrow |y_{pred} - y_{batch}|
             is\_noisy \leftarrow (error > noise\_threshold)
18:
             still\_noisy \leftarrow still\_noisy or any(is\_noisy)
19:
20:
             grad_X \leftarrow \nabla_{X_{batch}}
             norm \leftarrow \texttt{L2\_norm}(grad_X)
21:
22:
             if norm == 0 then
23:
                 norm = norm + \epsilon \# Avoid division by zero
24:
25:
             grad_X \leftarrow grad_X/norm
             for all sample i in batch do
26:
                 if is\_noisy[i] then
27:
                      X_{noisy}[i] \leftarrow X_{noisy}[i] - \eta \cdot grad_X[i]
28:
                 end if
29:
             end for
30:
31:
         end for
         epoch \leftarrow epoch + 1
32:
33: end while
34: X_{denoised} \leftarrow X_{noisy}
35: y_{denoised} \leftarrow X_{denoised}[y]. shift(future)
36: Remove y column from X_{denoised}
37: return (X_{denoised}, y_{denoised})
```

- **Train:** *Original* **Test:** *Original*: Evaluates the ideal performance of the model when both training and testing are conducted on clean data. Serves as the baseline for comparing other scenarios, reflecting both accuracy and explainability under optimal conditions. It is the supposed base case in synthetic scenarios.
- Train: *Original* Test: *Noisy*: Assesses the robustness of the model when exposed to degraded or corrupted data at deployment. Useful for understanding how performance deteriorates and whether the model's explanations remain coherent when facing out-of-distribution inputs.
- Train: *Original* Test: *Denoised*: Examines the model's ability to generalize to data that has been processed with a denoising technique. This scenario helps determine whether preprocessing improves or impairs both prediction accuracy and interpretability, and whether the model is sensitive to small changes in input representation.
- **Train:** *Noisy* **Test:** *Original*: Evaluates how a model trained on noisy data performs when tested on clean data. It may reveal whether the model has learned to ignore noise or has developed spurious patterns that do not transfer well. This setup also provides insights into how noise during training affects interpretability.
- Train: Noisy Test: Noisy: Analyzes the model's performance in consistently noisy environments, both during training and deployment. This simulates scenarios where data is inherently corrupted (e.g., faulty

sensors). It is essential for determining whether the model and its explanations remain functional under adverse conditions. It is the supposed base case in real-world scenarios.

- **Train:** *Noisy* **Test:** *Denoised*: Investigates the interaction between learning from noisy data and inferring from denoised inputs. Useful for evaluating whether post hoc denoising can compensate for suboptimal training, or whether the model fails to leverage the benefits of preprocessing.
- Train: *Denoised* Test: *Original*: Assesses how a model trained on artificially cleaned data (denoised) performs on real, unprocessed data. It helps identify whether the denoising process introduces biases or removes important information, thus affecting generalization.
- Train: *Denoised* Test: *Noisy*: Measures the generalization ability of a model trained on artificially cleaned data when confronted with noisy inputs. This setup reflects the model's vulnerability to unseen noise and is critical for risk assessment in real-world deployment scenarios. Additionally, it serves as a proxy to assess the effectiveness of the denoising process: if the model maintains its performance despite the mismatch, it suggests that the denoised data preserves essential structures of the original distribution.
- **Train:** *Denoised* **Test:** *Denoised*: Evaluates the performance of models entirely built on denoised data. This scenario quantifies the direct impact of denoising on the entire pipeline and helps determine whether systematic preprocessing is worthwhile, as well as its implications for model explainability.

These scenarios enable the analysis of several key aspects. First, they allow for the assessment of the resilience of model explanations in the presence of noise, providing insight into how interpretability holds under adverse conditions. Second, they offer a way to examine the transferability of knowledge across different data domains, such as moving from clean to noisy or denoised inputs. Third, they highlight the impact of preprocessing techniques, such as denoising, on the performance and explainability of the model. Finally, they help identify cases where certain combinations of training and testing conditions may compromise interpretability, even if the predictive accuracy remains acceptable. These evaluations are essential to ensure that Interpretable AI models are not only accurate but also trustworthy and understandable when deployed in real-world settings.

Although numerous analyses could be performed across the various training and testing scenarios described, in this work, we specifically focus on evaluating the effectiveness of the denoising method. Our primary goal is to assess whether the application of noise reduction techniques leads to measurable improvements in model performance and interpretability under realistic conditions.

In both synthetic contexts (where clean data is available) and real-world scenarios (where only noisy or denoised samples exist), the most insightful setup for evaluating denoising effectiveness is *Train: Denoised – Test: Noisy*. This configuration reveals whether the denoising process has preserved the essential structure and dependencies within the data. By exposing a model trained on denoised inputs to noisy data at inference time, we can test its ability to produce consistent predictions despite a possible drop in precision. Robust performance in this setting indicates that the preprocessing has retained the underlying data representation, while a marked degradation suggests that key relationships have been disrupted.

To contextualize the results, the performance is compared against a relevant baseline: *Train: Original – Test: Original* in synthetic cases and *Train: Noisy – Test: Noisy* in real-world ones. If the metrics remain comparable, it suggests that the denoising has not compromised the interpretable model's ability to learn meaningful patterns. However, a significant decline implies that the process has filtered out crucial information, rendering it ineffective or even harmful.

4.2 Metrics

We have selected four metrics to compare the different denoising methods. These are:

• \mathbf{R}^2 : R^2 is a measure of how well a regression model fits the actual data. In other words, it is an indicator of the model's overall accuracy. R-squared is also known as the coefficient of determination. It is measured on a scale from 0 to 1. A value of 1 indicates that the model perfectly predicts the values in the target field. A value of 0 indicates a model with no predictive value. Although the calculation of this metric allows for negative values, we clip its minimum to 0 in order to enhance interpretability and prevent extreme outliers from distorting subsequent analyses. If \hat{y}_i is the predicted value of the *i*-th sample and y_i is the corresponding true value for total n samples, the estimated R^2 is then computed as shown in Equation (5) where $\bar{y} = \frac{1}{n} \sum_{i=1}^{n} y_i$.

$$R^{2}(y,\hat{y}) = 1 - \frac{\sum_{i=1}^{n} (y_{i} - \hat{y}_{i})^{2}}{\sum_{i=1}^{n} (y_{i} - \bar{y})^{2}}$$
(5)

• Kullback-Leibler Divergence (D_{KL}): It is an asymmetric measure of the difference between two probability distributions, typically a true distribution P (the noisy dataset in real scenarios) and an approximate distribution Q (the denoised dataset). It is defined as we can see at Equation (6).

$$D_{\mathrm{KL}}(P||Q) = \sum_{x} P(x) \log \left(\frac{P(x)}{Q(x)}\right) \tag{6}$$

• **Correlation difference**: This is the difference between the means of the correlation matrices of both datasets, noisy and denoised. This metric is used to determine whether the relationships between pairs of variables have been preserved following the denoising process.

Furthermore, in addition to the aforementioned metrics, the following error metrics were calculated: mean squared error (MSE), root mean squared error (RMSE), mean absolute error (MAE) and symmetric mean absolute percentage error (SMAPE). However, the focus is on \mathbb{R}^2 as it is more interpretable independently of the dataset and the magnitude of the target variable.

In addition, we plotted several graphics that contribute to a better understanding of the results obtained. These plots are:

- Bayesian Signed Ranks Test: This graph summarizes the pairwise comparison of models using the Bayesian Signed Ranks test [67], allowing us to assess whether one model significantly outperforms another across datasets while accounting for uncertainty. It helps identify robust improvements with respect to baseline methods.
- Correlation Difference: This plot presents the difference between the average values of the correlation matrix before and after the application of the denoising method. It serves to quantify the extent to which the noise reduction process alters inter-variable dependencies, offering insight into the preservation or distortion of structural relationships within the data.
- Dataset Noisy-Denoised Comparison: This visualization contrasts the original noisy data with its denoised counterpart, allowing a qualitative evaluation of the performance of the denoising algorithm. It illustrates the degree of deviation introduced by the denoising process and provides a visual estimation of how effectively the method mitigates noise while retaining the intrinsic structure of the input signals.
- Kullback-Leibler Divergence (KL): The KL plot measures the distributional divergence between the original, noisy, and denoised datasets. This metric provides a quantitative assessment of the degree to which the denoised data approximate the statistical characteristics of the original clean data. A lower divergence indicates that the denoising process effectively preserves the underlying data distribution, whereas higher values may reveal the introduction of artifacts or structural distortions.
- Denoising Performance: This plot depicts R^2 performance metric in all possible combinations of training and testing datasets (see Section 4), categorized according to their denoising stage. Provides a comprehensive evaluation of the impact of the denoising method on predictive accuracy, allowing for a direct comparison of model performance under varying noise conditions and highlighting the generalization capabilities of the denoised models.
- Denoising Performance Comparison: This figure provides a comparative assessment between the proposed denoising method, DenoGrad, and the selection of baseline and state-of-the-art techniques presented in Section 2.2 attending to their R² score.

4.3 Datasets

The present study includes experiments conducted on a total of fourteen distinct datasets. As describe in Section 4, half of these datasets are static tabular data, while the other half consists of time series data. Among the seven datasets in each category, five are derived from real-world sources, and the remaining two are synthetically generated. A summary of all datasets is provided in Table 1.

With the datasets used in the experiments now introduced, we proceed to outline the configuration of the denoising models.

4.4 Denoising Methods Parameters

To prevent the experimentation process from becoming excessively extensive, common architectural configurations and hyperparameters were adopted across all datasets—including for our proposed algorithm—differentiating only when

| Dataset summary | | | | | | | | |
|----------------------|----------------|------------|-----------------|----------------|-----------|--|--|--|
| Name | Type | Source | N. of Instances | N. of Features | Frequency | | | |
| House Prices [68] | Static Tabular | Real World | 21436 | 19 | - | | | |
| Lattice Physics [69] | Static Tabular | Real World | 24000 | 40 | - | | | |
| Parkinsons [70] | Static Tabular | Real World | 5875 | 20 | - | | | |
| RT IOT 2022 [71] | Static Tabular | Real World | 117915 | 82 | - | | | |
| Support2 [72] | Static Tabular | Real World | 8579 | 33 | - | | | |
| 2D | Static Tabular | Synthetic | 10001 | 2 | - | | | |
| 3D | Static Tabular | Synthetic | 3000 | 3 | - | | | |
| Daily Climate [73] | Time Series | Real World | 1576 | 4 | daily | | | |
| ECL [74] | Time Series | Real World | 6000 | 320 | hourly | | | |
| ETT [74] | Time Series | Real World | 17420 | 7 | hourly | | | |
| Microsft Stock [75] | Time Series | Real World | 2192 | 5 | daily | | | |
| WTH [74] | Time Series | Real World | 35064 | 12 | hourly | | | |
| 1000s 5v 24w | Time Series | Synthetic | 1000 | 6 | - | | | |
| Seno | Time Series | Synthetic | 1000 | 4 | - | | | |

Table 1: Summary of the datasets used in the experiments, including their type, source, number of instances, number of features and frequency. These datasets were selected to evaluate the denoising performance across a range of data modalities and complexities.

necessary between time series and static datasets. Nevertheless, the selected parameters were chosen with the objective of ensuring optimal denoising performance, rather than being arbitrarily assigned.

• Denoising Autoencoder (DAE) [46]: The specific architecture employed can be observed in Table 2 where the parameter $input_dim$ is the number of variables of the noisy dataset and the parameter $latent_dim$ could be adjusted to achieve optimal performance. To ensure effective denoising while preserving the intrinsic structure of the data, the dimensionality of the latent space in the DAE was set to 8 across all experiments. This choice offers a consistent compression ratio suitable for a wide variety of datasets, as shown in Table 1, with input dimensionalities ranging from as few as 2 to as many as 320 features. A latent dimension of 8 strikes a balance between retaining sufficient representational capacity for reconstruction and enforcing a bottleneck that suppresses irrelevant or noisy variations in the input. Furthermore, this compact latent space enables fair comparisons across datasets of diverse complexity and modality, while avoiding overfitting and promoting generalization. The training parameters are specified at Table 5.

| Layer | Type | Output Dim. | Activation |
|-----------|--------|---------------|------------|
| Input | - | $input_dim$ | - |
| Encoder 1 | Linear | 256 | ReLU |
| Encoder 2 | Linear | 128 | ReLU |
| Encoder 3 | Linear | 64 | ReLU |
| Encoder 4 | Linear | 32 | ReLU |
| Latent | Linear | $latent_dim$ | - |
| Decoder 1 | Linear | 32 | ReLU |
| Decoder 2 | Linear | 64 | ReLU |
| Decoder 3 | Linear | 128 | ReLU |
| Decoder 4 | Linear | 256 | ReLU |
| Output | Linear | $input_dim$ | - |

Table 2: Denoising Autoencoder architecture.

• Empirical Mode Decomposition (EMD) [47]: The first two intrinsic mode functions (IMFs) are discarded, as they typically capture high-frequency components associated with noise. This is a widely adopted heuristic

| Variable | Description | Value | Justification |
|----------|-----------------------------|-------|---|
| F | State Transition Matrix | 1 | Assumes a stationary signal where each state depends linearly on the previous one. |
| H | Observation Matrix | 1 | Direct observation of the state without transformation. |
| Q | Process Noise Variance | 0.01 | Low process noise variance, assuming minimal unmodeled dynamics. |
| R | Measurement Noise Variance | 0.01 | Slightly higher measurement noise variance to filter out high-frequency fluctuations. |
| x | Initial State Estimate | 0 | Neutral initial condition. |
| P | Initial Estimate Covariance | 1 | Assumes high initial uncertainty in the state estimate. |

Table 3: Kalman Filter parameters.

in the literature to retain meaningful low-frequency signal content while removing spurious oscillations [76, 77, 78].

- Kalman Filter [48]: The values of the parameters used can be observed in Table 3.
- Moving Average (MA) [49]: A relatively small window of five time steps was chosen to attenuate high-frequency noise without overly distorting the local trends in the signal. The value was empirically selected based on performance across multiple samples.
- Principal Component Analysis (PCA) [50]: The threshold for explained variance is set to 0.95, ensuring that the selected principal components account for a minimum of 95% of the total variance in the data. This approach guarantees that the retained components contribute substantially to the overall variance, while components with minimal contribution to this variability are discarded.
- **ResNet [51]:** A deep learning-based approach utilizing residual connections to effectively filter out noise while preserving important signal features. The hidden dimension of the network is set to 64 as it provides sufficient capacity to learn complex noise patterns without overfitting. The DN-ResNet architechture can be seen at Table 4. The training parameters are specified at Table 5.

| Layer | Туре | Output Dim. | Activation |
|---------|---------------------------|--------------|------------|
| Input | Residual & Feedforward | $input_dim$ | - |
| Dense 1 | Linear | 64 | ReLU |
| Dense 2 | Linear | 64 | ReLU |
| Dense 3 | Linear | $input_dim$ | - |
| Output | $Residual\ Input-Dense 3$ | $input_dim$ | - |

Table 4: Denoising Residual Network architecture. The network learns to estimate noise, which is subtracted from the input via a residual connection to obtain the denoised signal.

• Wavelet Transform Decomposition (WTD) [52]: The sigma (σ) which the threshold is calculated from, is computed dynamically for each dataset. The wavelet type is fixed to *Daubechies 4 (DB4)* [79].

Now that the denoising models have been parameterized, we proceed to do the same with the Interpretable AI models.

4.5 Interpretable AI Models Parameters

As explained in Section 4.4, to avoid unnecessarily prolonging the experimentation process, a unified configuration has been adopted for the Interpretable AI models across all datasets. For datasets corresponding to time series, this configuration additionally includes an ARIMA model. The full set of parameters is detailed in Table 6. A brief description of each Interpretable AI model is provided below:

| Parameter | Value | Justification |
|------------|---------|---|
| lr | 0.001 | Standard learning rate for the Adam optimizer, ensuring stable convergence. |
| batch_size | 64 | Balanced choice for computational efficiency and gradient stability. |
| criterion | MSELoss | Mean squared error is appropriate for signal reconstruction tasks. |
| optimizer | Adam | Adaptive optimizer well-suited for noisy and sparse gradients. |
| epochs | 500 | Sufficient for convergence, particularly under early stopping. |
| patience | 15 | Prevents overfitting by halting training when no improvement is observed. |
| test_size | 0.2 | Commonly used ratio to ensure a representative validation/test split. |

Table 5: Training hyperparameters for DL-based denoising methods.

- **Ridge Regression:** Performs linear regression with L2 regularization by penalizing the squared magnitude of the coefficients. This constraint reduces variance and multicollinearity, promoting better generalization while preserving the linear structure of the model.
- Partial Least Squares (PLS) Regression: Projects both the predictors and the response variable into a lower-dimensional latent space by extracting components that maximize their covariance. This approach is particularly effective when dealing with high-dimensional, collinear data.
- **Decision Tree Regressor:** Builds a tree-based model by recursively splitting the input space to minimize variance within each resulting subset. The final prediction at each leaf is the average target value of the training points reaching that node, allowing for interpretable, rule-based regression.
- Support Vector Regressor (SVR): Estimates a regression function within a predefined error margin (ϵ -insensitive zone) by finding a hyperplane that balances flatness and tolerance to errors. The use of polynomial kernels enables the modeling of nonlinear relationships in the data.
- **k-Nearest Neighbors** (**kNN**) **Regressor:** Predicts the output value of a query point by averaging the target values of its *k* nearest neighbors in the feature space. Its non-parametric nature and local approximation capabilities make it intuitive and effective for regression tasks.
- ARIMA (AutoRegressive Integrated Moving Average): Applies to time series regression by combining autoregressive terms (past values), differencing (to achieve stationarity), and moving averages of past errors. It captures both trend and noise patterns to provide accurate forecasts of continuous values.

5 Results and Analysis

The following section presents and analyzes the experimental results obtained from applying the proposed denoising framework and all baseline methods. The discussion is divided into two main parts: first, we address the results obtained on tabular datasets, and subsequently, those derived from time series data.

Within each subsection, the analysis is structured in two stages. We begin by examining the ability of each denoising technique to preserve the original data distribution, identifying methods that introduce distortions or undesirable alterations. A study will be conducted under the train:denoised - test:noisy scenario. In this setup, we are interested in ensuring that the metrics do not differ significantly from those obtained under the train:noisy - test:noisy scenario. Such similarity would indicate that the distributions and relevant intrinsic relationships within the data have been preserved.

If performance improves, it means the model was able to learn the underlying relationships more effectively because the denoising process reduced noise in the training data. Even though inference is performed on noisy data, the model has learned more general and robust patterns, which allows it to make better predictions—even under noisy conditions.

If the performance drops below a certain threshold (set to 80% of the baseline performance in our case), we consider the degradation substantial enough to deem that denoising method inappropriate. Furthermore, if a denoising method is found to be inappropriate in more than 50% of the cases (i.e., across all Interpretable AI model per dataset combinations), it will be discarded and excluded from further analyses.

| Model | Parameters | Description |
|------------------------------|---|--|
| Ridge Regression | alpha = 1.0 | Provides moderate L2 regularization, reducing overfitting while maintaining interpretability. |
| Partial Least Squares (PLS) | n_components = 1 | Retains only the most informative latent component, simplifying the model for clearer interpretation. |
| Decision Tree | <pre>max_depth = 5</pre> | Limits tree complexity to avoid overfitting and ensures the resulting rules are easily traceable. |
| Support Vector Machine (SVM) | <pre>kernel = 'poly' degree = 2</pre> | A second-degree polynomial kernel introduces non-linearity while preserving decision boundary simplicity. |
| k-Nearest Neighbors (kNN) | <pre>n_neighbors = 5 weights = 'uniform'</pre> | Uses 5 neighbors to balance bias and variance. Uniform weighting simplifies vote aggregation. |
| ARIMA | order = (7, 0, 0) seasonal_order = (0, 0, 1, 30) | Autoregressive component of order 7 captures weekly lags. No differencing needed as the data is assumed stationary. Seasonal MA(1) models monthly seasonality effectively. |

Table 6: The hyperparameters have been chosen based on standard practices and preliminary experimentation to ensure stable and meaningful explanations. Unless explicitly stated, all other hyperparameters are set to their default values as defined in the respective implementations.

Once the most reliable techniques have been established, we proceed with a comparative performance analysis of the Interpretable AI models trained on the denoised data, assessing the extent to which denoising improves model accuracy and robustness.

To complement this section, two appendices are provided. Appendix A includes the auxiliary code used to generate synthetic datasets, while Appendix B presents a complete collection of visual results (plots) obtained during experimentation for detailed consultation.

5.1 Tabular Data

In this subsection, the results obtained on static tabular datasets are analyzed. The real-world datasets considered include *House Prices, Lattice Physics, Parkinsons, RT IOT 2022*, and *Support*, while the synthetic datasets comprise *2D* and *3D*. For more information on the datasets, refer to Section 4.3.

5.1.1 Tabular Data: Distribution Preservation of Denoising Methods

In Table 7, we present the metrics obtained by the Interpretable AI models across all static tabular datasets. Cells where performance falls below the defined threshold are highlighted in red, while those exceeding the baseline score are shown in green. In the row labeled "Underperformance Rate", the red cells correspond to the denoising methods that will be discarded. Based on this criterion, the following denoising methods are discarded due to underperformance in more than 50% of the evaluated scenarios: EMD, Kalman Filter, MA, and WTD. This outcome aligns with theoretical expectations, as these four methods are primarily designed for time series data rather than static tabular datasets. Furthermore, DenoGrad displays the highest number of green cells (>34%), indicating that it improves performance in more cases than any other denoising method. We also performed the signed ranked Bayes test in this scenario, and we can see at Figures 9 and 10 how DenoGrad is, without doubt, the best statistically preserving the internal structure of the data.

To further support the analysis of distributional changes introduced by the denoising process, we compute the D_{KL} (definition in Section 4.2), which quantifies the extent to which the original data distribution is altered. In parallel, we assess the correlation difference, which captures how much the intrinsic relationships between pairs of variables deviate from those in the noisy dataset.

| Dataset | AI_model | Baseline | DAE | DenoGrad | EMD | Kalman | MA | PCA | ResNet | Wavelet |
|------------------------------|--------------------------|------------|----------|----------|----------|----------|----------|----------|-----------|-----------|
| | Ridge | 0.6751 | 0.6827 | 0.6752 | 0.644 | 0.6700 | 0.6839 | 0.5883 | 0.6863 | -0.666 |
| ss se | PLS | 0.5273 | 0.5415 | 0.5371 | 0.487 | 0.4332 | 0.5439 | 0.5366 | 0.5366 | 0.4824 |
| House Prices | Tree | 0.6695 | 0.6548 | 0.6743 | 0.558 | 0.2493 | 0.4977 | 0.6050 | 0.6560 | -14.038 |
| H | SVR | 0.5074 | 0.4872 | 0.5536 | -0.1862 | -73.7796 | -7.5782 | 0.4346 | 0.5247 | -6.3216 |
| | k-NN | 0.7869 | 0.8129 | 0.7888 | 0.569 | 0.2356 | 0.5430 | 0.7382 | 0.8051 | 0.3129 |
| | Ridge | 0.9868 | 0.9361 | 0.9862 | 0.954 | 0.9860 | 0.9868 | 0.9863 | 0.9868 | 0.1750 |
| ce | PLS | 0.9839 | 0.9273 | 0.9837 | 0.944 | 0.9390 | 0.9776 | 0.9815 | 0.9839 | 0.0275 |
| Lattice Physics | Tree | 0.1217 | -0.02638 | 0.1262 | 0.094 | 0.0403 | 0.0963 | 0.1260 | 0.1217 | -0.3587 |
| 7 | SVR | -0.13858 | -6.4082 | -0.14117 | -0.63967 | -30.50 | -1.253 | -0.2463 | -0.1385 | -23.7767 |
| | k-NN | 0.6321 | 0.6162 | 0.6341 | 0.318 | 0.1202 | 0.3402 | 0.6372 | 0.6321 | 0.0301 |
| 8 | Ridge | 0.1577 | 0.0940 | 0.1558 | 0.022 | -2.7751 | -0.1356 | -26.2459 | 0.1577 | -0.0711 |
| nos. | PLS | 0.0534 | 0.0603 | 0.0531 | 0.018 | -2.7751 | 0.0196 | 0.0524 | 0.0534 | 0.0045 |
| kin | Tree | 0.5292 | 0.4575 | 0.5044 | -0.0597 | 0.0405 | 0.5359 | 0.5265 | 0.5337 | 0.0340 |
| Parkinsons | SVR | -0.0243 | -0.5872 | 0.0087 | -0.0597 | -2.7751 | -0.1356 | -26.2459 | -0.02423 | -0.0711 |
| , | k-NN | 0.6435 | 0.6383 | 0.6397 | 0.037 | 0.2462 | 0.5752 | 0.5988 | 0.6451 | 0.2460 |
| 22 | Ridge | -1.7076 | -26.6157 | -0.5705 | -2.892 | -0.1788 | 0.0298 | -38.0799 | -1.5709 | -1.701 |
| RT 10T 2022 | PLS | 0.2185 | -0.4621 | 0.2236 | -2.585 | -1.6324 | 0.3039 | 0.3315 | 0.2185 | 0.2220 |
| OT | Tree | 0.8485 | 0.6413 | 0.8785 | -1.0703 | 0.5868 | -1.2526 | 0.5703 | 0.8484 | 0.8485 |
| TI | SVR | -1796.1979 | -30.3484 | -552.23 | -0.5460 | -110.833 | -31.0936 | -61.698 | -1798.285 | -1690.589 |
| × | k-NN | -1.6336 | 0.7240 | -0.3147 | -0.28939 | 0.6148 | 0.7233 | -1.7298 | -1.6336 | -1.6336 |
| 2 | Ridge | 0.4980 | 0.4870 | 0.4945 | 0.190 | 0.4395 | 0.4847 | -0.54996 | 0.4980 | -0.507 |
| SUPPORT 2 | PLS | 0.2164 | 0.1940 | 0.2183 | 0.071 | -0.198 | 0.1053 | 0.2158 | 0.2164 | -0.055 |
| P0 | Tree | 0.3680 | 0.2049 | 0.3064 | 0.077 | 0.0256 | 0.0559 | 0.2378 | 0.3221 | -0.3783 |
| UF | SVR | 0.2572 | 0.2286 | 0.2541 | -0.2443 | -32.4186 | -3.960 | 0.1155 | 0.2573 | -4.1672 |
| J 1 | k-NN | 0.2311 | 0.2249 | 0.2399 | 0.059 | 0.0681 | 0.1361 | 0.2411 | 0.2311 | -0.01009 |
| | Ridge | 0.7893 | 0.7892 | 0.7886 | 0.789 | 0.7899 | 0.7893 | 0.7892 | 0.7891 | 0.7893 |
| | PLS | 0.7893 | 0.7892 | 0.7886 | 0.789 | 0.7899 | 0.7894 | 0.7892 | 0.7892 | 0.7893 |
| 2D | Tree | 0.9953 | 0.9942 | 0.9917 | 0.995 | 0.9953 | 0.9950 | 0.9942 | 0.9943 | 0.9932 |
| | SVR | -0.1472 | -0.1318 | -0.1375 | -0.1375 | -0.1383 | -0.13786 | -0.1333 | -0.1330 | -0.15663 |
| | k-NN | 0.9999 | 0.9954 | 0.9951 | 0.999 | 0.9998 | 0.9993 | 0.9957 | 0.9954 | 0.9967 |
| | Ridge | 0.0039 | 0.0038 | 0.0031 | 0.006 | -0.0397 | 0.0006 | 0.0037 | 0.0036 | -0.1756 |
| _ | PLS | 0.0039 | 0.0038 | 0.0031 | 0.006 | -0.041 | 0.0006 | 0.0037 | 0.0036 | -0.0907 |
| 30 | Tree | 0.8023 | 0.8007 | 0.7830 | -0.0892 | -0.007 | 0.0294 | 0.7909 | 0.7886 | -0.022 |
| | SVR | 0.9967 | 0.9974 | 0.9958 | 0.467 | 0.2331 | 0.3056 | 0.9974 | 0.9974 | -3.4859 |
| | k-NN | 0.9499 | 0.9511 | 0.9425 | 0.092 | 0.0086 | 0.1346 | 0.9494 | 0.9494 | -0.39636 |
| Total Bad Performance | | 8 | 2 | 21 | 22 | 19 | 8 | 0 | 24 | |
| % Total | Bad Perform | ance | 22.86 | 5.71 | 60 | 62.86 | 54.29 | 22.86 | 0.0 | 68.57 |
| Total Go | od Performa | nce | 9 | 15 | 5 | 5 | 9 | 8 | 9 | 2 |
| % Total | % Total Good Performance | | 25.710 | 42.86 | 14.29 | 14.29 | 25.71 | 22.86 | 25.71 | 5.71 |

Table 7: R^2 scores for static tabular datasets under the train:denoised-test:noisy setting. The "Baseline" column shows results for train:noisy-test:noisy. Red cells mark $\geq 20\%$ drops vs. baseline. In the "% Total Bad Performance" row, methods equal or above 50% are marked in red. Green cells mark a higher score vs. baseline.

To provide a comprehensive view of these effects, we include Figures 13 and 14, which present the mean correlation differences grouped by the denoising method. Similarly, Figures 17 and 18 show the D_{KL} results both as mean values per denoising method and as heat maps showing the divergence for each variable and method.

In Figures 13 and 14, it is evident that the previously discarded methods are those that consistently exhibit the largest changes in correlation. In contrast, DenoGrad and ResNet consistently preserve intervariable relationships, showing the lowest correlation differences across datasets. The only exception is the 2D synthetic dataset, where DenoGrad shows a slightly higher correlation difference compared to other methods. However, because of the very small scale of the plots and the reduce number of variables (just two), this difference is negligible and is not of practical significance.

Turning to Figures 17 and 18, we observe a similar trend in terms of D_{KL} . EMD, Kalman Filter, MA, and WTD are again the methods that introduce the greatest distributional shifts. The only case where DenoGrad exhibits a relatively high D_{KL} is in the 2D synthetic dataset, which, due to having only two variables, is particularly sensitive to small variations. Even so, the scale of the plot is so small that the observed divergence remains negligible and does not carry practical significance. DAE and PCA show a significant D_{KL} in the RT_IOT2022 dataset (see Figure 2), with both performing the worst in that case. PCA also performs poorly in the House Prices dataset, showing one of the highest D_{KL} values.

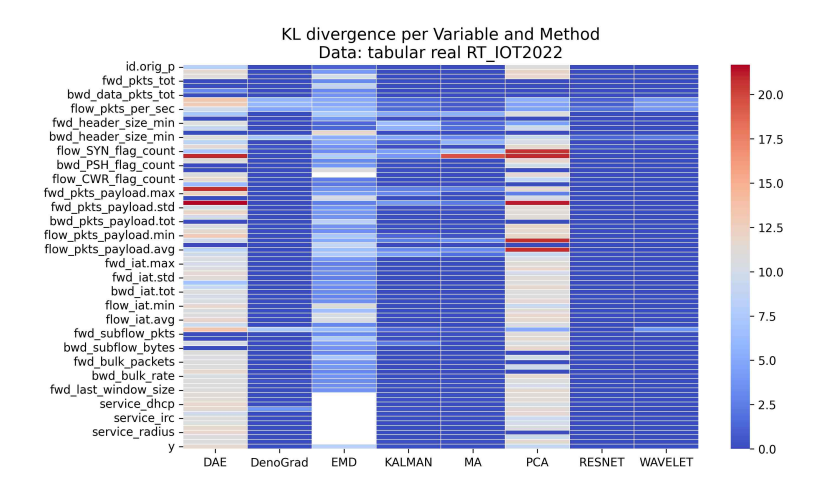


Figure 2: D_{KL} heatmap for the real-world static tabular RT IOT 2022 dataset.

5.1.2 Tabular Data: Comparative Performance

As a result of the previous analyses, four denoising methods/frameworks remain viable for static tabular data: DAE, PCA, ResNet, and DenoGrad. Among these, DAE and PCA exhibit higher D_{KL} and correlation differences in certain scenarios, particularly on the RT_IOT2022 and House Prices datasets. DenoGrad shows slightly elevated values only in the 2D synthetic dataset, where, as we argued before, the differences are less meaningful. However, in the signed ranked Bayes tests presented in Figures 9 and 10, DenoGrad emerges as the statistically undisputed winner. Meanwhile, ResNet demonstrates consistently strong performance across all datasets, maintaining minimal distributional shifts and preserving inter-variable relationships effectively.

However, one might argue that maintaining high R^2 in the *train:denoised – test:noisy* scenario, preserving variable correlations and showing minimal D_{KL} could indicate that the denoising method does not alter the data meaningfully, that is, it is not actually denoising. To address this concern, we now turn to a focused analysis of the denoising performance of these four selected methods.

We now analyze the train:denoised - test:denoised scenario to assess which denoising method enables Interpretable AI models to achieve better predictive performance. As shown in Figure 3, which presents the signed ranked Bayes test for this setting, DenoGrad consistently outperforms ResNet in real-world datasets, performs similarly to DAE, and is consistently outperformed by PCA. However, if we exclude the datasets in which PCA obtained bad D_{KL} values, the comparison becomes less conclusive: DenoGrad has a 23% probability of outperforming PCA, versus a 77% probability of the opposite. In contrast, for synthetic datasets, DenoGrad emerges as the preferred method, either outperforming or matching all alternatives.

For a detailed analysis of \mathbb{R}^2 scores across all train-test scenarios and datasets, we refer the reader to Figure 4 as an illustrative example of the full set of results presented in Appendix B, specifically in Figures 21 to 27. These results

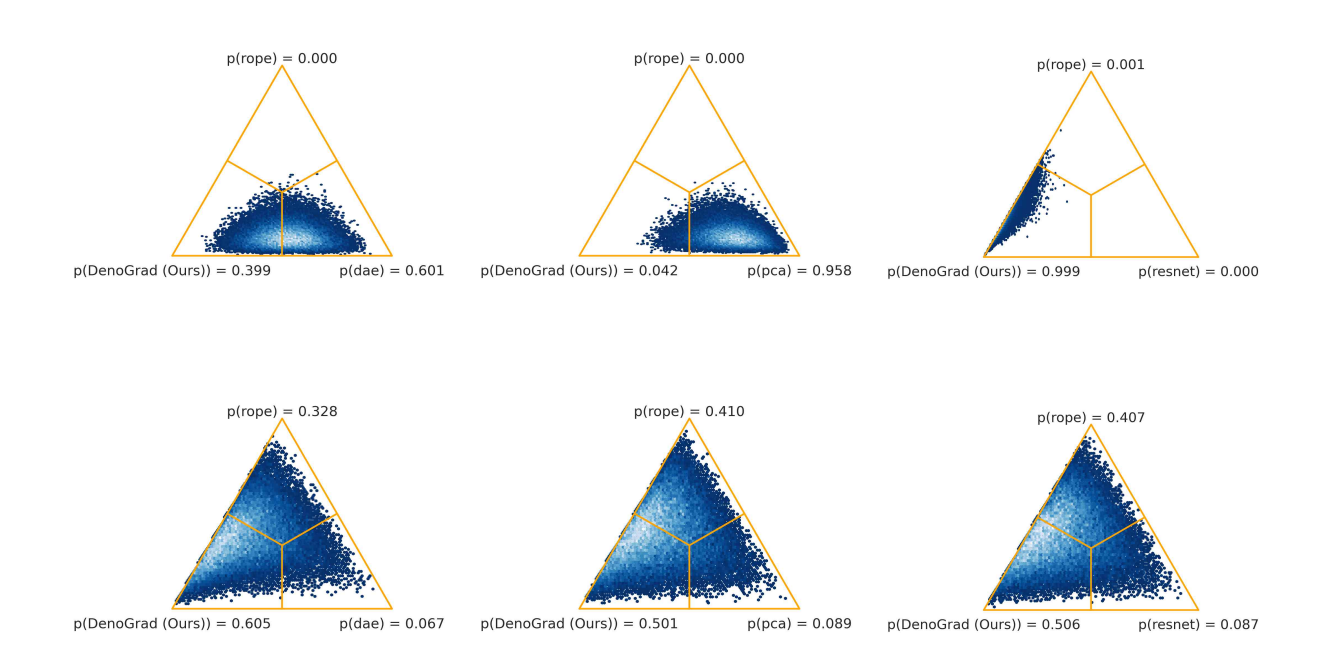


Figure 3: Signed ranked Bayes tests in *train:denoised - test:denoised* scenario confronting DenoGrad with the other valid state-of-the-art denoising alternatives in real-world and synthetic static tabular datasets.

also help resolve the earlier question regarding ResNet's denoising effectiveness: does a method that preserves a perfect R^2 score, shows no correlation difference, and exhibits no D_{KL} actually perform denoising? The answer appears to be negative for this case. ResNet's R^2 scores remain nearly unchanged across most scenarios, with only minor variations, suggesting that it is not effectively denoising the data.

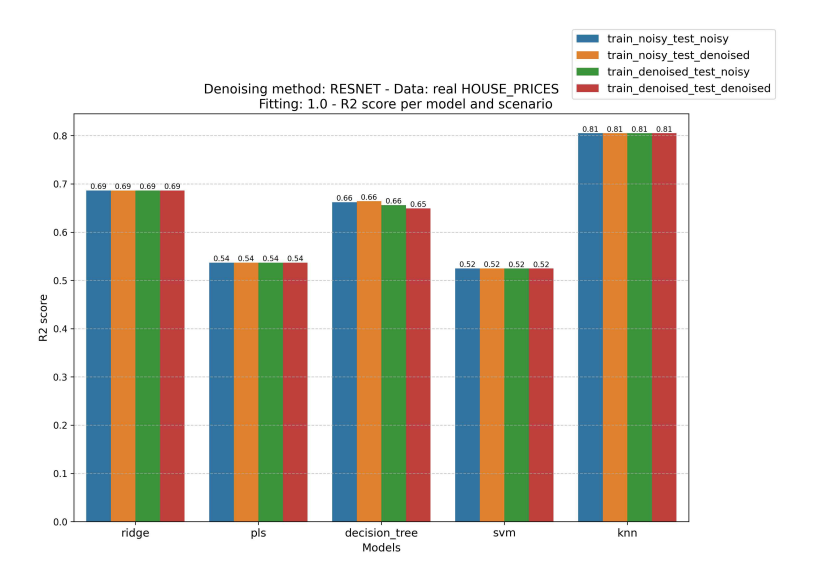


Figure 4: R^2 score obtained by the Interpretable AI models in the *House Prices* real-world static tabular dataset in all train-test scenarios applying ResNet as denoiser method.

Based on the complete analysis, we conclude that DenoGrad is the most suitable denoising framework for static tabular data in most scenarios. It consistently preserves both the overall data distribution and the internal relationships between variables across all evaluated cases, while still achieving competitive performance compared to state-of-the-art

alternatives. In contrast, methods such as DAE and PCA may yield better results in specific scenarios, but their application requires careful evaluation (such as the one conducted in this study) as they can potentially alter the underlying structure of the data.

5.2 Time Series

In this subsection, the results obtained on static tabular datasets are analyzed. The real-world datasets considered include *Daily Climate*, *ECL*, *ETT*, *Microsoft Stock*, and *Weather*, while the synthetic datasets comprise *1000s 5v 24w* and *Sinus*. For more information on the datasets, refer to Section 4.3.

5.2.1 Time Series: Distribution Preservation of Denoising Methods

As previously done for static tabular data (see Section 5.1.1), we now evaluate the denoising performance of each method in the train:denoised - test:noisy scenario. The goal is to verify that the performance of the model remains close to the baseline (train:noisy - test:noisy), indicating that key distributional properties and variable relationships are preserved.

We consider a method unsuitable if its performance drops below 80% of the baseline and this occurs in more than half of the Interpretable AI model–dataset combinations. The results of this evaluation are presented in Table 8 and, for time series datasets, no method meets the exclusion criteria. The same four methods/frameworks identified as best for static tabular data – DAE, PCA, ResNet, and DenoGrad – remain the most reliable options, as they have the best trade-off between "Total Bad Performace" and "Total Good Performance". Among them, DenoGrad once again stands out as the framework that effectively enhances model performance in more cases (>26%), enabling the Interpretable AI models to better capture the underlying data relationships.

To complement Table 8, we conducted signed ranked Bayes tests for R^2 scores in the train:denoised -test:noisy scenario. The results are presented in Figures 11 and 12 for real-world and synthetic datasets, respectively. In Figure 11, DenoGrad is statistically superior to EMD, Kalman Filter, MA, and WTD, and outperforms DAE with lower probability. It performs on par with ResNet, but is outperformed by PCA. In the synthetic scenario (Figure 12), the results are less favorable: DenoGrad again outperforms EMD, Kalman Filter, and WTD, and narrowly beats MA, but is consistently outperformed by DAE, PCA, and ResNet.

Overall, DenoGrad emerges as the statistically preferred framework in 9 out of 14 pairwise comparisons (approximately 64% of the cases), reinforcing its robustness in this scenario. To further validate this finding, we now examine correlation differences (Figures 15 and 16) and D_{KL} (Figures 19 and 20) to assess whether the denoising process preserves the original data distribution and inter-variable relationships.

DenoGrad consistently outperforms other alternatives across all datasets and in both metrics, positioning it as one of the most effective – if not the most effective – denoising alternatives in time series scenarios. In the correlation difference plots (Figures 15 and 16), the largest deviations appear in the Kalman Filter and WTD columns for real-world datasets, and in the Kalman Filter, EMD, and WTD columns for synthetic datasets.

The D_{KL} analysis that takes place in Figures 19 and 20 reveals clear differences in denoising quality among the evaluated methods. Kalman Filter stands out as the most consistently underperforming technique across all datasets. We refer to Figure 5 as an example of all the plots from Figures 19 and 20 to illustrate how EMD, WTD, and MA also exhibit poor results in several cases, with EMD notably distorting the distribution of the target variable in the WTH dataset. Although MA slightly outperforms DenoGrad in that same dataset, both EMD and MA generally yield higher D_{KL} values across datasets, indicating that they degrade the original data distribution rather than preserving it.

The D_{KL} analysis presented in Figures 19 and 20 highlights clear disparities in denoising quality among the evaluated methods. Kalman Filter consistently underperforms across all datasets, while EMD, WTD, and MA also show poor results in several cases as we can see, for example, in Figure 5. Furthermore, EMD significantly distorts the distribution of the target variable in the WTH dataset and, although MA slightly outperforms DenoGrad in that specific case, both EMD and MA tend to produce higher D_{KL} values across the rest of datasets, suggesting that they alter the original data distribution rather than preserving it.

PCA presents highly inconsistent behavior, with particularly high D_{KL} values for certain variables in the ECL, WTH, and $1000s_5v_24w$ datasets. In contrast, DAE and DenoGrad show more stable and reliable performance. DAE underperforms only on Daily Climate but outperforms DenoGrad in WTH. Overall, both DenoGrad and DAE achieve a good balance between preserving the original data distribution and enabling strong predictive performance. Notably, DenoGrad improves the performance of Interpretable AI models in the train:denoised-test:noisy scenario in slightly more cases (11 vs. 9), suggesting a marginally better ability to correct noisy instances while retaining the underlying structure and variable relationships.

| Dataset | AI_model | Baseline | DAE | DenoGrad | EMD | Kalman | MA | PCA | ResNet | Wavelet |
|-------------------------------|--------------------------|------------------|------------------|------------------|------------------|-------------------|------------------|------------------|-------------------|------------------|
| | Ridge | 0.9377 | 0.9377 | 0.9374 | 0.936 | 0.9324 | 0.9354 | 0.9377 | 0.9377 | 0.9341 |
| <i>a</i> | PLS | 0.6616 | 0.6626 | 0.6664 | 0.538 | -0.0055 | 0.4475 | 0.6621 | 0.6621 | 0.3372 |
| Daily Climate | Tree | 0.9286 | 0.9264 | 0.9295 | 0.931 | 0.9348 | 0.9358 | 0.9286 | 0.9324 | 0.9364 |
| Cii | SVR | -1.3398 | -4.2166 | -6.2085 | -0.2192 | -14.675 | -4.41354 | -1.31951 | -1.36387 | -4.718 |
| | k-NN | 0.9177 | 0.9230 | 0.9200 | 0.900 | 0.8616 | 0.9103 | 0.9177 | 0.9186 | 0.8859 |
| | ARIMA | 0.1761 | 0.0601 | 0.0362 | -0.0834 | 0.3432 | -0.0853 | 0.0548 | 0.0552 | -0.17287 |
| | Ridge | 0.7436 | 0.6771 | 0.8470 | 0.884 | 0.8841 | 0.8799 | 0.8358 | 0.7422 | 0.7800 |
| | PLS | -0.2975 | -0.3431 | -0.2635 | -0.24596 | -0.09481 | -0.2302 | -0.30152 | -0.2987 | -0.19373 |
| ECL | Tree | 0.7900 | 0.7884 | 0.8394 | 0.844 | 0.6987 | 0.8487 | 0.8380 | 0.7896 | 0.8535 |
| E | SVR | -0.3769 | -0.54624 | -0.26098 | -1.74314 | -7.9991 | -2.3929 | -0.3003 | -0.377 | -1.4126 |
| | k-NN | 0.7003 | 0.7127 | 0.7047 | 0.522 | 0.2573 | 0.6935 | 0.7290 | 0.6997 | 0.6743 |
| | ARIMA | -1.141 | -1.20629 | -1.1071 | -1.141 | -0.73518 | -1.1098 | -1.148 | -1.1422 | -1.1153 |
| | Ridge | 0.9649 | 0.9650 | 0.9637 | 0.965 | 0.9649 | 0.9651 | 0.9648 | 0.9648 | 0.9658 |
| | PLS | -1.6659 | -1.7605 | -1.6844 | -1.8187 | -6.0172 | -2.3417 | -1.6831 | -1.6662 | -3.0941 |
| ETT | Tree | 0.9544 | 0.9551 | 0.9549 | 0.955 | 0.9550 | 0.9562 | 0.9539 | 0.9551 | 0.9535 |
| E | SVR | -5.4207 | -5.59145 | -9.45776 | -6.5585 | -144.5168 | -11.0169 | -5.098 | -5.4388 | -8.7827 |
| | k-NN | 0.7592 | 0.7581 | 0.7624 | 0.722 | -0.92478 | 0.6137 | 0.7639 | 0.7592 | 0.2900 |
| | ARIMA | -3.31074 | -3.2917 | -3.43563 | -2.89279 | -0.31668 | -2.636 | -3.4354 | -3.4357 | -2.7779 |
| | Ridge | 0.9817 | 0.9811 | 0.9816 | 0.982 | 0.9810 | 0.9813 | 0.9810 | 0.9817 | 0.9813 |
| tfo 3 | PLS | 0.9671 | 0.9681 | 0.9670 | 0.961 | 0.7748 | 0.9457 | 0.9678 | 0.9670 | 0.9354 |
| Microsoft Stock | Tree | -2.31058 | -2.3566 | -2.3073 | -2.2946 | -3.8278 | -2.79158 | -2.31557 | -2.3198 | -2.3294 |
| Mic | SVR | -118.3594 | -113.671 | -118.3581 | -117.973 | -144.3748 | -122.7387 | -117.9405 | -118.4855 | -125.1431 |
| | k-NN | -2.5967 | -2.5828 | -2.59725 | -2.6656 | -3.85168 | -2.9958 | -2.6024 | -2.604 | -2.6792 |
| | ARIMA | -13.2756 | -7.5119 | -14.3404 | -6.91459 | -4.17 | -15.1613 | -7.7627 | -12.7342 | -8.1346 |
| | Ridge | 0.4553 | 0.4353 | 0.3893 | 0.326 | 0.3178 | 0.3362 | 0.4582 | 0.4553 | 0.4189 |
| + | PLS | 0.2639 | 0.2645 | 0.2804 | -0.2137 | 0.2621 | 0.2908 | 0.2635 | 0.2639 | 0.2231 |
| WTH | Tree | 0.4588 | 0.4673 | 0.4212 | 0.336 | 0.3946 | 0.3426 | 0.4377 | 0.4420 | 0.4009 |
| _ | SVR k-NN | 0.4273 0.3907 | 0.4284 0.3833 | 0.3725 0.4389 | -0.1664 0.336 | -1.7712 0.4388 | 0.1955 0.4054 | 0.4226 0.3892 | 0.4274 | 0.3957 0.3555 |
| | ARIMA | -0.0155 | -0.0155 | -0.011 | -0.00417 | -0.0148 | -0.0155 | -0.0157 | 0.3910 -0.0155 | -0.0155 |
| | Ridge | 0.8910 | 0.8969 | 0.8887 | -0.93237 | -0.0769 | 0.5381 | 0.7863 | 0.8895 | -0.7907 |
| <u> </u> | PLS | 0.75486 | 0.7592 | 0.8887 | -2.36689 | -0.0703 | 0.6871 | 0.7803 | 0.8893 | -0.0215 |
| 1000s 5v 24w | Tree | 0.75480 | 0.7392 | 0.7338 | -0.2406 | -1.2491 | -0.01669 | 0.7411 | 0.7501 | -0.0213 |
|)s 5 | SVR | 0.4805 | 0.4555 | 0.4612 | -239.596 | -39.463 | 0.0005 | 0.3402 | 0.4633 | -28.113 |
| 000 | k-NN | 0.9811 | 0.9802 | 0.9815 | -0.2181 | 0.0243 | 0.1066 | 0.9541 | 0.9814 | 0.5038 |
| | ARIMA | 0.1769 | -0.1288 | -0.1198 | -0.0064 | -0.02249 | -0.3154 | -0.0418 | -0.1162 | -0.0545 |
| | Ridge | 0.9128 | 0.9108 | 0.9126 | 0.903 | 0.9088 | 0.9109 | 0.9116 | 0.9127 | 0.9065 |
| | PLS | 0.9109 | 0.9096 | 0.9111 | 0.885 | -2.2838 | 0.9094 | 0.9111 | 0.9110 | 0.9023 |
| ns | Tree | -3.4158 | -3.145 | -3.1752 | -2.9679 | -5.6982 | -3.2275 | -3.2046 | -4.2925 | -3.8482 |
| Sinus | SVR | -171.448 | -170.789 | -170.3575 | -244.661 | -203.485 | -170.8129 | -170.223 | -170.804 | -174.9363 |
| | k-NN | -3.5869 | -3.4908 | -3.635 | -2.3726 | -5.5304 | -3.8516 | -3.6311 | -3.5976 | -3.5083 |
| | ARIMA | -4.3862 | -2.8405 | -3.036 | -2.8219 | -12.856 | -3.7369 | -2.8518 | -2.5932 | -4.9136 |
| Total Bad Performance | | 4 | 4 | 15 | 22 | 15 | 3 | 3 | 13 | |
| % Total | Bad Perform | ance | 9.52 | 9.52 | 35.71 | 52.38 | 35.71 | 7.14 | 7.14 | 30,95 |
| Total Good Performance | | | 19 | 23 | 15 | 10 | 12 | 16 | 14 | 9 |
| % Total | % Total Good Performance | | 45.24 | 54.76 | 35.71 | 23.81 | 28.57 | 38.10 | 33.33 | 21.43 |

Table 8: R^2 scores for time series datasets under the train:denoised-test:noisy setting. The "Baseline" column shows results for the train:noisy-test:noisy setup. Red cells indicate $\geq 20\%$ drop from baseline. Green cells mark a higher score vs baseline.

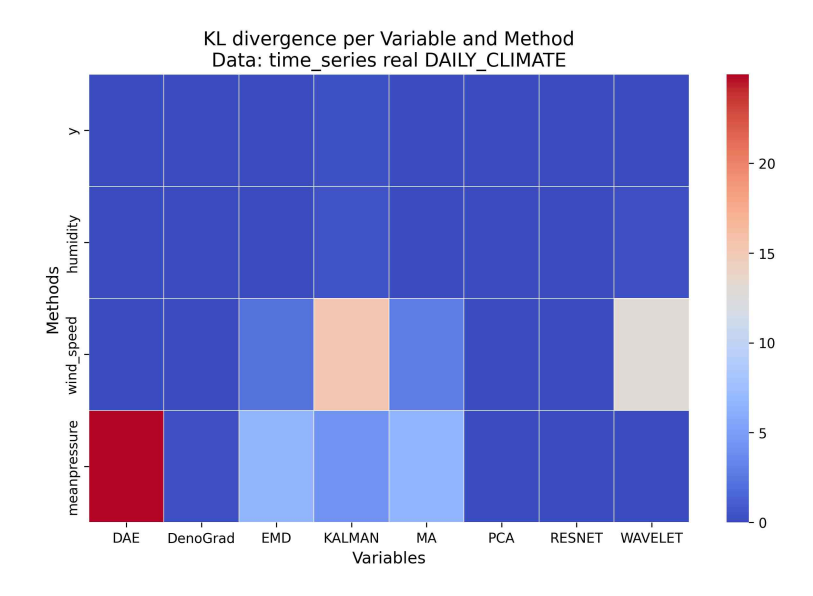


Figure 5: D_{KL} heatmap for the real-world time series Daily Climate dataset.

As in the static tabular setting, ResNet consistently achieves the lowest D_{KL} and correlation differences across all datasets. However, this pattern raises the same doubts as before: whether such stability is due to actual denoising or simply a lack of any meaningful transformation. This will be explored in more detail in the following sections.

Given these findings, we discard EMD, Kalman Filter, MA, and WTD from further analysis, as they consistently show poor performance in both D_{KL} and correlation metrics. This leaves DAE, PCA, ResNet and DenoGrad for further study.

5.2.2 Time Series: Comparative Performance

Summarizing the analysis of distribution preservation, four denoising methods/frameworks are identified as suitable for time series data: DAE, PCA, ResNet, and DenoGrad. However, a closer inspection of ResNet reveals that it does not perform effective denoising. As shown in Figure 6, using the WTH dataset as an example, ResNet leaves the input unchanged, resulting in identical R^2 scores across all train-test scenarios. This indicates that no real denoising is taking place, and thus ResNet is discarded from further analysis. Additional results can be found in Figures 28 to 34. These figures also help identify which methods are most effective in time series scenarios, showing that EMD and MA lead to the highest predictive performance for the Interpretable AI models across most datasets. However, as previously discussed in Section 5.2.1, both methods perform poorly in terms of actual denoising quality, suggesting that their improved performance may result from distorting the original data distribution rather than genuinely removing noise. Furthermore, the results suggest that when Interpretable AI models already perform well on noisy data, it likely means the noise level is low or negligible. In such cases, applying denoising may offer little to no benefit and can even lead to a decline in performance.

To explore this further, we examine the *train:denoised* – *test:denoised* scenario, assessing which method makes the Interpretable AI models to obtain the best predictive performance. As illustrated in Figures 7 and 8, which show the signed ranked Bayes test results, DenoGrad emerges as the best performer in only 1 out of all 4 real-world and synthetic scenarios and shows moderate chances of outperforming PCA (around 38%) in real-world settings.

Looking at Figures 28 to 34, we observe that the best denoising method really depends on the dataset but, as specified in Section 5.2.1, the results in ECL and WTH for PCA are not valid as the data distribution is hardly distorted. This means that PCA only outperforms DenoGrad in synthetic scenarios and that choosing between DAE and DenoGrad really depends on the data and the Interpretable AI model. These results are remarkable, considering that our method competes with an approach specifically designed and trained for the denoising task, with a carefully crafted architecture and fine-tuned parameters. In contrast, DenoGrad relies on an external DL model that was trained for a different task using the same data, requires no additional training, and does not involve any hyperparameter optimization.

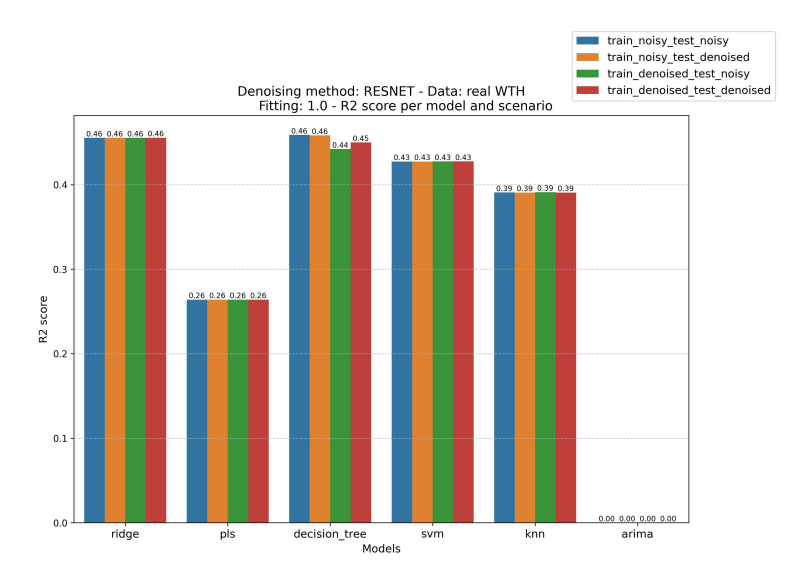


Figure 6: \mathbb{R}^2 score obtained by the Interpretable AI models in the WTH real-world time series dataset in all train-test scenarios applying ResNet as denoiser.

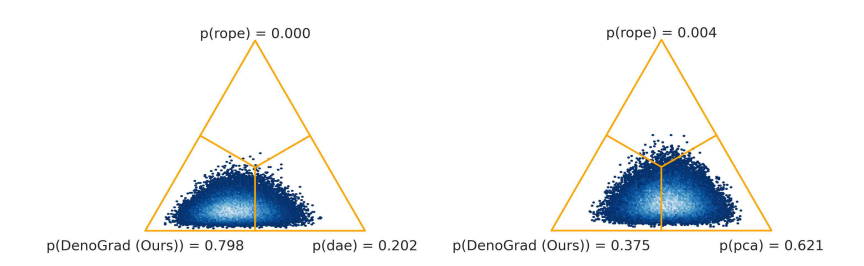


Figure 7: Signed ranked Bayes tests in *train:denoised - test:denoised* scenario confronting DenoGrad with the other valid state-of-the-art denoising alternatives in real-world time series datasets.

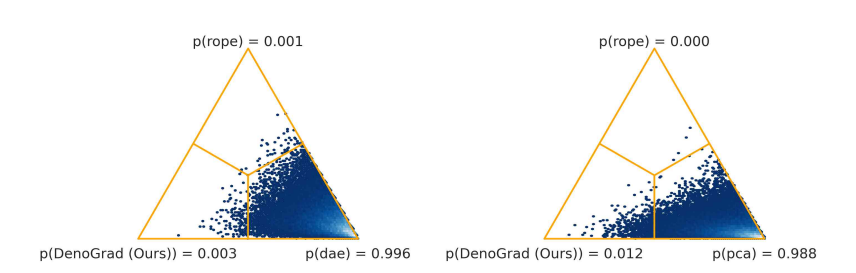


Figure 8: Signed ranked Bayes tests in *train:denoised - test:denoised* scenario confronting DenoGrad with the other valid state-of-the-art denoising alternatives in synthetic time series datasets.

In summary, DenoGrad stands out as one of the most effective methods for denoising time series data, as it best preserves the data distribution and intervariable correlations while also being among the top performers in enhancing the accuracy of Interpretable AI models.

6 Conclusions and Future Work

We proposed DenoGrad, a gradient-based denoising framework that operates using a pretrained DL model as its backbone. The main advantage of DenoGrad is that it does not require access to clean data nor any training process at all, since it can directly leverage an existing DL model already deployed in production. DenoGrad is entirely agnostic to the architecture of the underlying model: it works regardless of the type, number of layers, or specific design, as long as it was trained to perform regression on the same data we aim to denoise. DenoGrad is mathematically grounded and straightforward to implement, providing along with this manuscript a Python library publicly available on GitHub to facilitate its adoption.

As shown in Section 5, DenoGrad performs competitively with state-of-the-art denoising methods in all 14 datasets analyzed in both static tabular and time series domains, emerging as the most effective alternative in the majority of evaluated scenarios. It preserves data distribution and the intervariable correlations in the majority of cases and, even so, it performs real denoising allowing improvement in \mathbb{R}^2 score for the Interpretable AI models.

As future work derived from this study, we find several ways to improve DenoGrad as outlined below:

- 1 Automatic hyperparameter tuning: Integrate an optimizer for the noise reduction rate similar to learning rate schedulers used in DL training. This would allow DenoGrad to dynamically adapt the denoising strength depending on the characteristics of the data or the learning progress.
- 2 Alternative backbone architectures: Evaluate the use of Transformer-based models as the underlying DL model for DenoGrad. Their strong performance in both tabular and sequence modeling tasks makes them a promising candidate for enhancing denoising capabilities.
- 3 Extension to classification tasks. A natural next step is to extend DenoGrad to classification problems using tabular data, in order to evaluate its effectiveness beyond regression. This would allow for testing the generalizability of the framework across different learning paradigms.
 - A particularly application would be image classification: if DenoGrad proves successful in tabular classification, it could be adapted to handle visual data, where it might effectively mitigate Gaussian noise in input images. Such an extension would demonstrate the versatility and scalability of DenoGrad across multiple data modalities and problem domains.

Appendices

This section provides additional material that supports the main content of the paper. Appendix A contains auxiliary code functions used during the development. These functions are included to facilitate reproducibility and to provide further implementation details. Appendix B presents a collection of plots illustrating various metrics obtained during the experiments, offering a more comprehensive view of the model behavior and performance across different settings.

A Code

This appendix provides the auxiliary code functions developed to support the implementation and experimentation of DenoGrad.

```
def linear_combination_ts_generator(window_size: int, n_var: int, n_samples: int,
      seed: int = 42) -> pd.DataFrame:
       Generate synthetic time series data with temporal dependencies.
       Each new sample is a linear combination of the previous 'window_size' samples,
       with added Gaussian noise and L2 normalization.
       Parameters:
8
           window_size (int): Number of past steps to base each new sample on.
           n_var (int): Number of variables (features).
           n_samples (int): Number of time steps to generate after the initial
              window.
           seed (int): Random seed for reproducibility.
14
           pd.DataFrame: Generated time series data of shape (n_samples, n_var),
                         with each row representing a time step.
16
       np.random.seed(seed)
18
19
       # Initialize base window
20
       X = 2 * np.random.rand(window_size, n_var) - 1
       A = 2 * np.random.rand(1, window_size) - 1 # Temporal dependency weights
       X_df = pd.DataFrame(X)
24
       A_{matrix} = A
26
       for _ in range(n_samples):
           window = X_df.iloc[-window_size:].values
28
29
           new_sample = A_matrix @ window + np.random.normal(0, 0.1, (1, n_var))
           new_sample /= np.linalg.norm(new_sample) # L2 normalization
30
           X_df = pd.concat([X_df, pd.DataFrame(new_sample)], ignore_index=True)
       # Remove initial window
34
       X_df = X_df.iloc[window_size:].reset_index(drop=True)
       return X_df.astype(np.float32)
```

Listing 1: Function used to generate the 1000s 5v 24w time series dataset.

B Images

This appendix presents a collection of plots illustrating the metrics obtained during the experimental phase. These visualizations complement the quantitative results discussed in Section 5 by providing additional insight into the behavior of the different denoising alternatives.

B.1 Signed Ranked Bayes Tests

This subsection presents the plots corresponding to the Signed Ranked Bayes Tests performed during the experimental evaluation. These tests provide a Bayesian alternative to traditional non-parametric significance tests, allowing for a probabilistic comparison between denoising alternatives. The resulting visualizations illustrate the posterior probability distributions and support the interpretation of the relative performance differences between DenoGrad and other denoising alternatives.

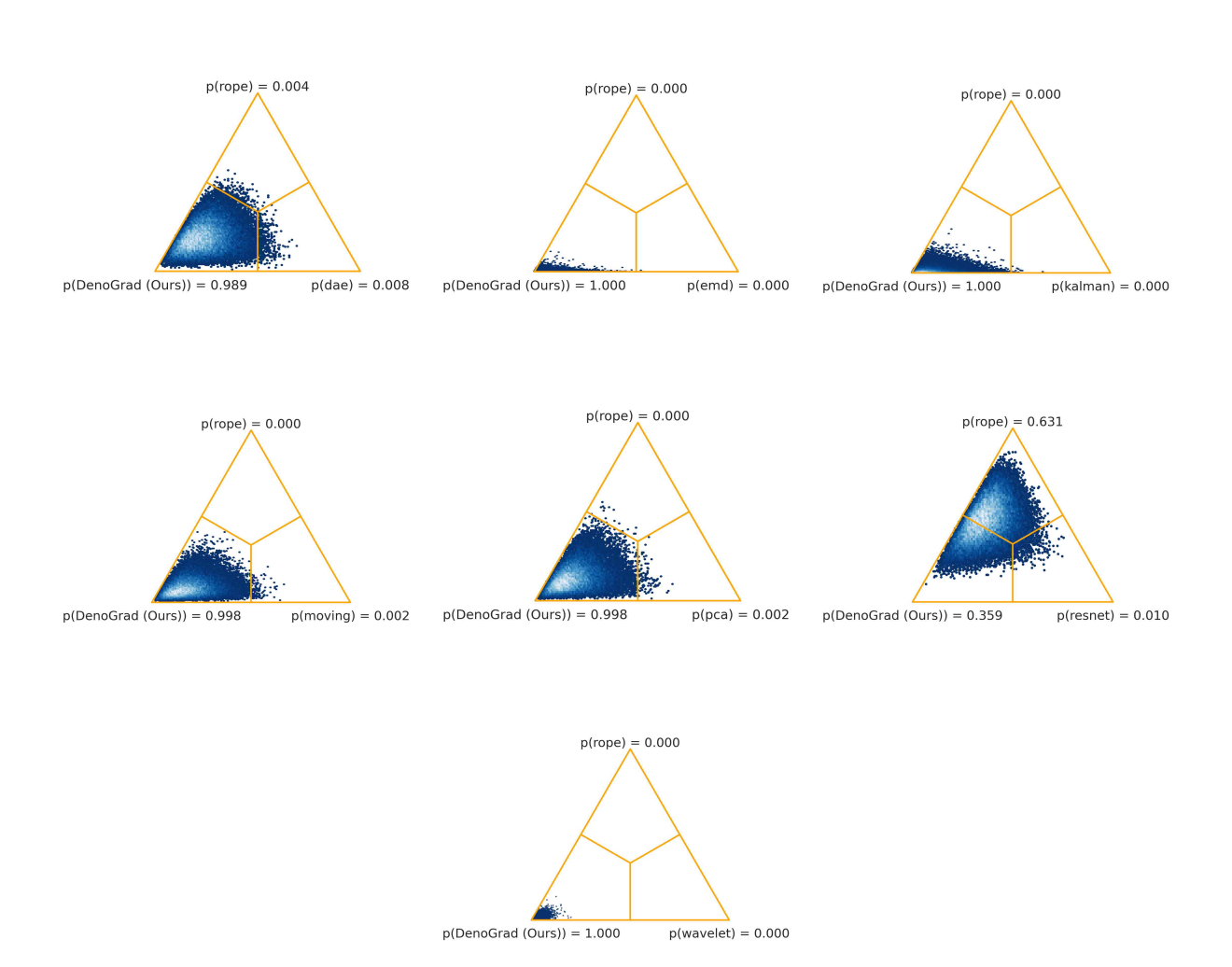


Figure 9: Signed ranked Bayes tests in *train:denoised - test:noisy* scenario confronting DenoGrad with every other state-of-the-art denoising alternative in real-world static tabular datasets.

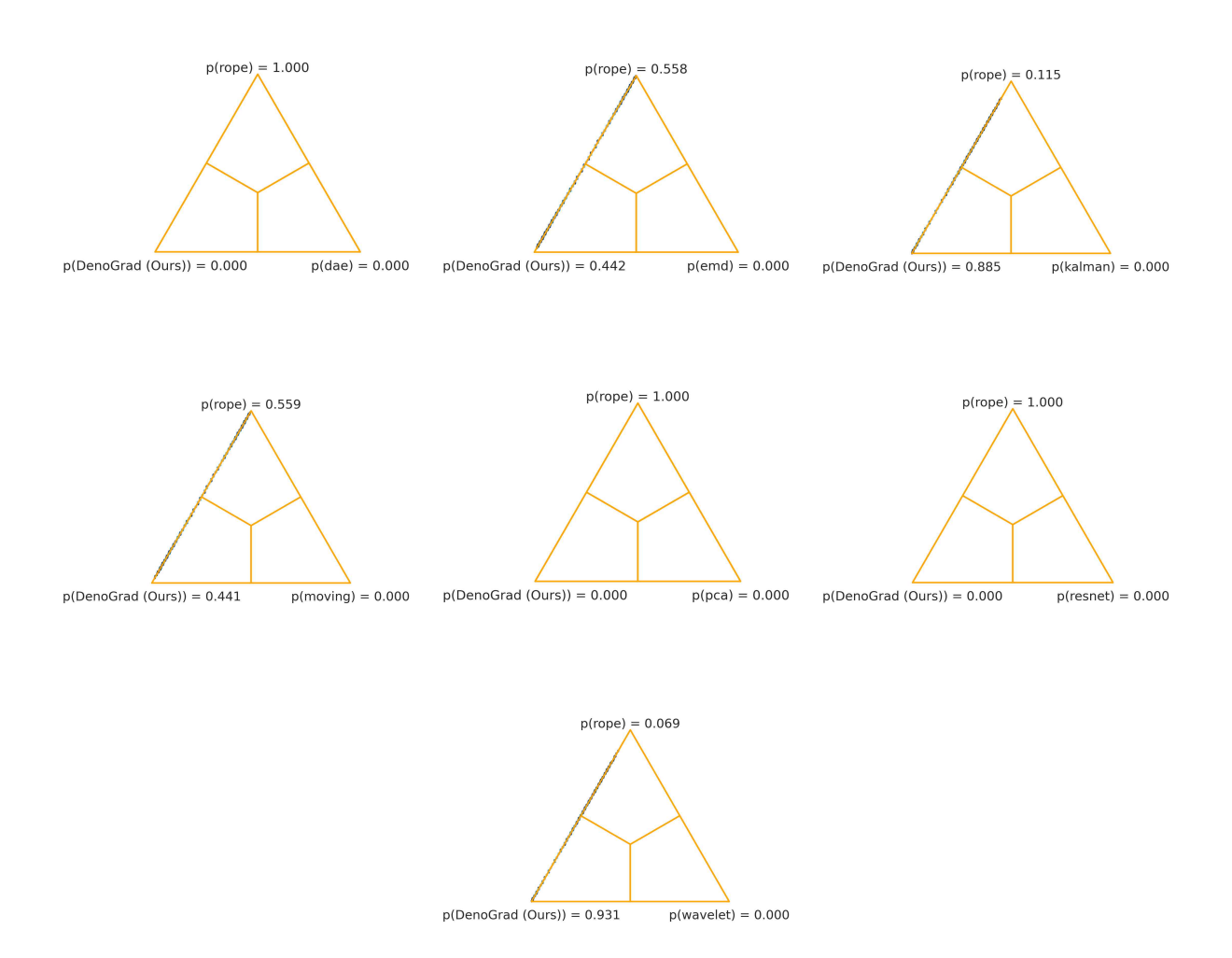


Figure 10: Signed ranked Bayes tests in *train:denoised - test:noisy* scenario confronting DenoGrad with every other state-of-the-art denoising alternative in synthetic static tabular datasets.

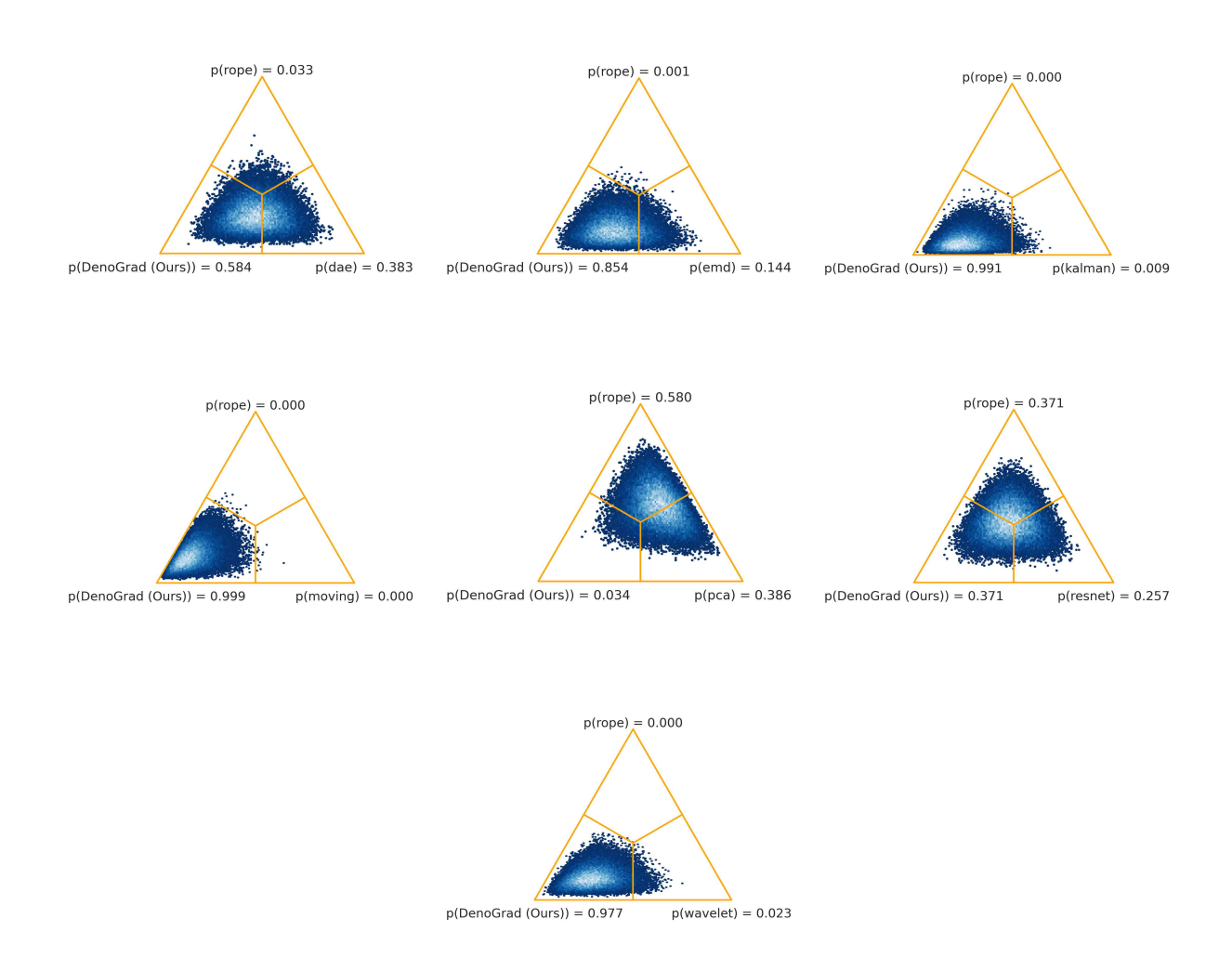


Figure 11: Signed ranked Bayes tests in *train:denoised - test:noisy* scenario confronting DenoGrad with the other valid state-of-the-art denoising alternatives in real-world time series datasets.

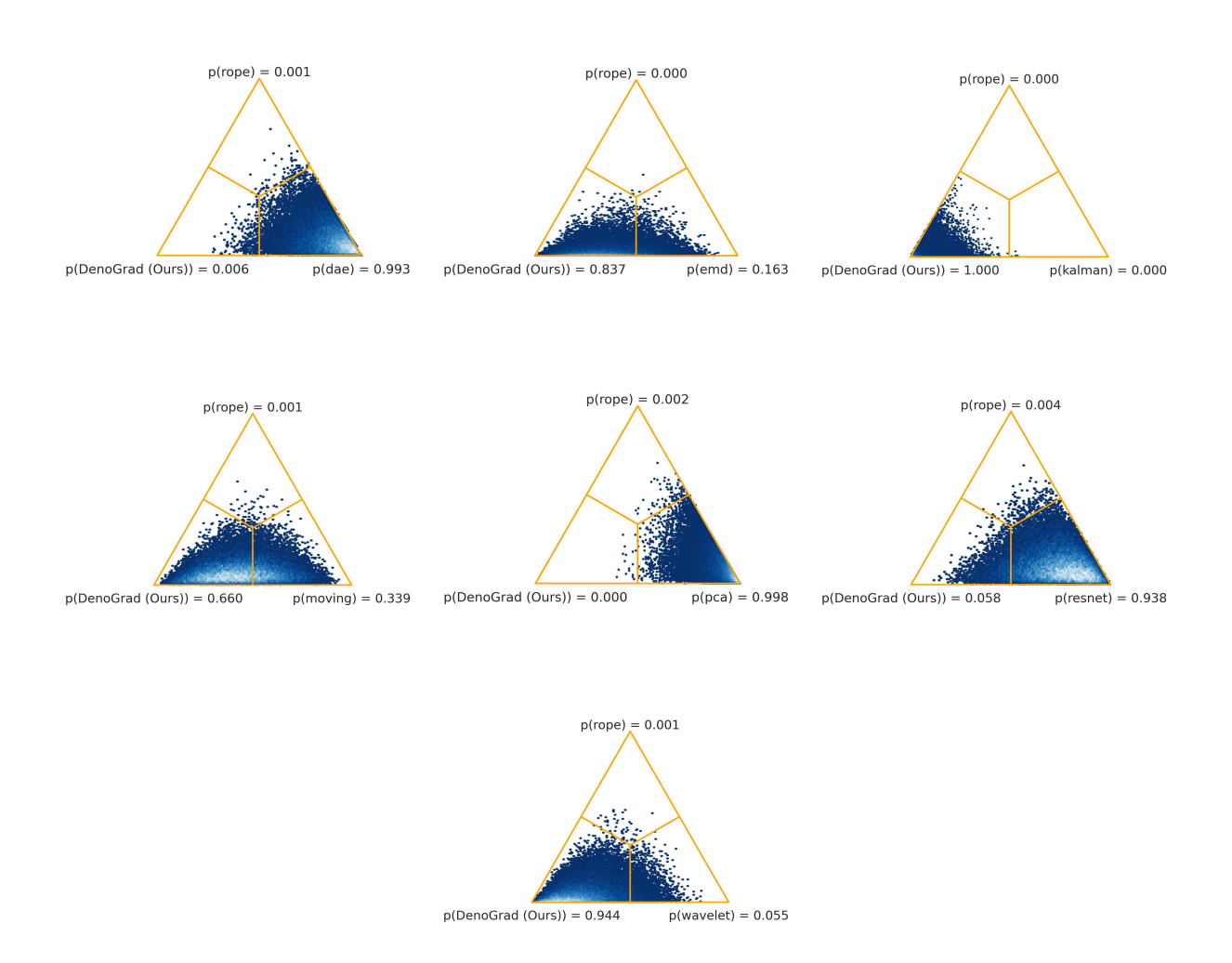


Figure 12: Signed ranked Bayes tests in *train:denoised - test:noisy* scenario confronting DenoGrad with the other valid state-of-the-art denoising alternatives in synthetic time series datasets.

B.2 Absolute Correlation Mean Differences

This subsection presents plots showing the Absolute Correlation Mean Differences calculated during the denoising experiments. These visualizations provide insight into the magnitude of the differences in correlation between the different denoising alternatives and the original data.

B.2.1 Static Tabular

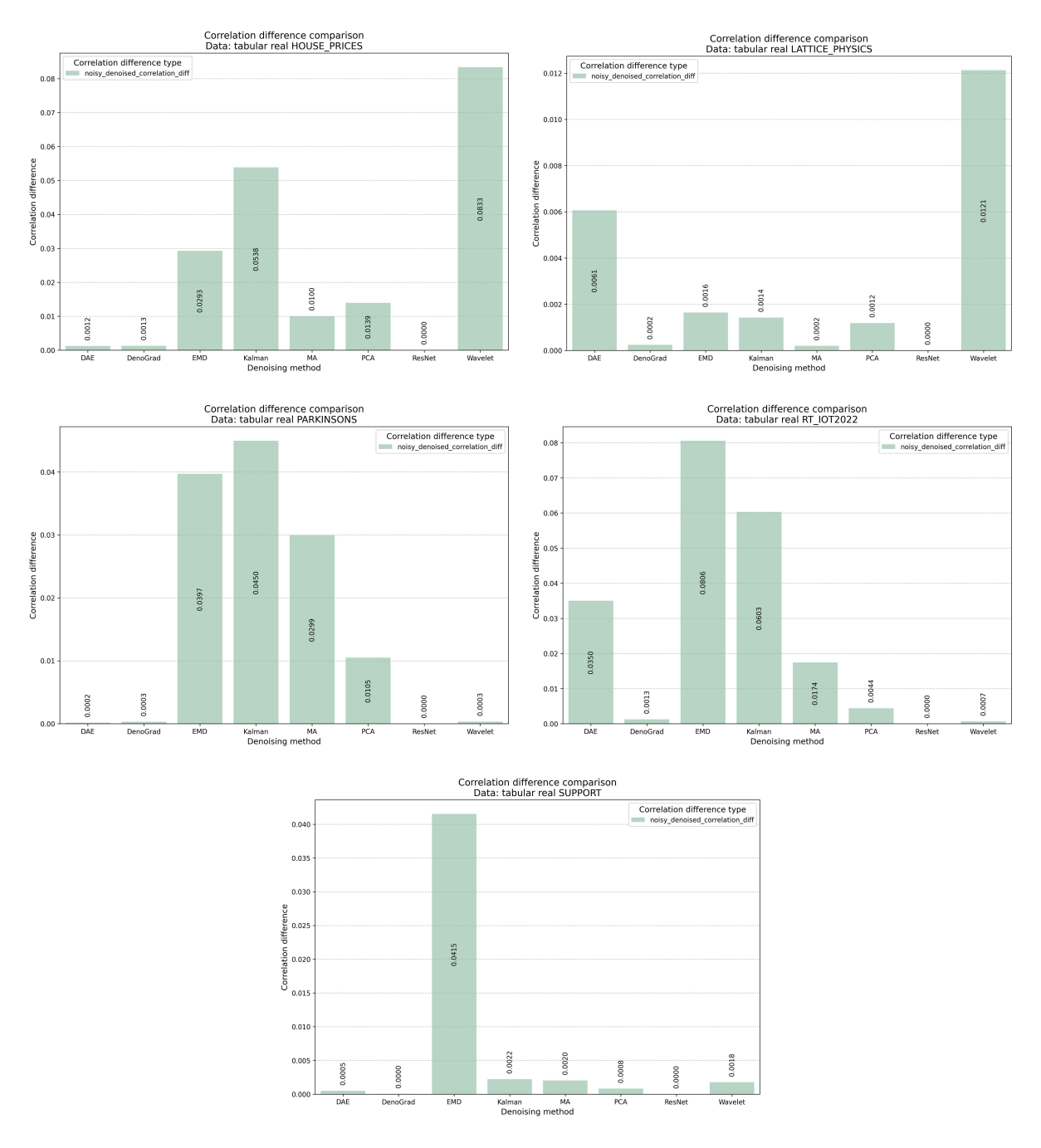


Figure 13: Absolute difference between the average values of the correlation matrices before and after applying each denoising method to each real-world static tabular dataset.

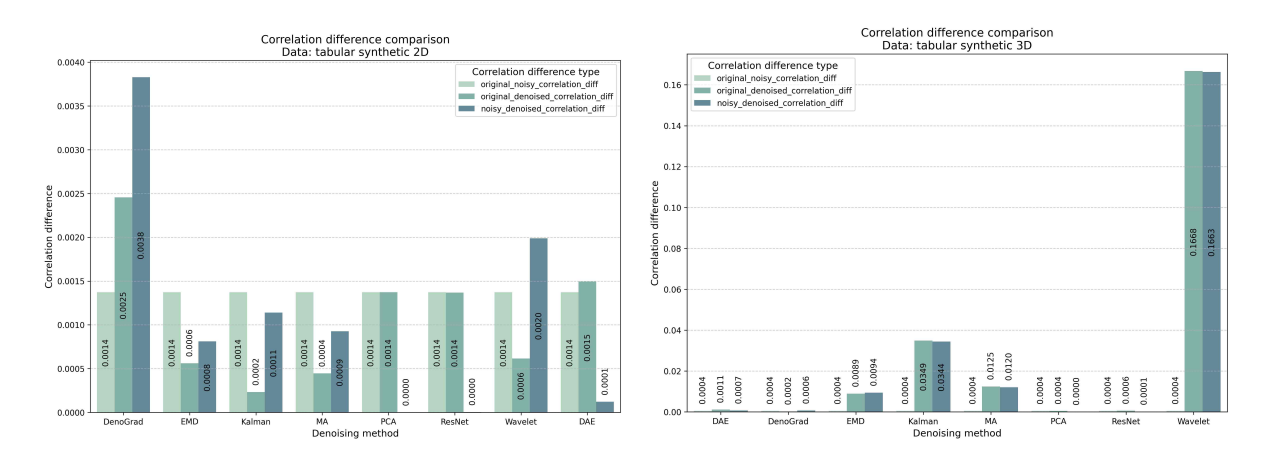


Figure 14: Absolute difference between the average values of the correlation matrices before and after applying each denoising method to each synthetic static tabular dataset.

B.2.2 Time Series

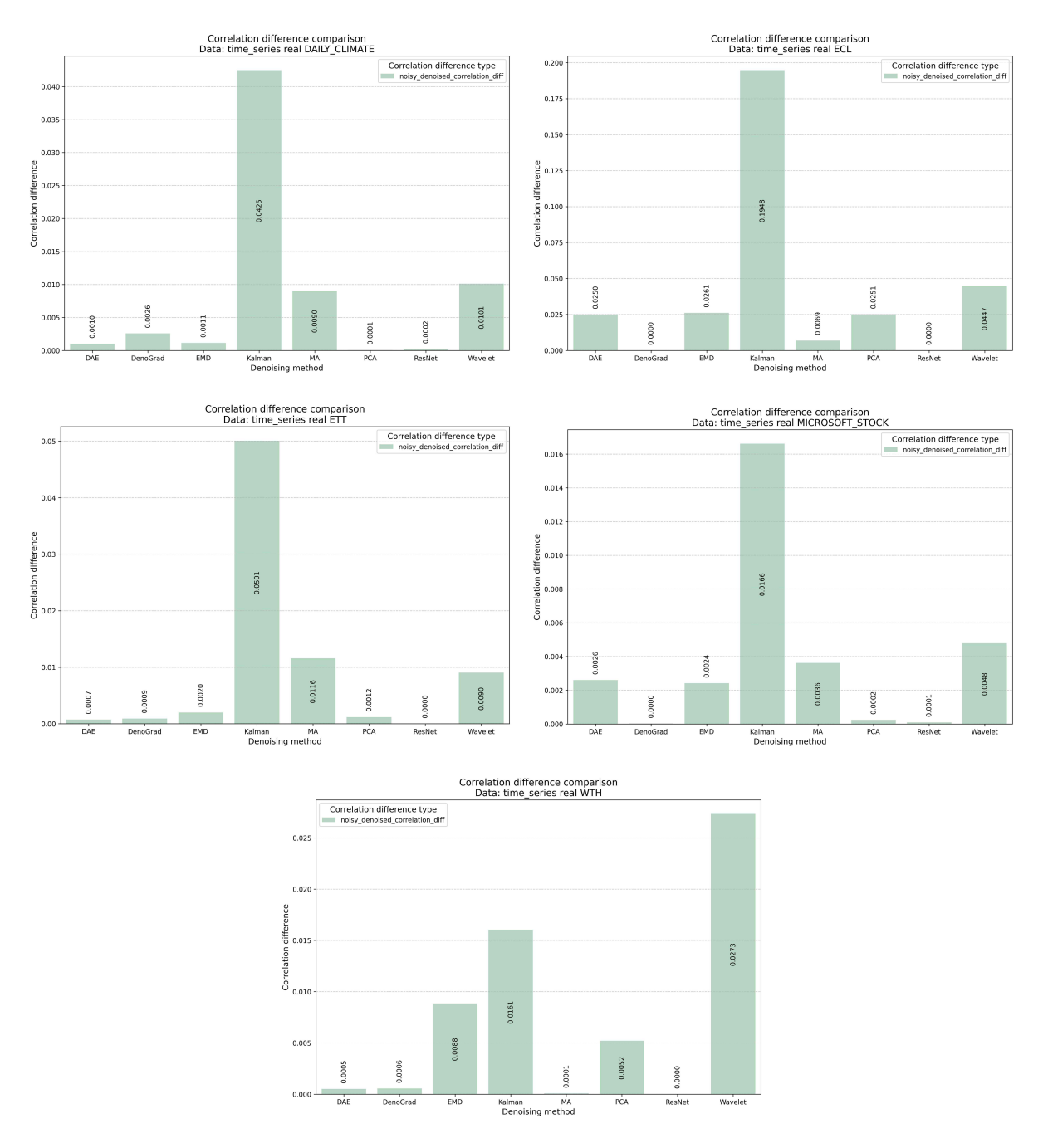


Figure 15: Absolute difference between the average values of the correlation matrices before and after applying each denoising method to each real-world time series dataset.

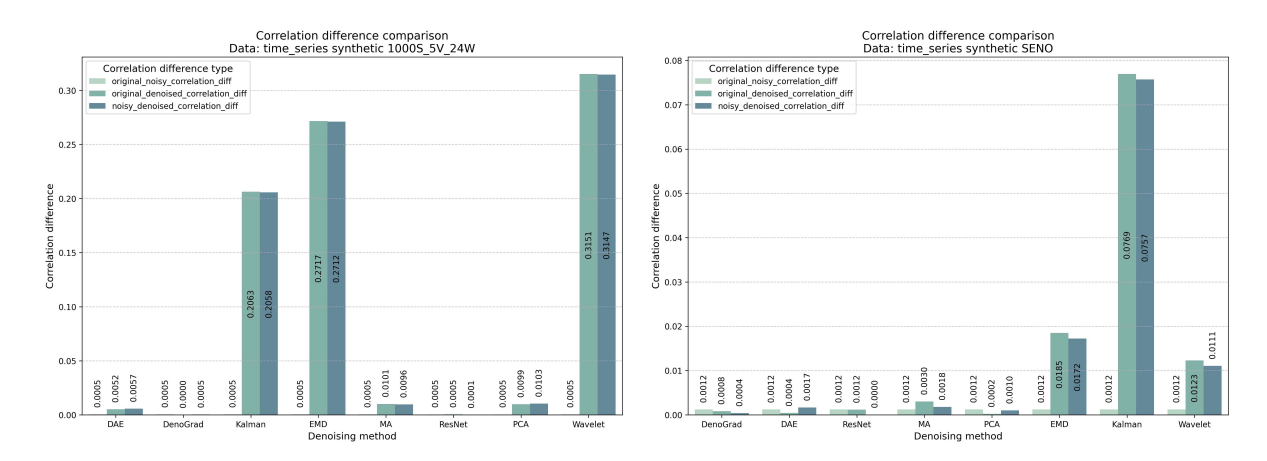


Figure 16: Absolute difference between the average values of the correlation matrices before and after applying each denoising method to each synthetic time series dataset.

B.3 Kullback-Leibler Divergence

This subsection presents the results related to the KL Divergence analysis. It includes plots showing the differences in mean KL values for each noise reduction method, as well as a heatmap displaying the KL values for each method across all variables. These visualizations provide a detailed comparison of how each denoising approach affects the distributional similarity between denoised and original data.

B.3.1 Static Tabular

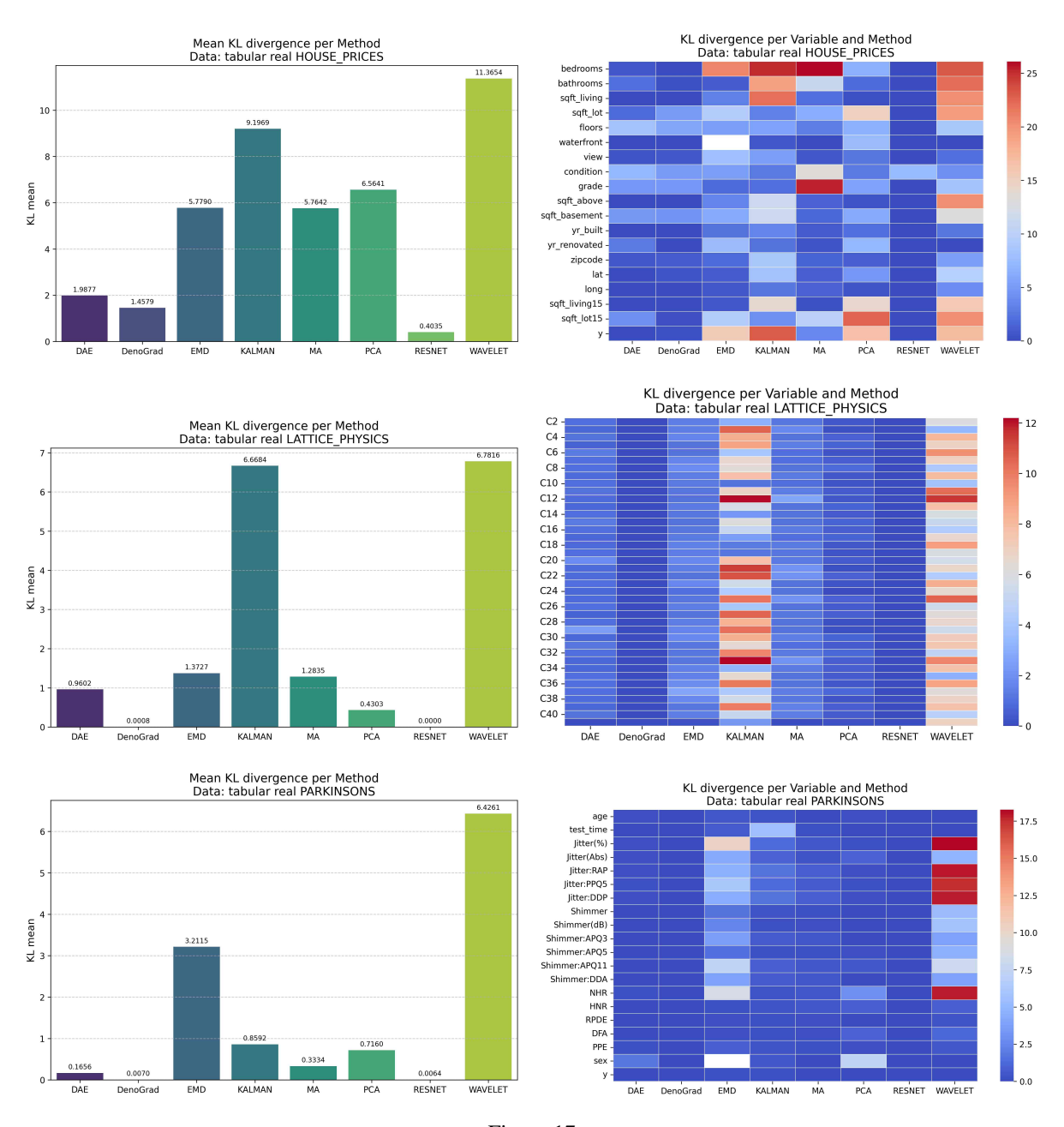


Figure 17

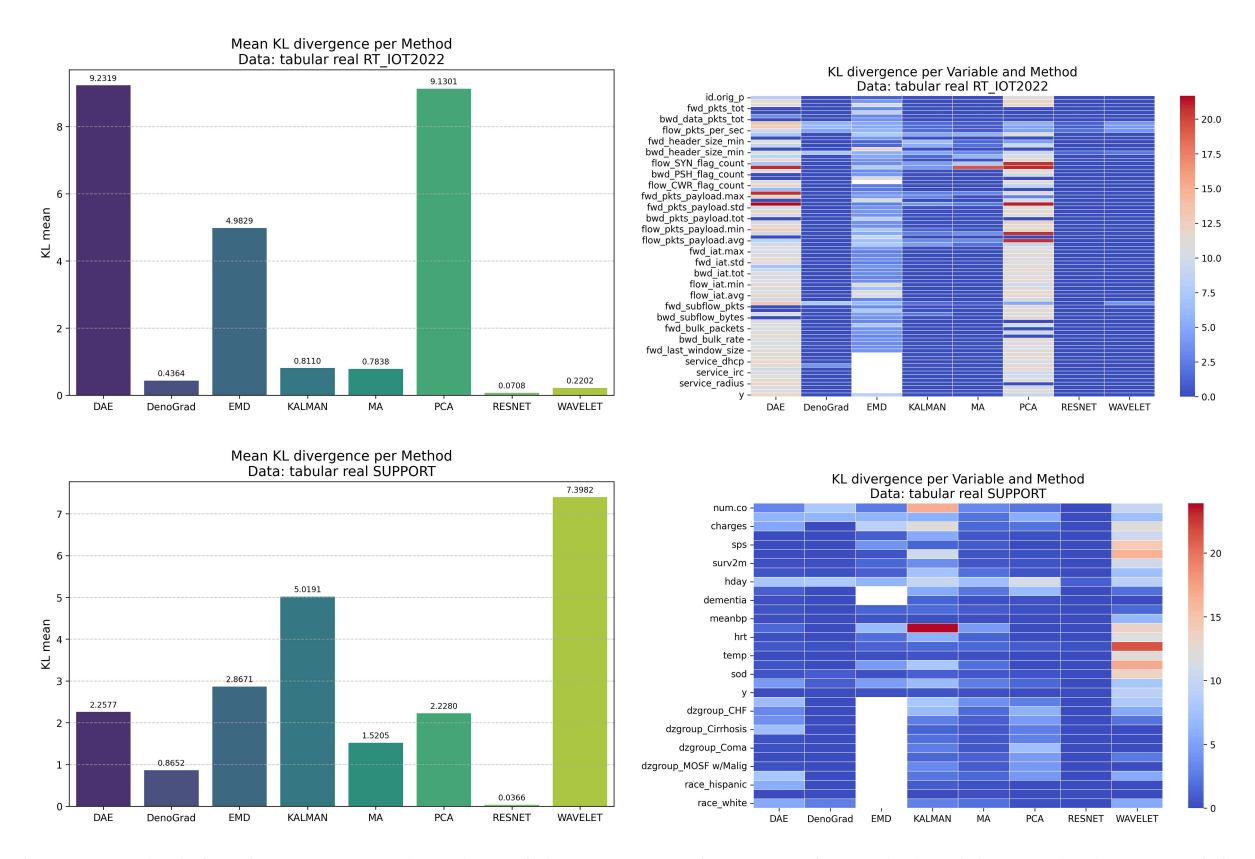


Figure 17: The left column presents bar plots of the mean KL divergence for each denoising method, summarizing the overall distributional shift introduced by each approach. The right column displays heatmaps representing the KL divergence computed for each individual variable and denoising method. All plots correspond to real-world static tabular datasets.

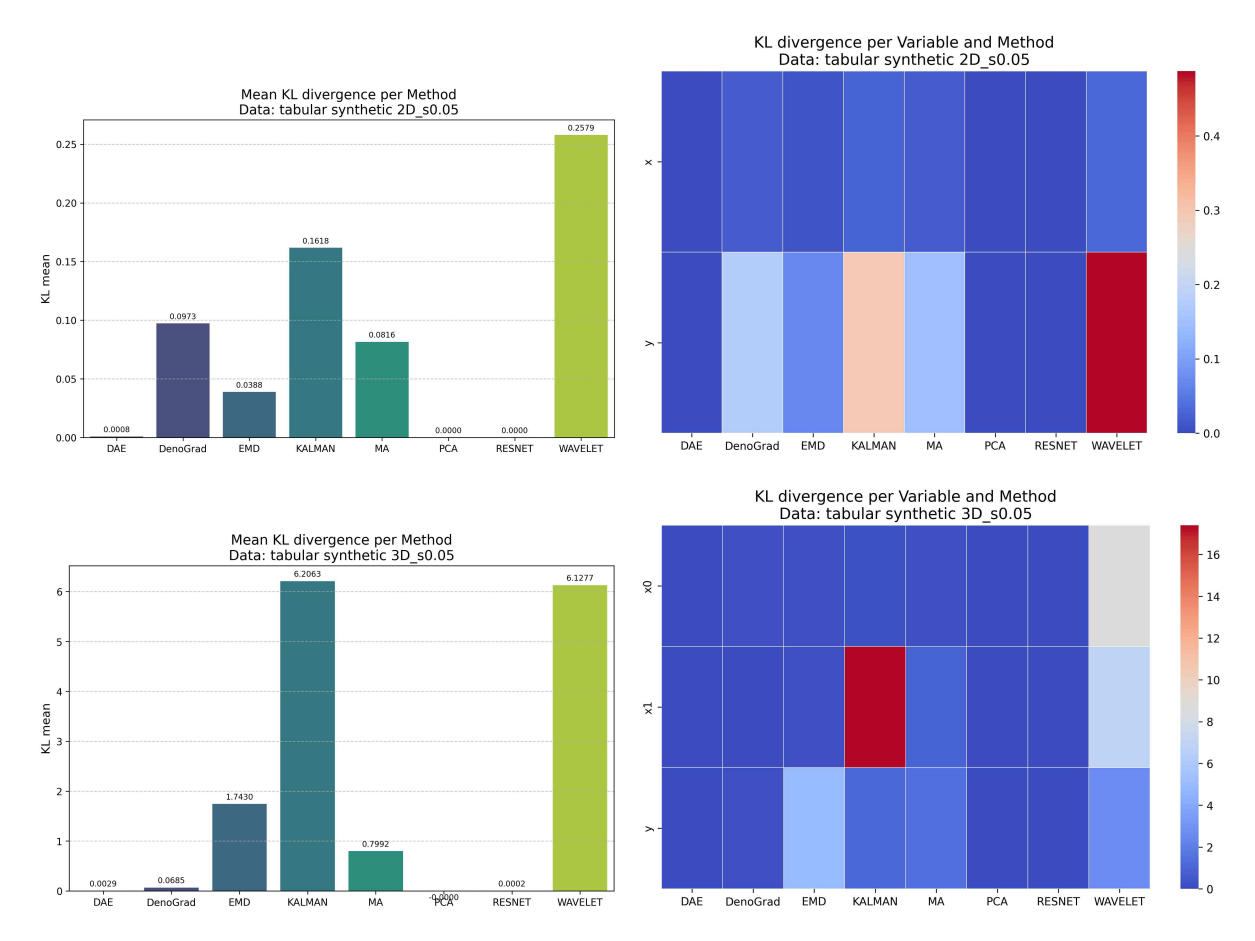


Figure 18: The left column presents bar plots of the mean KL divergence for each denoising method, summarizing the overall distributional shift introduced by each approach. The right column displays heatmaps representing the KL divergence computed for each individual variable and denoising method. The plots correspond to synthetic static tabular datasets.

B.3.2 Time Series

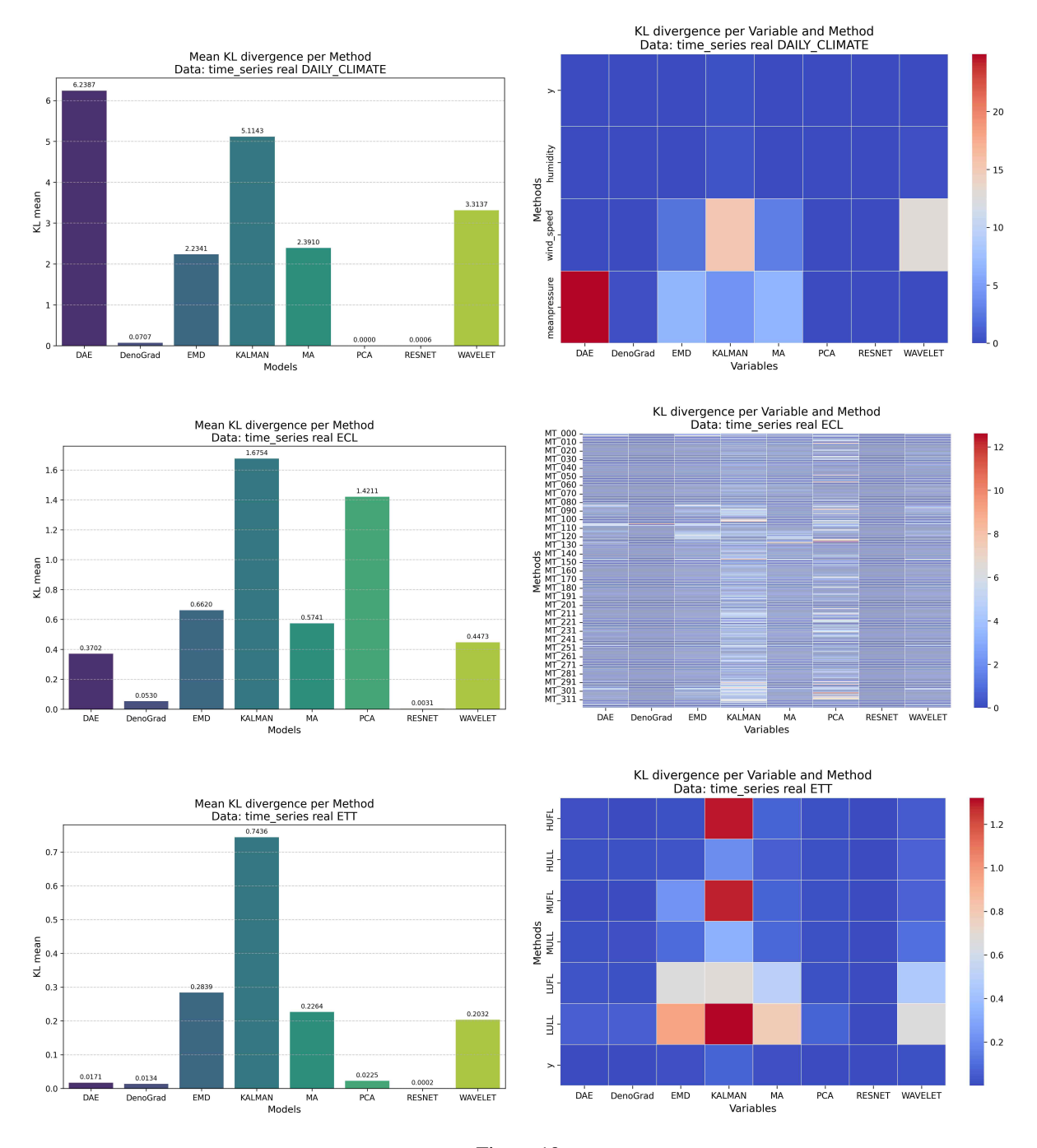


Figure 19

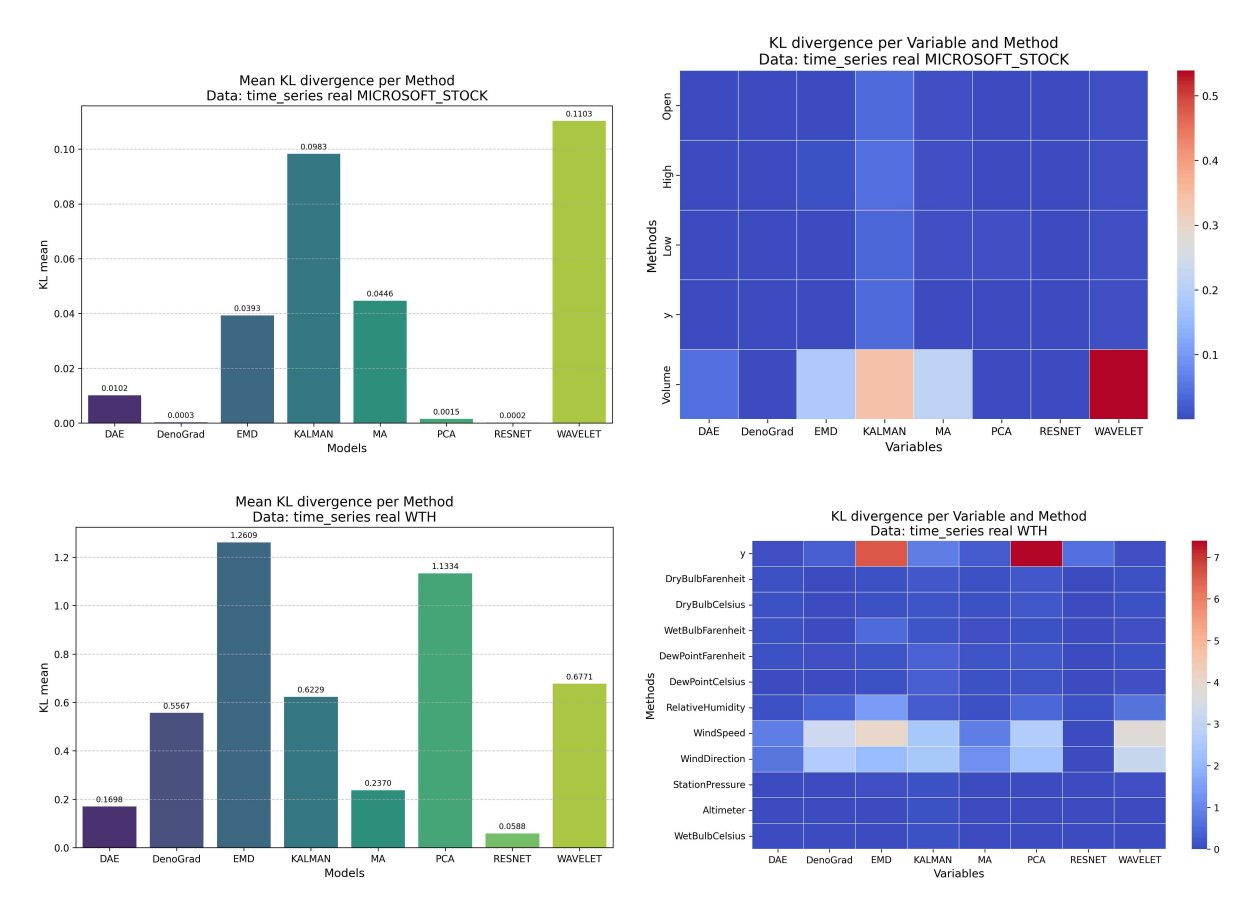


Figure 19: The left column presents bar plots of the mean KL divergence for each denoising method, summarizing the overall distributional shift introduced by each approach. The right column displays heatmaps representing the KL divergence computed for each individual variable and denoising method. All plots correspond to real-world time series datasets.

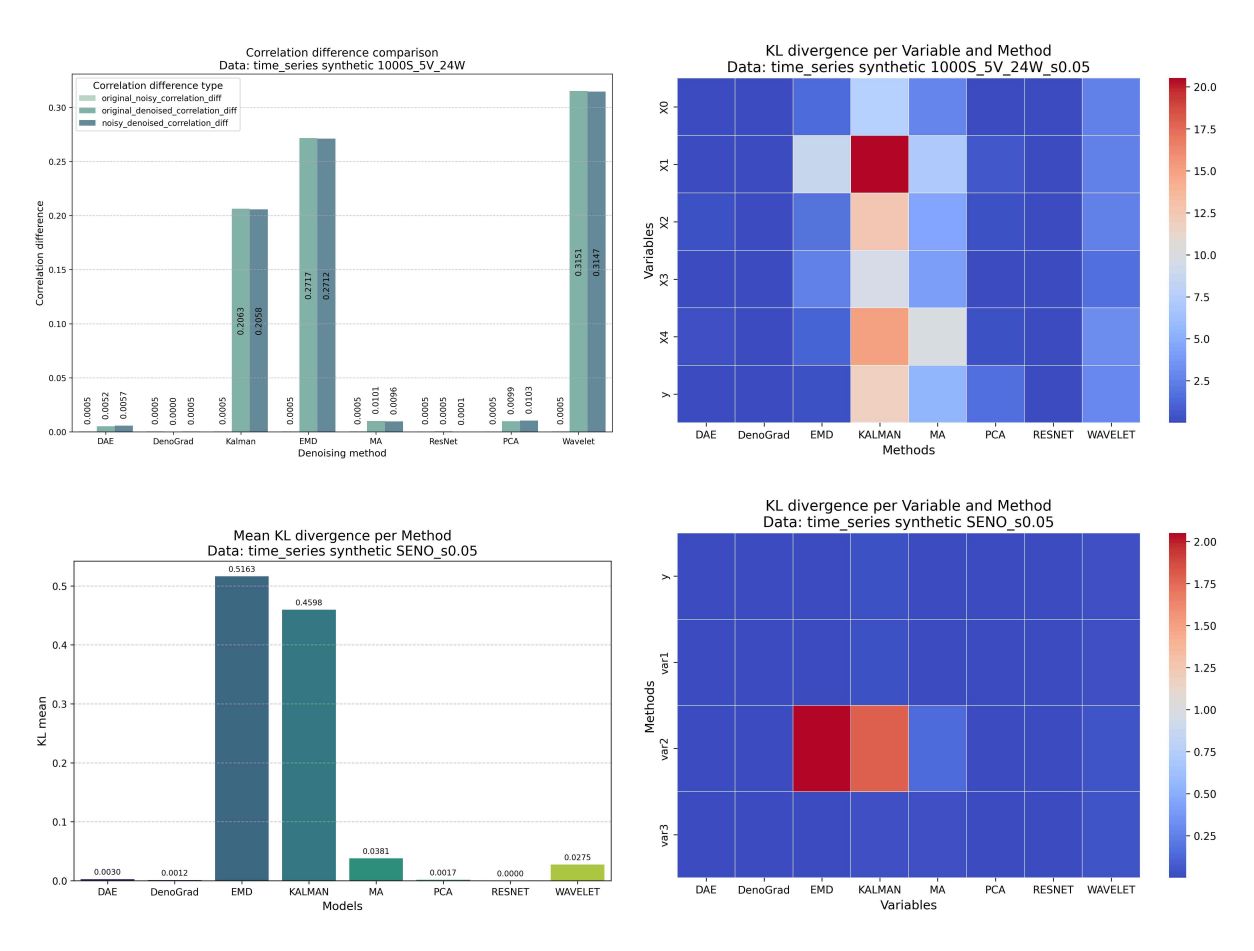


Figure 20: The left column presents bar plots of the mean KL divergence for each denoising method, summarizing the overall distributional shift introduced by each approach. The right column displays heatmaps representing the KL divergence computed for each individual variable and denoising method. The plots correspond to synthetic time series datasets.

B.4 R² Scores of Interpretable AI models

This subsection presents plots of the R² scores obtained by the Interpretable AI models under different train-test combinations, reflecting the denoising state of the datasets. The combinations include train_noisy – test_noisy, train_noisy – test_denoised, train_denoised – test_noisy, and train_denoised – test_denoised. For synthetic datasets, an additional 'original' state is included in the combinations. These visualizations illustrate how the denoising process impacts the models' predictive performance across varying conditions.

B.4.1 Static Tabular

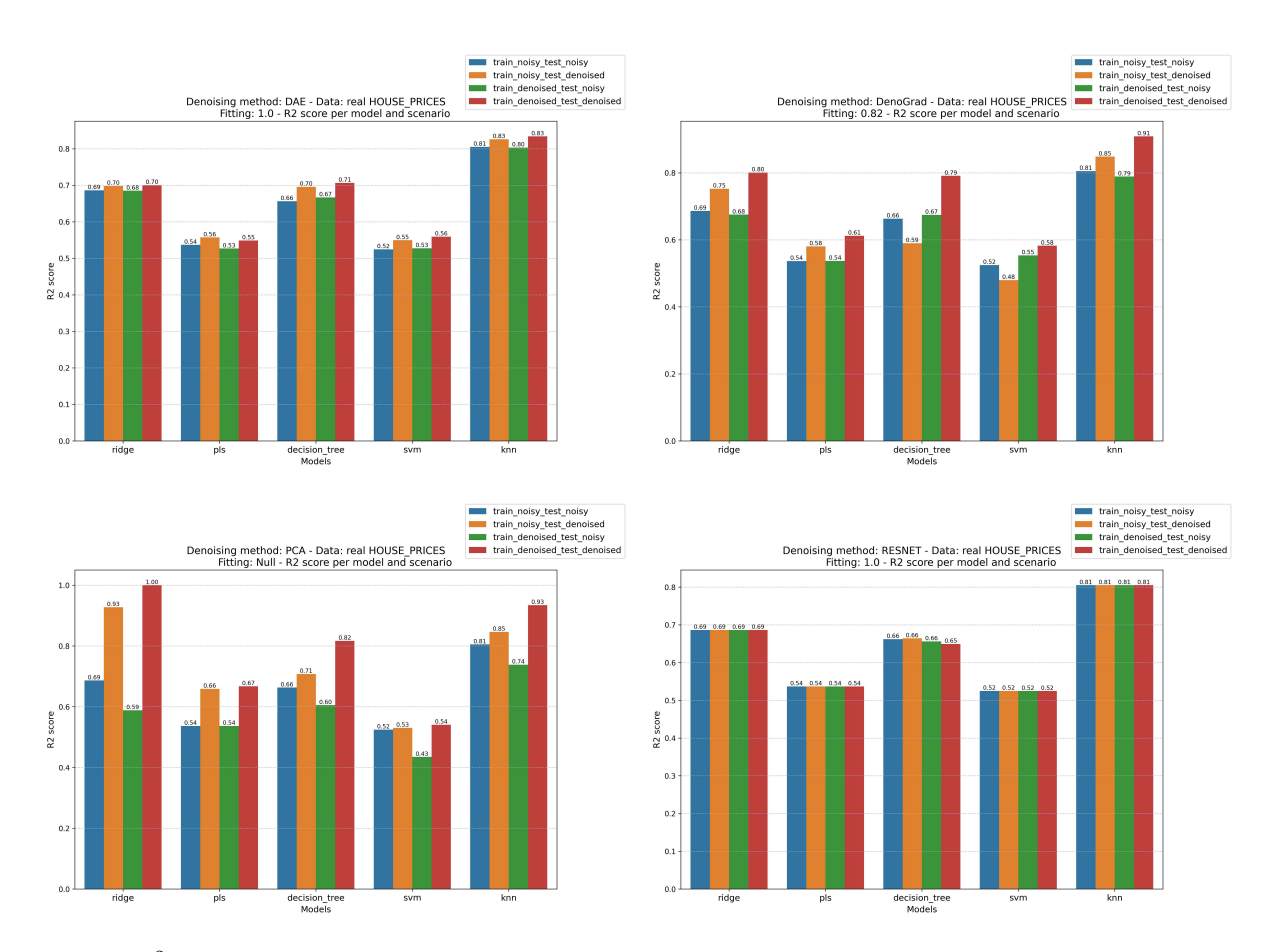


Figure 21: R^2 score obtained by the XAI models in the *House Prices* real-world static tabular dataset in all train-test scenarios applying the four denoising algorithms that passed the previous filter: DAE, DenoGrad, PCA and ResNet.

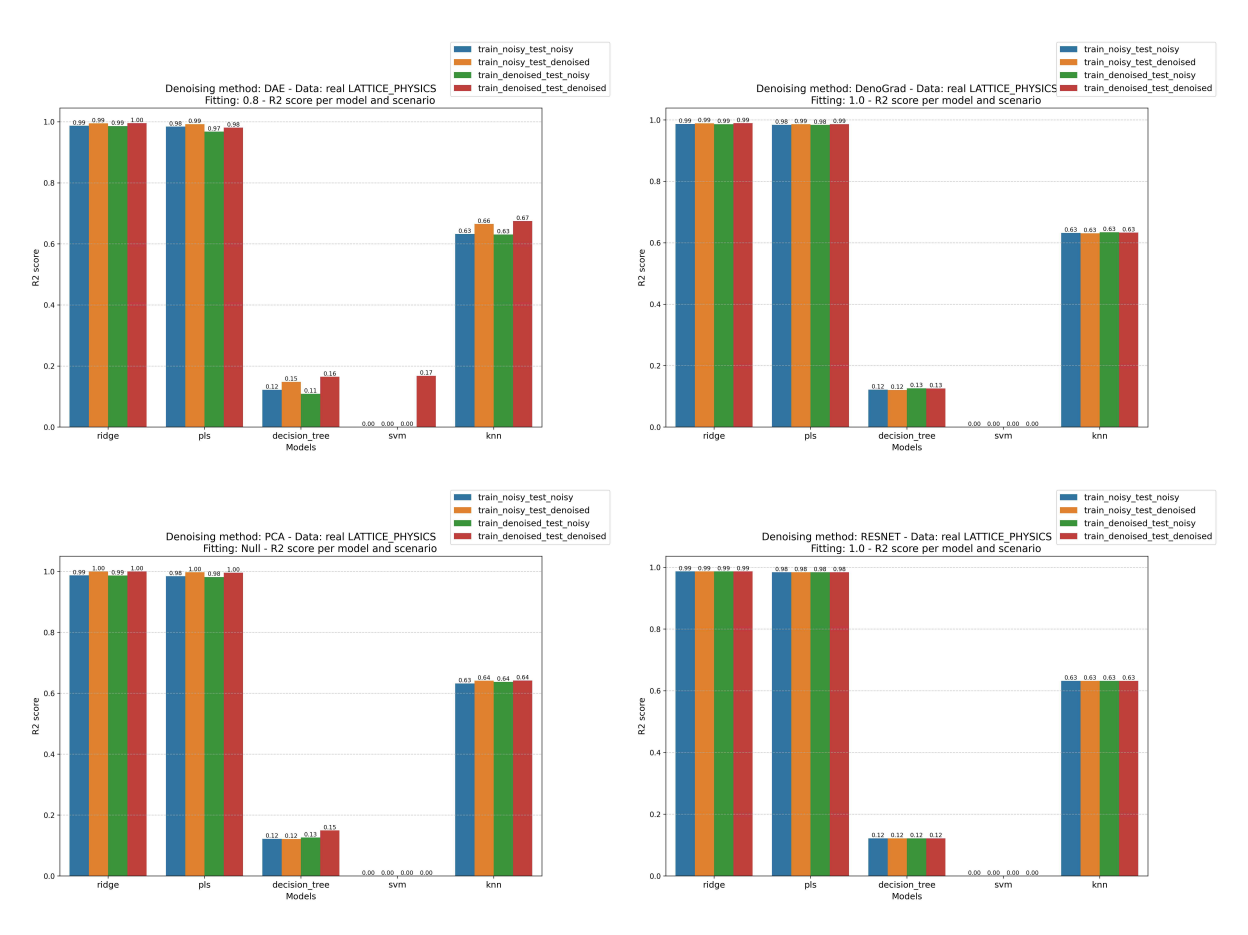


Figure 22: \mathbb{R}^2 score obtained by the XAI models in the *Lattice Physics* real-world static tabular dataset in all train-test scenarios applying the four denoising algorithms that passed the previous filter: DAE, DenoGrad, PCA and ResNet.

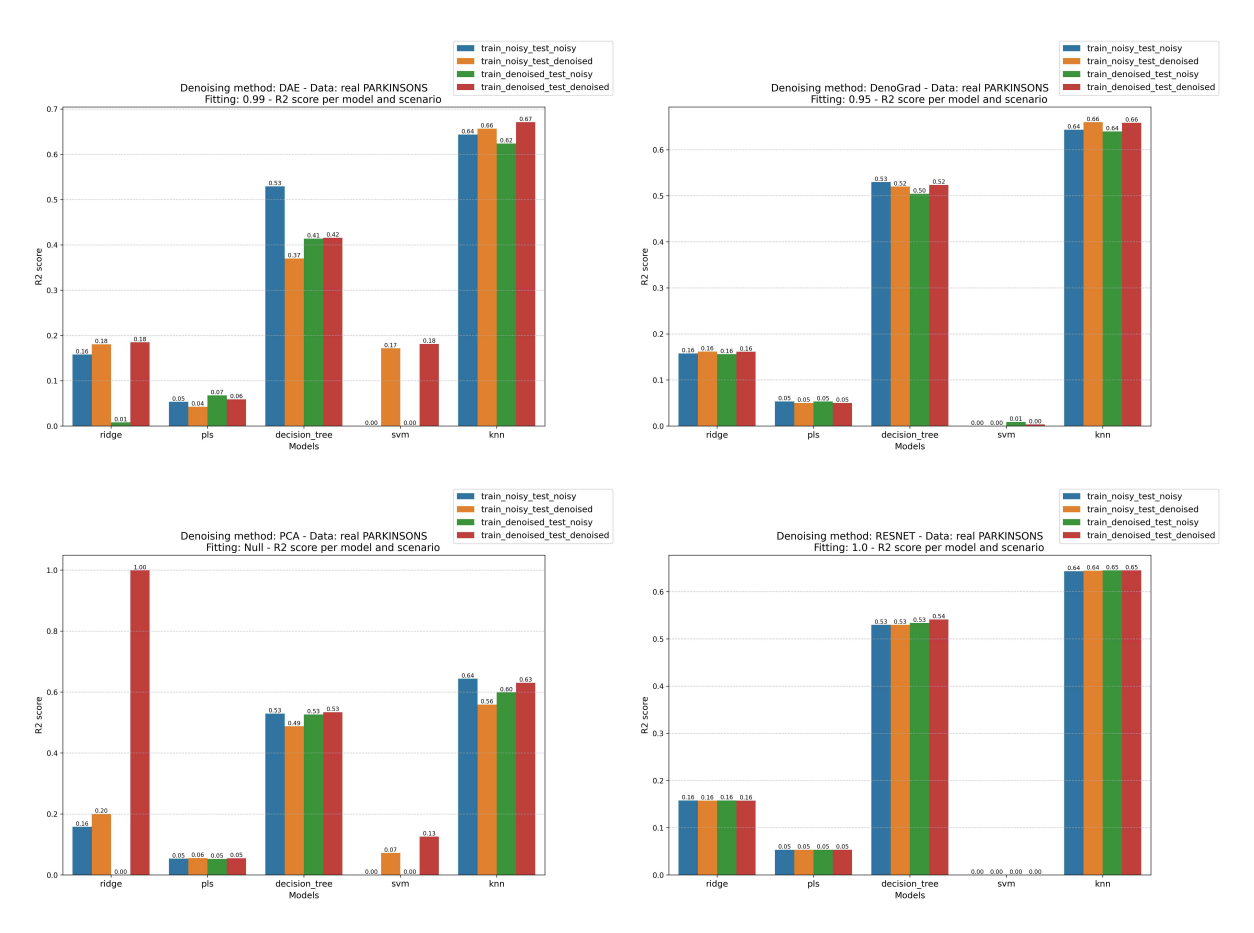


Figure 23: \mathbb{R}^2 score obtained by the XAI models in the *Parkinsons* real-world static tabular dataset in all train-test scenarios applying the four denoising algorithms that passed the previous filter: DAE, DenoGrad, PCA and ResNet.

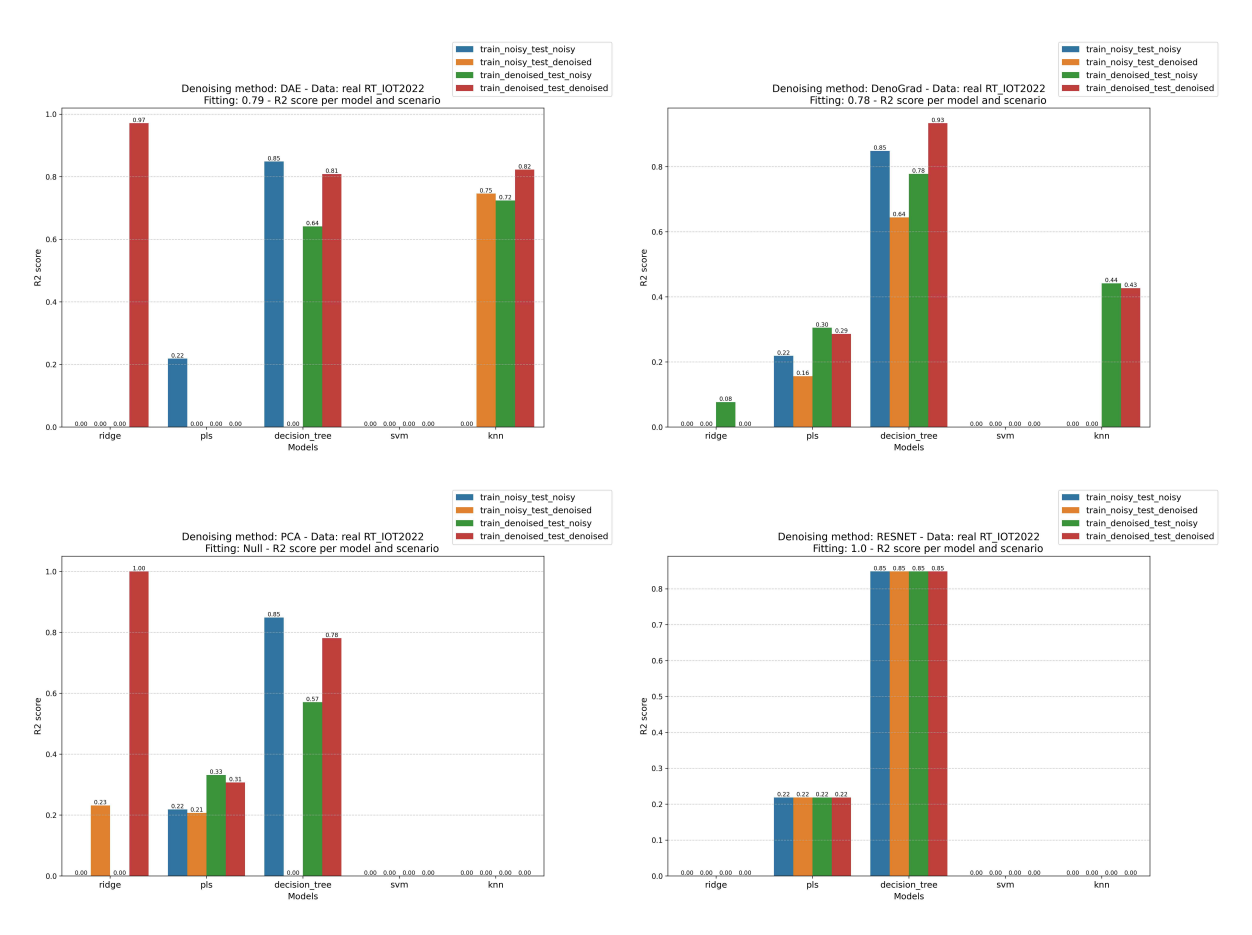


Figure 24: \mathbb{R}^2 score obtained by the XAI models in the RT IOT 2022 real-world static tabular dataset in all train-test scenarios applying the four denoising algorithms that passed the previous filter: DAE, DenoGrad, PCA and ResNet.

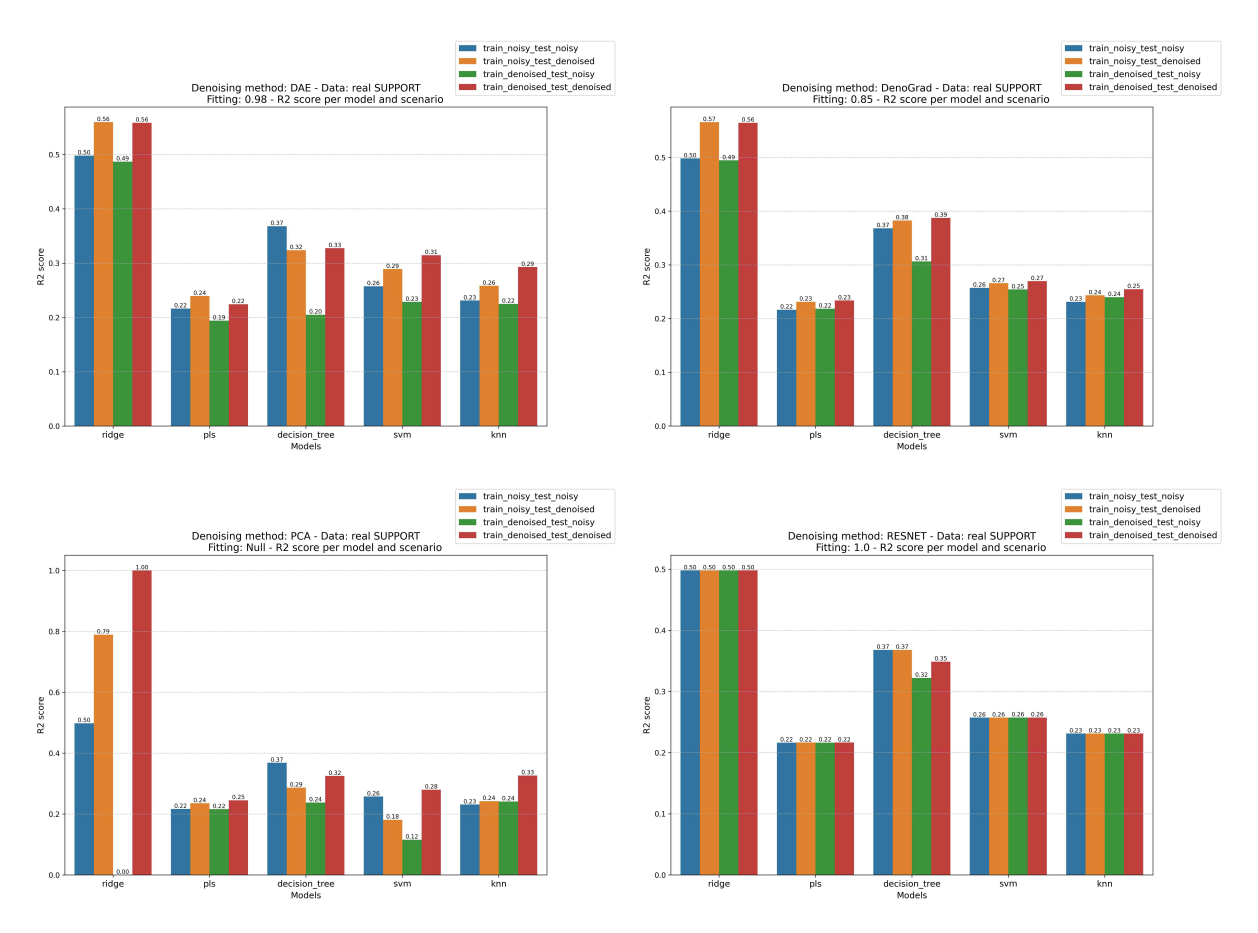


Figure 25: \mathbb{R}^2 score obtained by the XAI models in the SUPPORT2 real-world static tabular dataset in all train-test scenarios applying the four denoising algorithms that passed the previous filter: DAE, DenoGrad, PCA and ResNet.

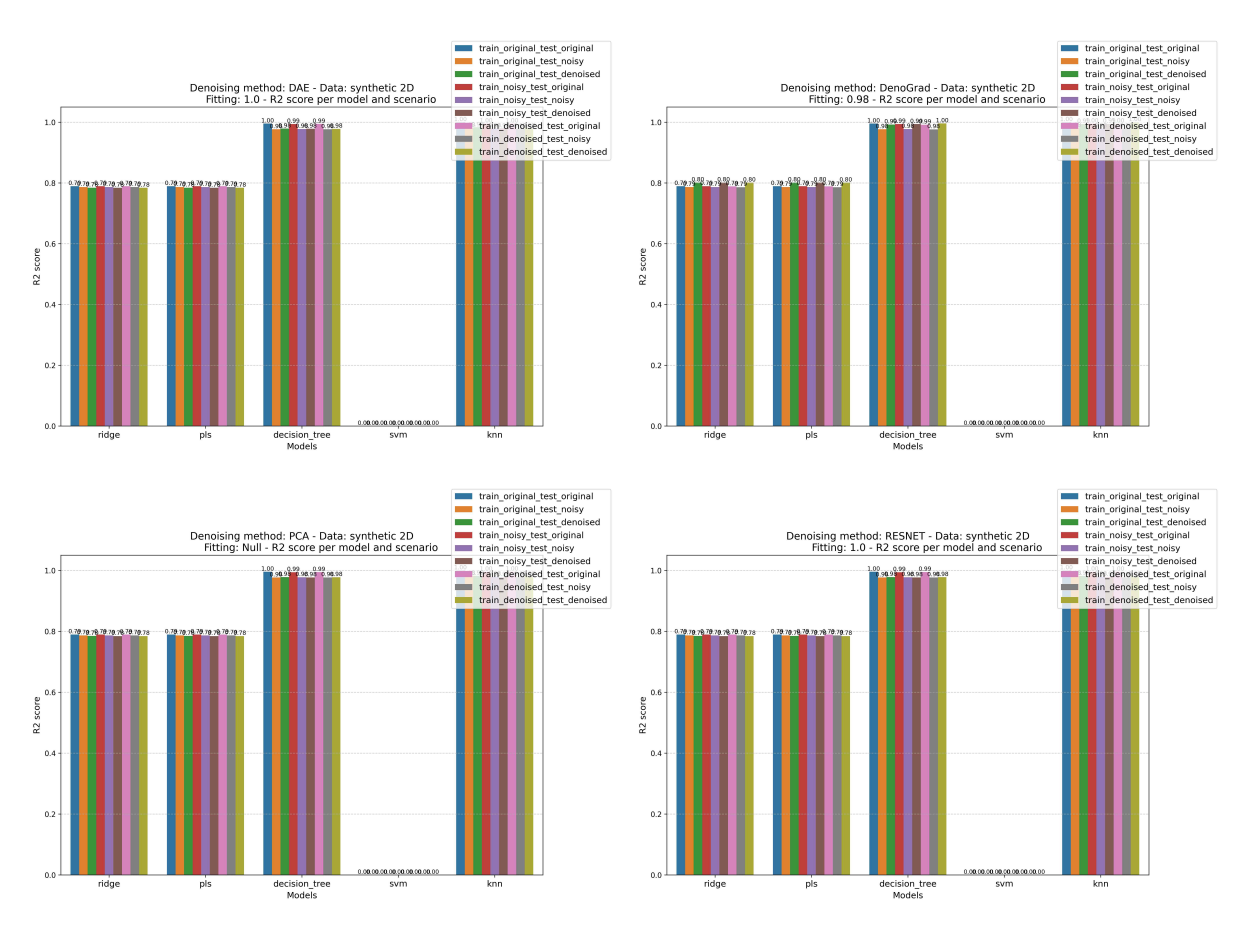


Figure 26: \mathbb{R}^2 score obtained by the XAI models in the 2D synthetic static tabular dataset in all train-test scenarios applying the four denoising algorithms that passed the previous filter: DAE, DenoGrad, PCA and ResNet.

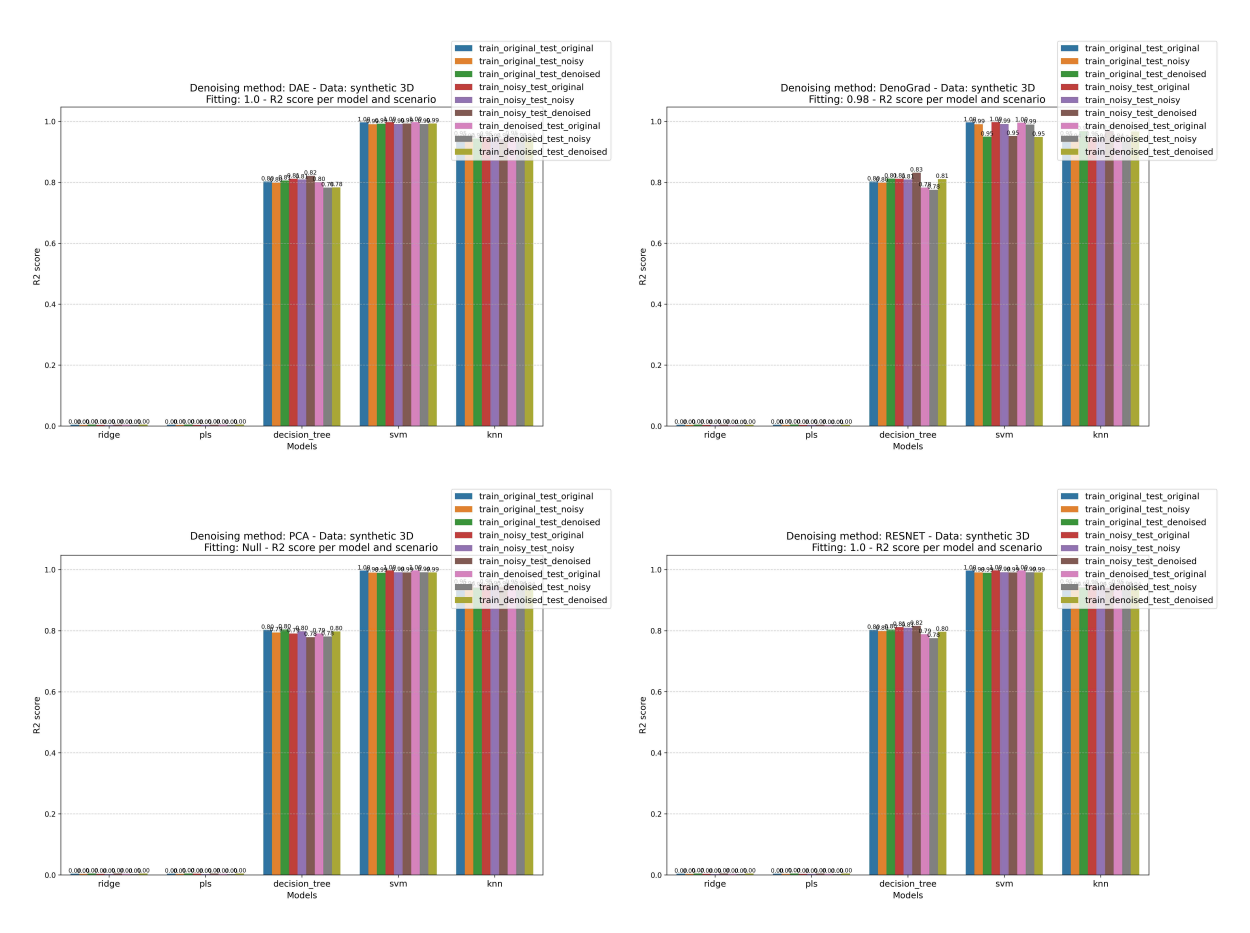


Figure 27: \mathbb{R}^2 score obtained by the XAI models in the 3D synyhetic static tabular dataset in all train-test scenarios applying the four denoising algorithms that passed the previous filter: DAE, DenoGrad, PCA and ResNet.

B.4.2 Time Series

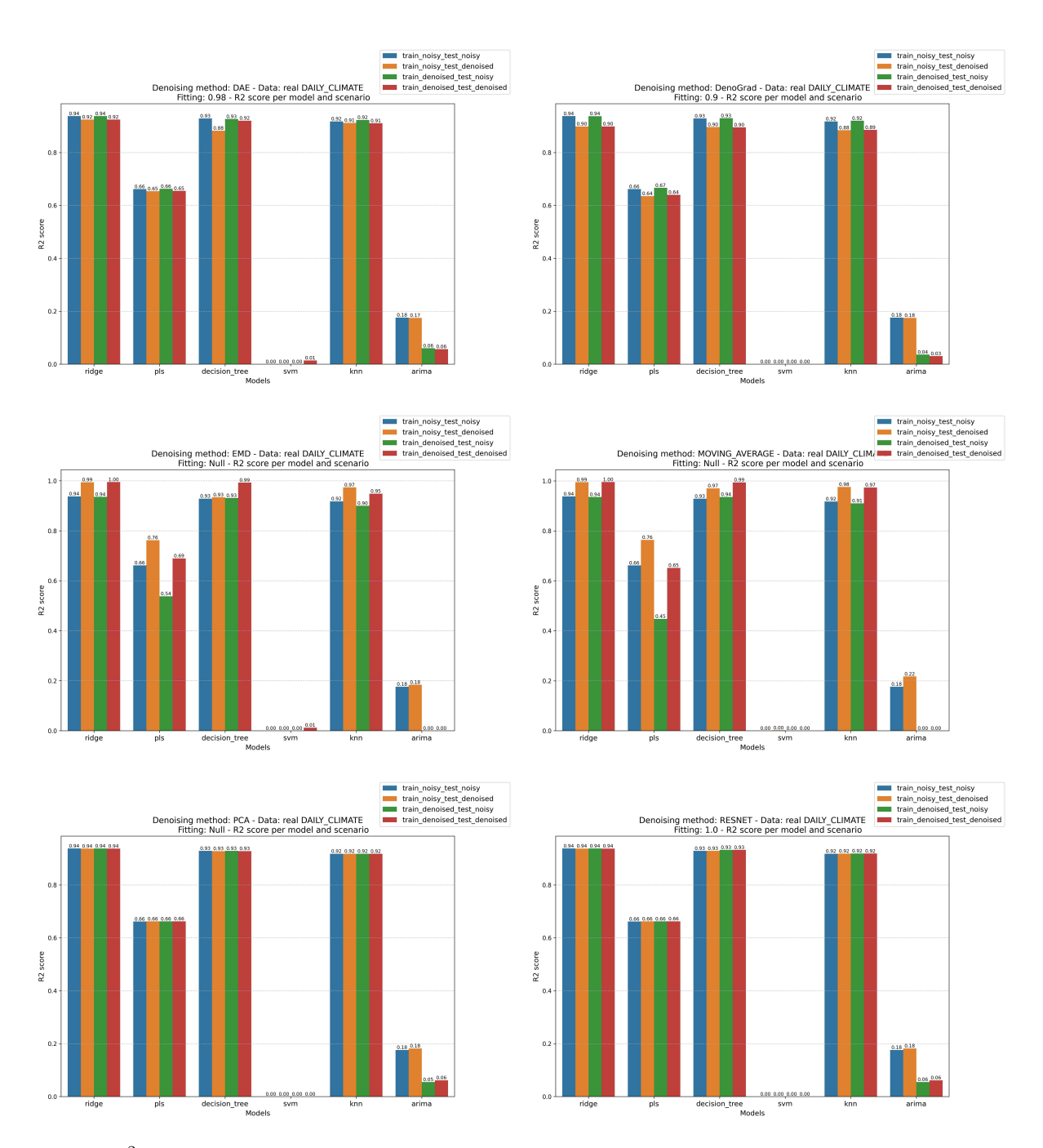


Figure 28: R^2 score obtained by the XAI models in the *Daily Climate* real-world time series dataset in all train-test scenarios applying the six denoising algorithms that passed the previous filter: DAE, DenoGrad, EMD, MA, PCA and ResNet.

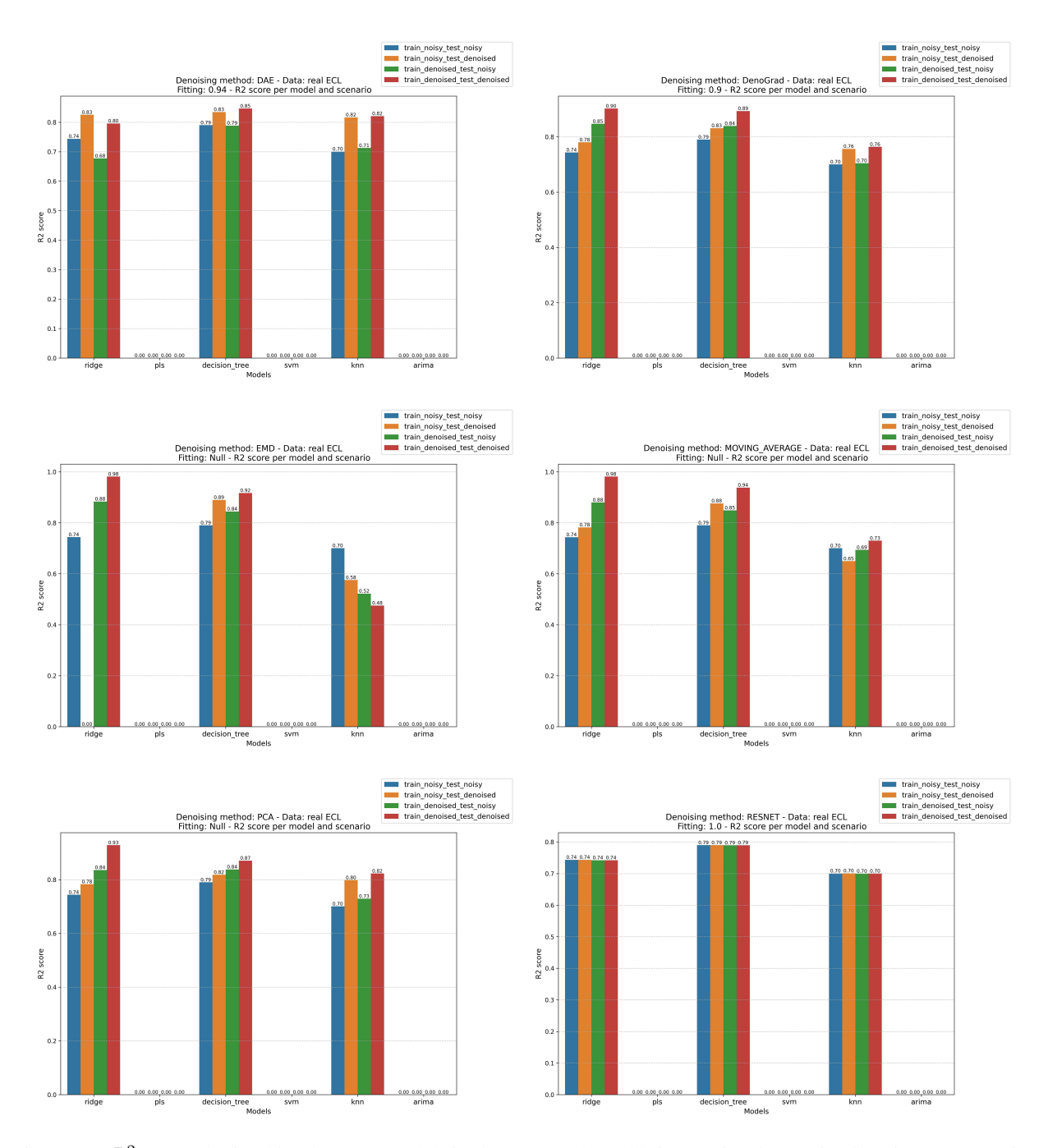


Figure 29: R^2 score obtained by the XAI models in the ECL real-world time series dataset in all train-test scenarios applying the six denoising algorithms that passed the previous filter: DAE, DenoGrad, EMD, MA, PCA and ResNet.

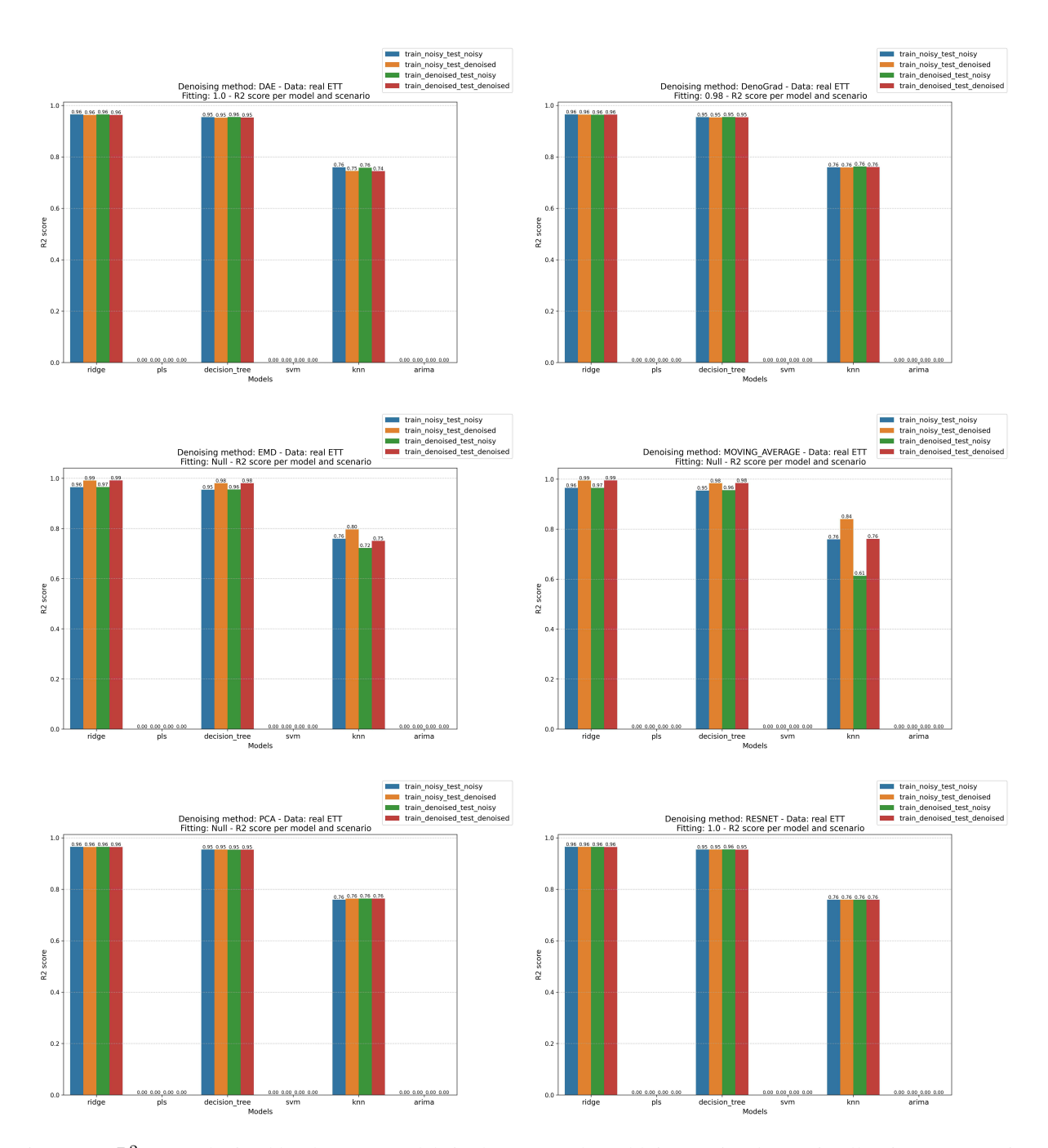


Figure 30: R^2 score obtained by the XAI models in the ETT real-world time series dataset in all train-test scenarios applying the six denoising algorithms that passed the previous filter: DAE, DenoGrad, EMD, MA, PCA and ResNet.

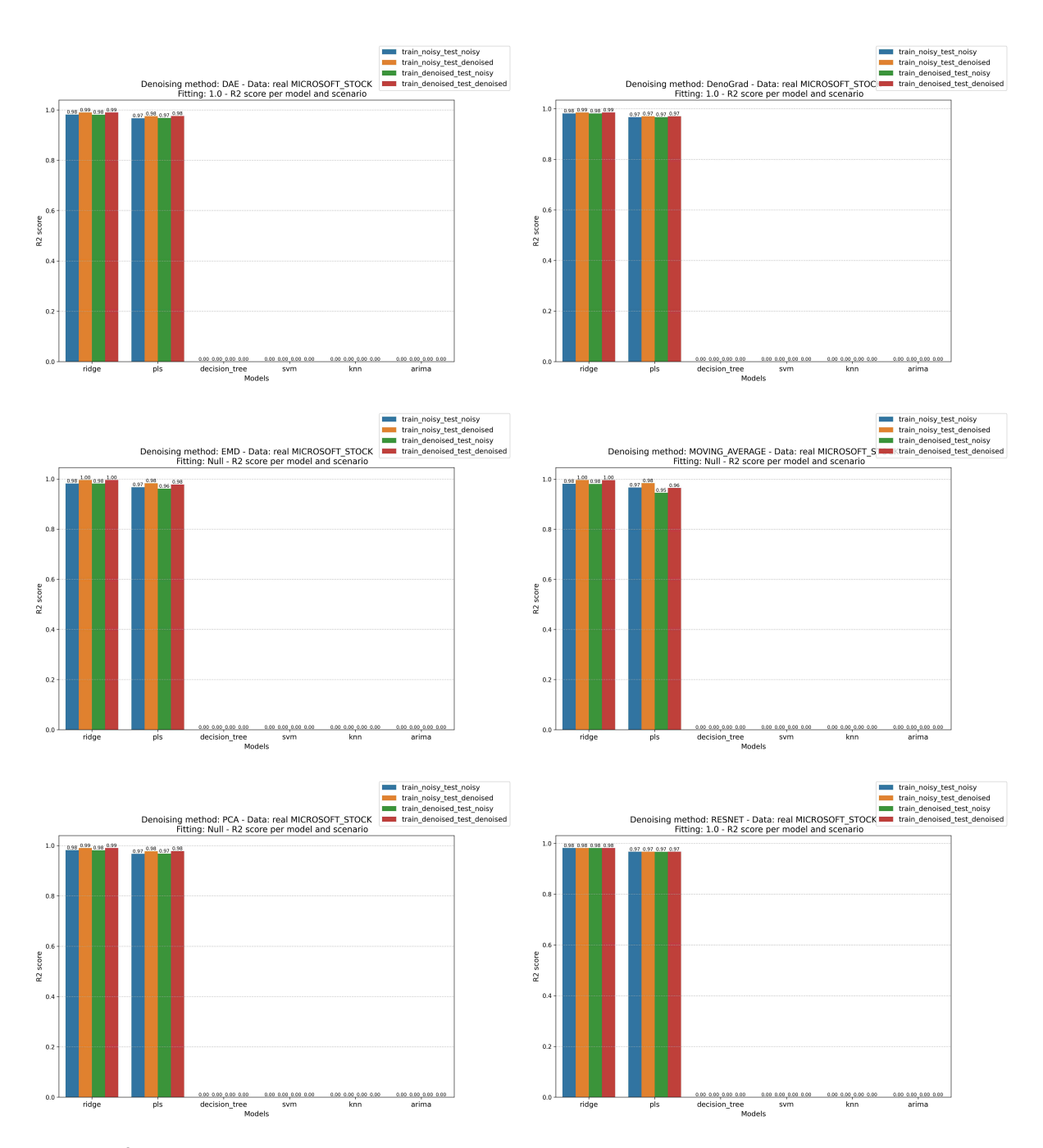


Figure 31: R^2 score obtained by the XAI models in the *Microsoft Stock* real-world time series dataset in all train-test scenarios applying the six denoising algorithms that passed the previous filter: DAE, DenoGrad, EMD, MA, PCA and ResNet.

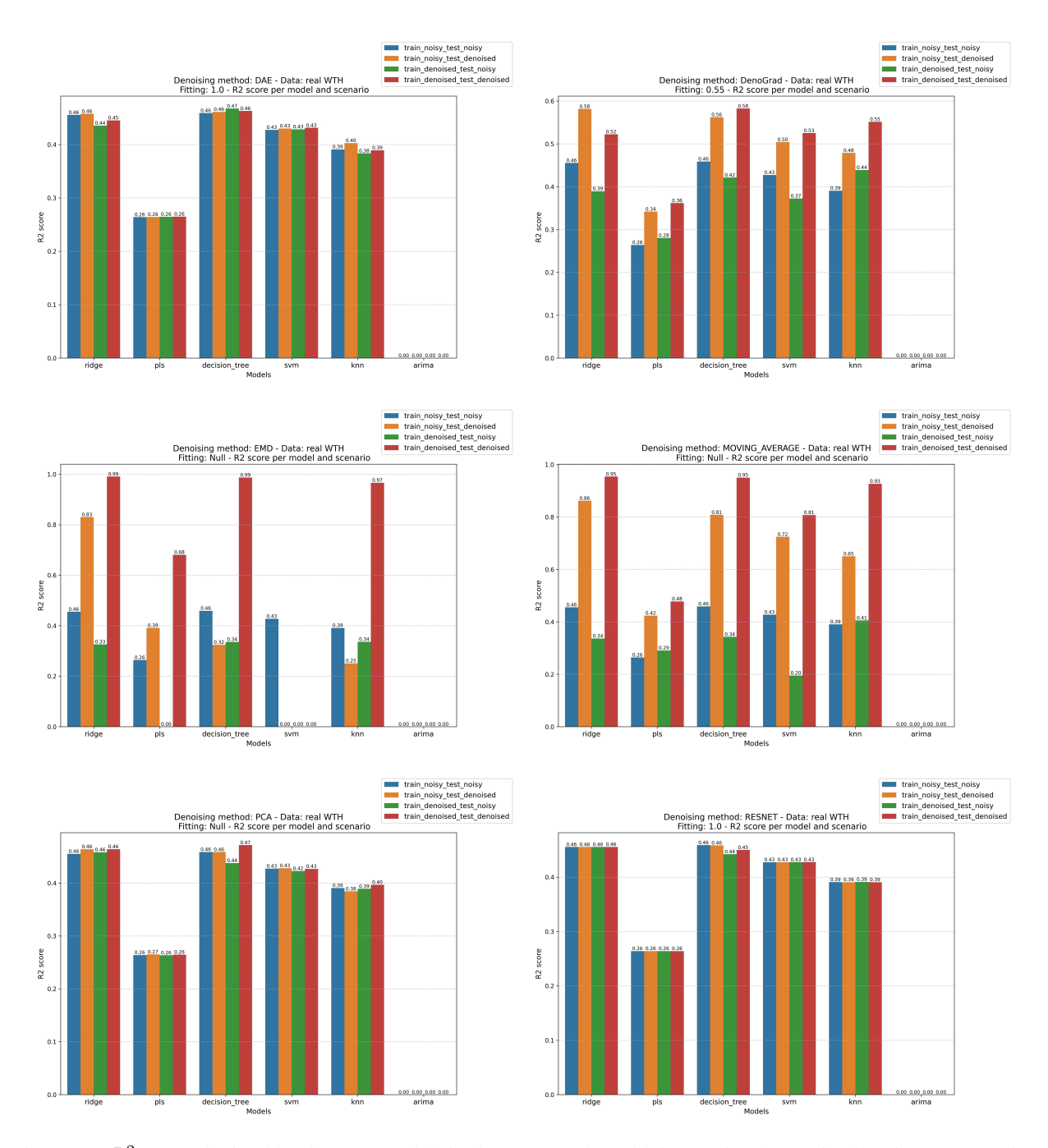


Figure 32: R^2 score obtained by the XAI models in the WTH real-world time series dataset in all train-test scenarios applying the six denoising algorithms that passed the previous filter: DAE, DenoGrad, EMD, MA, PCA and ResNet.

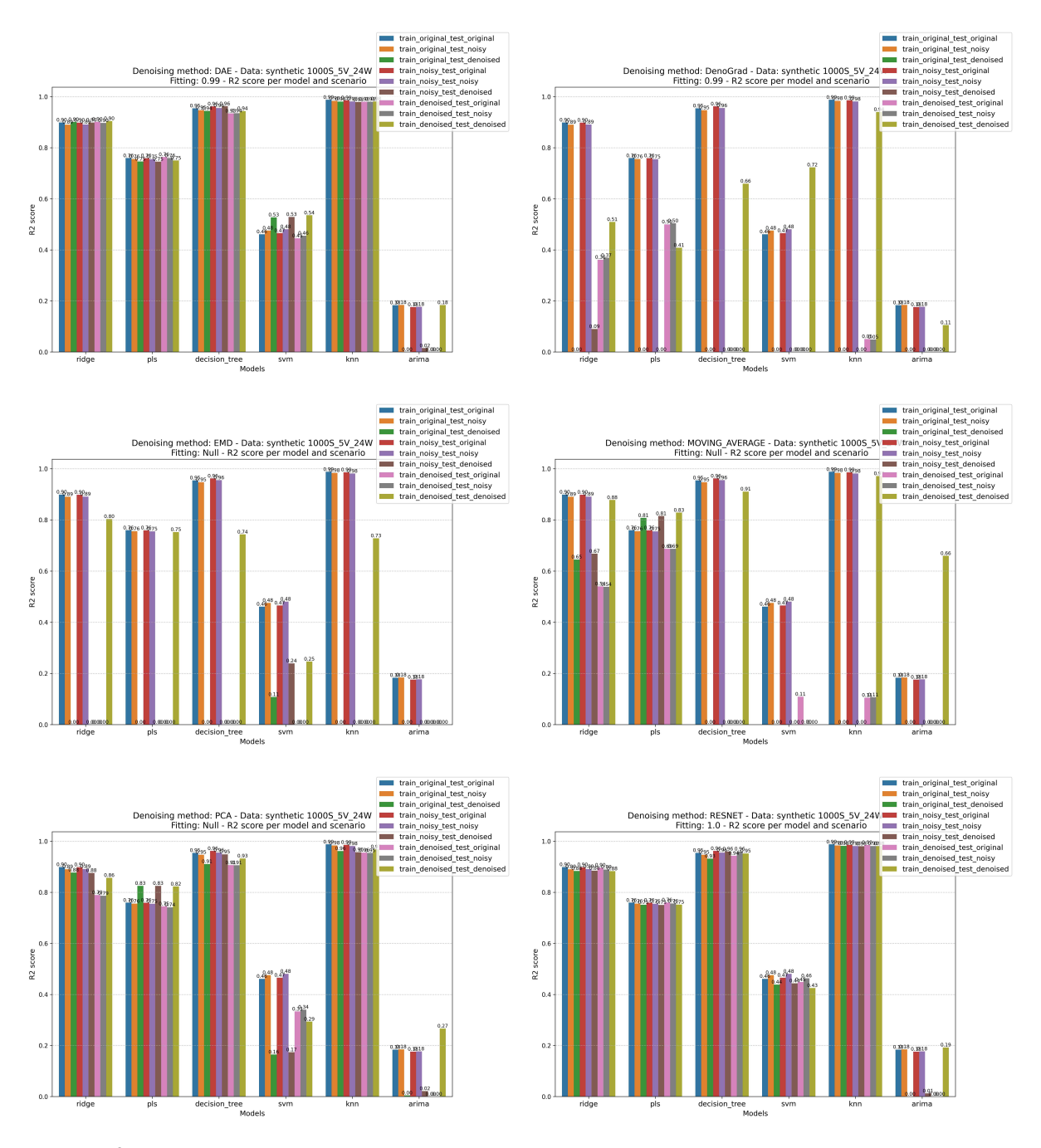


Figure 33: R^2 score obtained by the XAI models in the *Linear Combination* synthetic time series dataset in all train-test scenarios applying the six denoising algorithms that passed the previous filter: DAE, DenoGrad, EMD, MA, PCA and ResNet.

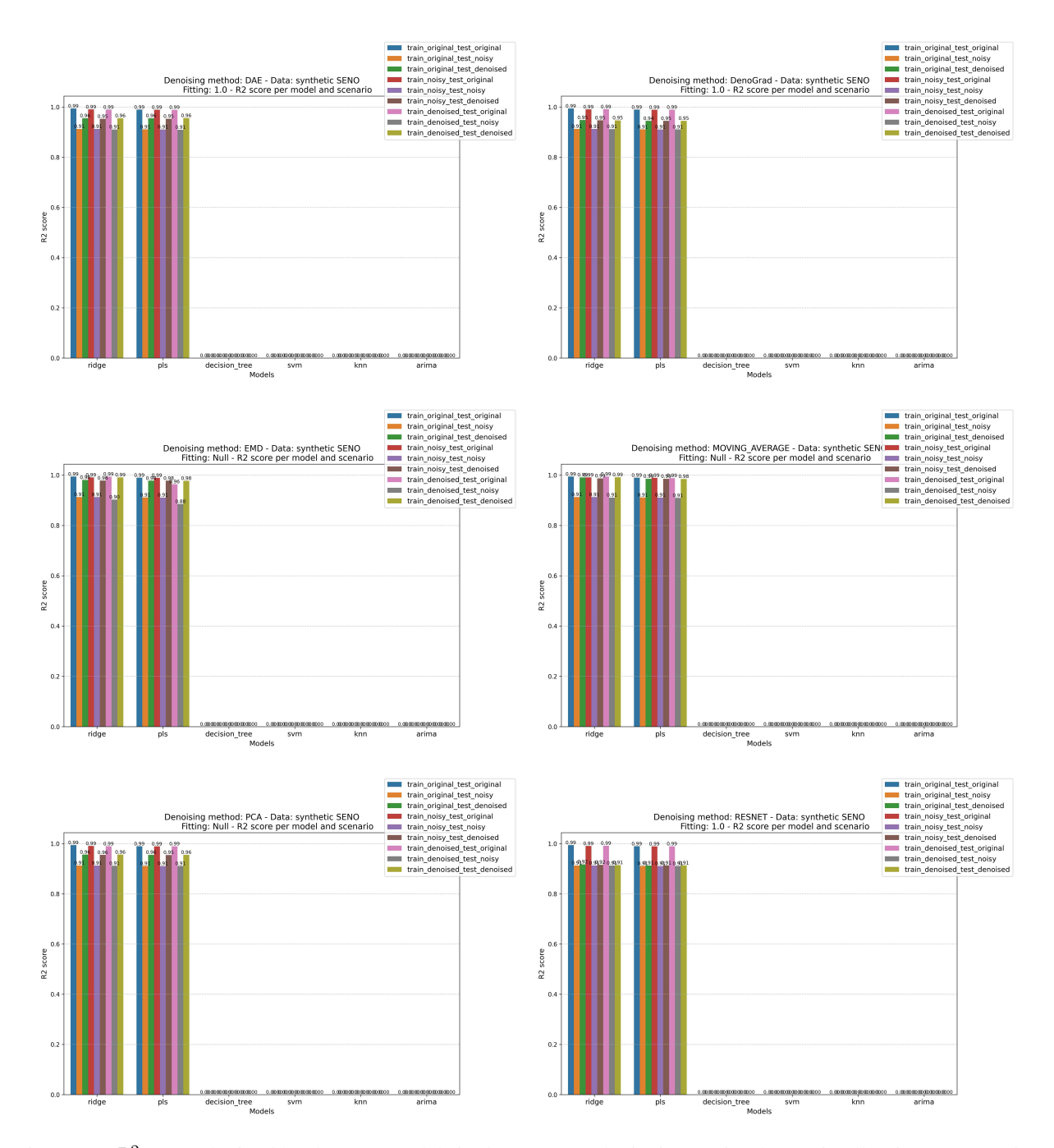


Figure 34: R^2 score obtained by the XAI models in the *Sinus* synthetic time series dataset in all train-test scenarios applying the six denoising algorithms that passed the previous filter: DAE, DenoGrad, EMD, MA, PCA and ResNet.

Acknowledgements

This publication is part of the Project "Ethical, Responsible and General Purpose Artificial Intelligence: Applications In Risk Scenarios" (IAFER) Exp.:TSI-100927-2023-1 funded through the Creation of university-industry research programs (Enia Programs), aimed at the research and development of artificial intelligence, for its dissemination and education within the framework of the Recovery, Transformation and Resilience Plan from the European Union Next Generation EU through the Ministry for Digital Transformation and the Civil Service. Ignacio Aguilera-Martos was supported by the Ministry of Science of Spain under the FPI programme PRE2021-100169.

References

- [1] M. Sidahmed, Attribute noise-sensitivity impact: Model performance and feature ranking, in: Americas Conference on Information Systems, 2008, p. no info.

 URL https://api.semanticscholar.org/CorpusID:2960577
- [2] R. Hasan, C. H. Chu, Drn: Detection and removal of noisy instances with self organizing map, in: International Conferences on Pattern Recognition and Artificial Intelligence, 2022, p. no info. URL https://api.semanticscholar.org/CorpusID:249318257
- [3] Y. Li, H. Han, S. Shan, X. Chen, Disc: Learning from noisy labels via dynamic instance-specific selection and correction, 2023 IEEE/CVF Conference on Computer Vision and Pattern Recognition (CVPR) (2023) 24070– 24079.
 - URL https://api.semanticscholar.org/CorpusID:260068694
- [4] A. Papenmeier, D. Kern, G. Englebienne, C. Seifert, It's complicated: The relationship between user trust, model accuracy and explanations in ai, ACM Trans. Comput.-Hum. Interact. (2022). doi:10.1145/3495013. URL https://doi.org/10.1145/3495013
- [5] A. Mokari, S. Eiserloh, O. Ryabchykov, U. Neugebauer, T. Bocklitz, A comparative study of robustness to noise and interpretability in u-net-based denoising of raman spectra., Spectrochimica acta. Part A, Molecular and biomolecular spectroscopy 344 Pt 1 (2025) 126577.

 URL https://api.semanticscholar.org/CorpusID:279965738
- [6] Z. He, Y. Wang, Y. Yang, P. Sun, L. Wu, H. Bai, J. Gong, R. Hong, M. Zhang, Double correction framework for denoising recommendation, in: Proceedings of the 30th ACM SIGKDD Conference on Knowledge Discovery and Data Mining, 2024, p. 1062–1072. doi:10.1145/3637528.3671692. URL https://doi.org/10.1145/3637528.3671692
- [7] C. Kausik, K. Srivastava, R. Sonthalia, Double descent and overfitting under noisy inputs and distribution shift for linear denoisers, in: arxiv, 2023, p. no info. URL https://api.semanticscholar.org/CorpusID:258959152
- [8] I. Larsen-Ledet, Embracing data noise, in: microsoft, 2023, p. no info. URL https://api.semanticscholar.org/CorpusID:259300333
- [9] R. Hasan, C. H. Chu, Noise in datasets: What are the impacts on classification performance?, in: Proceedings of the 11th International Conference on Pattern Recognition Applications and Methods ICPRAM, INSTICC, SciTePress, 2022, pp. 163–170. doi:10.5220/0010782200003122.
- [10] D. García-Gil, J. Luengo, S. García, F. Herrera, Enabling smart data: noise filtering in big data classification, Information Sciences 479 (2019) 135–152.
- [11] K. W. Al-Sabbagh, M. Staron, R. Hebig, Improving test case selection by handling class and attribute noise, J. Syst. Softw. 183 (2021) 111093.
 URL https://api.semanticscholar.org/CorpusID:244245120
- [12] R. K. L. Kennedy, J. M. Johnson, T. M. Khoshgoftaar, The effects of class label noise on highly-imbalanced big data, 2021 IEEE 33rd International Conference on Tools with Artificial Intelligence (ICTAI) (2021) 1427–1433. URL https://api.semanticscholar.org/CorpusID:245388536
- [13] Schreiber, Determination of the noise level of chaotic time series., Physical review. E, Statistical physics, plasmas, fluids, and related interdisciplinary topics 48 1 (1993) R13–R16.

 URL https://api.semanticscholar.org/CorpusID:12164904
- [14] J. M. Johnson, T. M. Khoshgoftaar, A survey on classifying big data with label noise, ACM Journal of Data and Information Quality 14 (2022) 1 – 43. URL https://api.semanticscholar.org/CorpusID:248070196
- [15] M. Pontil, S. Mukherjee, F. Girosi, On the noise model of support vector machines regression, in: International Conference on Algorithmic Learning Theory, 2000, p. no info. URL https://api.semanticscholar.org/CorpusID:6244043
- [16] C. M. Bishop, C. S. Quazaz, Regression with input-dependent noise: A bayesian treatment, in: Neural Information Processing Systems, 1996, p. no info. URL https://api.semanticscholar.org/CorpusID:14474914
- [17] P. W. Goldberg, C. K. I. Williams, C. M. Bishop, Regression with input-dependent noise: A gaussian process treatment, in: Neural Information Processing Systems, 1997, p. no info. URL https://api.semanticscholar.org/CorpusID:7482528

- [18] S. Shankar, D. Sheldon, T. Sun, J. Pickering, T. G. Dietterich, Three-quarter sibling regression for denoising observational data, in: Proceedings of the Twenty-Eighth International Joint Conference on Artificial Intelligence, IJCAI-19, International Joint Conferences on Artificial Intelligence Organization, 2019, pp. 5960–5966. doi: 10.24963/ijcai.2019/826.
 URL https://doi.org/10.24963/ijcai.2019/826
- [19] P. Chaudhary, I. Chauhan, B. R. Manoj, M. R. Bhatnagar, Linear regression-based channel estimation for non-gaussian noise, 2024 IEEE 99th Vehicular Technology Conference (VTC2024-Spring) (2024) 1–6. URL https://api.semanticscholar.org/CorpusID:272858899
- [20] S. G. Kwak, J. H. Kim, Central limit theorem: the cornerstone of modern statistics, Korean journal of anesthesiology 70 (2) (2017) 144.
- [21] S. Santhosh, P. Soori, V. Shashidhar, Impact of additive noise on information loss characteristics of datasets, 2023 International Conference on the Confluence of Advancements in Robotics, Vision and Interdisciplinary Technology Management (IC-RVITM) (2023) 1–8. URL https://api.semanticscholar.org/CorpusID:267772787
- [22] E. Barnett, O. Kaiser, J. Masci, E. C. Wit, S. Fulda, Generative models for periodicity detection in noisy signals, Clocks & Sleep 6 (3) (2024) 359–388.
- [23] E. Jafarigol, T. Trafalis, The paradox of noise: An empirical study of noise-infusion mechanisms to improve generalization, stability, and privacy in federated learning (2023). arXiv:2311.05790. URL https://arxiv.org/abs/2311.05790
- [24] S. Gupta, A. Gupta, Dealing with noise problem in machine learning data-sets: A systematic review, Procedia Computer Science 161 (2019) 466–474.
- [25] S. Wang, H. Chen, A novel deep learning method for the classification of power quality disturbances using deep convolutional neural network, Applied energy 235 (2019) 1126–1140.
- [26] A. Barredo Arrieta, N. Díaz-Rodríguez, J. Del Ser, A. Bennetot, S. Tabik, A. Barbado, S. Garcia, S. Gil-Lopez, D. Molina, R. Benjamins, R. Chatila, F. Herrera, Explainable artificial intelligence (XAI): Concepts, taxonomies, opportunities and challenges toward responsible AI, Information Fusion 58 (2020) 82–115. doi: 10.1016/j.inffus.2019.12.012.
- [27] D. Gunning, Explainable artificial intelligence (xai), Defense advanced research projects agency (DARPA), nd Web 2 (2) (2017) 1.
- [28] F. Doshi-Velez, B. Kim, Towards a rigorous science of interpretable machine learning, arXiv preprint arXiv:1702.08608 (2017).
- [29] A. E. Hoerl, R. W. Kennard, Ridge regression: Biased estimation for nonorthogonal problems, Technometrics 12 (1) (1970) 55–67.
- [30] S. Wold, A. Ruhe, H. Wold, W. Dunn, Iii, The collinearity problem in linear regression. the partial least squares (pls) approach to generalized inverses, SIAM Journal on Scientific and Statistical Computing 5 (3) (1984) 735–743.
- [31] L. Breiman, J. Friedman, R. A. Olshen, C. J. Stone, Classification and regression trees, Routledge, 2017.
- [32] H. Drucker, C. J. Burges, L. Kaufman, A. Smola, V. Vapnik, Support vector regression machines, Advances in neural information processing systems 9 (1996).
- [33] E. Fix, J. L. Hodges Jr, Discriminatory analysis. nonparametric discrimination: Consistency properties, Tech. rep., USA Air Force School of Aviation Medicine, Randolph Field (1951).
- [34] G. E. Box, G. M. Jenkins, Time series analysis: Forecasting and control, Holden-Day, 1970.
- [35] B. Crook, M. Schlüter, T. Speith, Revisiting the performance-explainability trade-off in explainable artificial intelligence (xai), in: 2023 IEEE 31st International Requirements Engineering Conference Workshops (REW), IEEE, 2023, pp. 316–324.
- [36] L. Peracchio, G. Nicora, T. M. Buonocore, R. Bellazzi, E. Parimbelli, Do you trust your model explanations? an analysis of xai performance under dataset shift, in: International Conference on Artificial Intelligence in Medicine, Springer, 2024, pp. 257–266.
- [37] P. Milanfar, M. Delbracio, Denoising: a powerful building block for imaging, inverse problems and machine learning, Philosophical transactions. Series A, Mathematical, physical, and engineering sciences 383 (2024). URL https://api.semanticscholar.org/CorpusID:272550819
- [38] X. Gu, Y.-J. Wang, X. Zhu, C. Shi, Y. Guo, Y. Liu, J. Chen, Advancing humanoid locomotion: Mastering challenging terrains with denoising world model learning (2024). arXiv:2408.14472. URL https://arxiv.org/abs/2408.14472

- [39] G. Frusque, O. Fink, Robust time series denoising with learnable wavelet packet transform, Advanced Engineering Informatics 62 (2024) 102669.
- [40] D. Makwana, G. Deshmukh, O. Susladkar, S. Mittal, et al., Livenet: A novel network for real-world low-light image denoising and enhancement, in: Proceedings of the IEEE/CVF Winter Conference on Applications of Computer Vision, 2024, pp. 5856–5865.
- [41] P. Zhao, W. Zhang, X. Cao, X. Li, Denoising diffusion probabilistic model-enabled data augmentation method for intelligent machine fault diagnosis, Engineering Applications of Artificial Intelligence 139 (2025) 109520.
- [42] L. P. F. Garcia, A. C. Lorena, A. C. P. de Leon Ferreira de Carvalho, A study on class noise detection and elimination, 2012 Brazilian Symposium on Neural Networks (2012) 13–18. URL https://api.semanticscholar.org/CorpusID:14146586
- [43] S. Zhou, Z. He, X. Chen, W. Chang, An anomaly detection method for uav based on wavelet decomposition and stacked denoising autoencoder, Aerospace 11 (5) (2024) 393.
- [44] S. García, J. Luengo, F. Herrera, Dealing with noisy data, in: Dealing with Noisy Data, 2015, p. no info. URL https://api.semanticscholar.org/CorpusID:268092955
- [45] J. Shi, K. Zhang, C. Guo, Y. Yang, Y. Xu, J. Wu, A survey of label-noise deep learning for medical image analysis, Medical Image Analysis 95 (2024) 103166. doi:https://doi.org/10.1016/j.media.2024.103166.
- [46] A. Majumdar, Blind denoising autoencoder, IEEE transactions on neural networks and learning systems 30 (1) (2018) 312–317.
- [47] A.-O. Boudraa, J.-C. Cexus, et al., Denoising via empirical mode decomposition, Proc. IEEE ISCCSP 4 (2006) (2006).
- [48] I. de Vries, A. de Jong, M. van der Hout-van der Jagt, J. van Laar, R. Vullings, Deep learning for sparse domain kalman filtering with applications on ecg denoising and motility estimation, IEEE Transactions on Biomedical Engineering 71 (8) (2024) 2321–2329. doi:10.1109/TBME.2024.3368105.
- [49] Z. Shan, J. Yang, M. A. Sanjuán, C. Wu, H. Liu, A novel adaptive moving average method for signal denoising in strong noise background, The European Physical Journal Plus 137 (1) (2022) 50.
- [50] W. Dong, M. Woźniak, J. Wu, W. Li, Z. Bai, Denoising aggregation of graph neural networks by using principal component analysis, IEEE Transactions on Industrial Informatics 19 (3) (2023) 2385–2394. doi:10.1109/TII. 2022.3156658.
- [51] H. Kang, C. Park, H. Yang, Evaluation of denoising performance of resnet deep learning model for ultrasound images corresponding to two frequency parameters, Bioengineering 11 (7) (2024) 723.
- [52] C. Tian, M. Zheng, W. Zuo, B. Zhang, Y. Zhang, D. Zhang, Multi-stage image denoising with the wavelet transform, Pattern Recognition 134 (2023) 109050.
- [53] D. L. Donoho, De-noising by soft-thresholding, IEEE transactions on information theory 41 (3) (2002) 613–627.
- [54] W. S. McCulloch, W. Pitts, A logical calculus of the ideas immanent in nervous activity, The bulletin of mathematical biophysics 5 (1943) 115–133.
- [55] Z. L. Liu, Artificial neural networks, in: Artificial Intelligence for Engineers: Basics and Implementations, Springer, 2025, pp. 175–190.
- [56] H. Robbins, S. Monro, A stochastic approximation method, The annals of mathematical statistics (1951) 400–407.
- [57] K. Cho, B. van Merriënboer, C. Gulcehre, D. Bahdanau, F. Bougares, H. Schwenk, Y. Bengio, Learning phrase representations using RNN encoder–decoder for statistical machine translation, in: A. Moschitti, B. Pang, W. Daelemans (Eds.), Proceedings of the 2014 Conference on Empirical Methods in Natural Language Processing (EMNLP), Association for Computational Linguistics, Doha, Qatar, 2014, pp. 1724–1734. doi:10.3115/v1/D14-1179.
 URL https://aclanthology.org/D14-1179/
- [58] R. Pascanu, T. Mikolov, Y. Bengio, On the difficulty of training recurrent neural networks, in: International conference on machine learning, Pmlr, 2013, pp. 1310–1318.
- [59] S. Hochreiter, The vanishing gradient problem during learning recurrent neural nets and problem solutions, International Journal of Uncertainty, Fuzziness and Knowledge-Based Systems 6 (02) (1998) 107–116.
- [60] V. Nair, G. E. Hinton, Rectified linear units improve restricted boltzmann machines, in: Proceedings of the 27th international conference on machine learning (ICML-10), 2010, pp. 807–814.
- [61] K. He, X. Zhang, S. Ren, J. Sun, Deep residual learning for image recognition, in: Proceedings of the IEEE conference on computer vision and pattern recognition, 2016, pp. 770–778.

- [62] A. Camuto, M. Willetts, U. Simsekli, S. J. Roberts, C. C. Holmes, Explicit regularisation in gaussian noise injections, Advances in Neural Information Processing Systems 33 (2020) 16603–16614.
- [63] S. Hochreiter, J. Schmidhuber, Long short-term memory, Neural computation 9 (8) (1997) 1735–1780.
- [64] M. Beck, K. Pöppel, M. Spanring, A. Auer, O. Prudnikova, M. Kopp, G. Klambauer, J. Brandstetter, S. Hochreiter, xlstm: Extended long short-term memory, Advances in Neural Information Processing Systems 37 (2024) 107547–107603.
- [65] J. J. Hopfield, Neural networks and physical systems with emergent collective computational abilities., Proceedings of the national academy of sciences 79 (8) (1982) 2554–2558.
- [66] D. Svozil, V. Kvasnicka, J. Pospichal, Introduction to multi-layer feed-forward neural networks, Chemometrics and intelligent laboratory systems 39 (1) (1997) 43–62.
- [67] J. van Doorn, A. Ly, M. Marsman, E.-J. Wagenmakers, Bayesian rank-based hypothesis testing for the rank sum test, the signed rank test, and spearman's ρ , Journal of Applied Statistics 47 (16) (2020) 2984–3006.
- [68] harlfoxem, House Sales in King County, USA, Kaggle, https://www.kaggle.com/datasets/harlfoxem/housesalesprediction (2014).
- [69] N. Huu Tiep, Lattice-physics (PWR fuel assembly neutronics simulation results), UCI Machine Learning Repository, DOI: https://doi.org/10.24432/C5BK64 (2024).
- [70] A. Tsanas, M. Little, Parkinsons Telemonitoring, UCI Machine Learning Repository, DOI: https://doi.org/10.24432/C5ZS3N (2009).
- [71] B. S., R. Nagapadma, RT-IoT2022, UCI Machine Learning Repository, DOI: https://doi.org/10.24432/C5P338 (2023).
- [72] F. Harrel, SUPPORT2, UCI Machine Learning Repository, DOI: https://doi.org/10.3886/ICPSR02957.v2 (2023).
- [73] W. U. API, Daily Climate time series data, Kaggle, URL: https://www.kaggle.com/datasets/sumanthvrao/daily-climate-time-series-data (2019).
- [74] H. Zhou, S. Zhang, J. Peng, S. Zhang, J. Li, H. Xiong, W. Zhang, Informer: Beyond efficient transformer for long sequence time-series forecasting, in: The Thirty-Fifth AAAI Conference on Artificial Intelligence, AAAI 2021, Virtual Conference, Vol. 35, AAAI Press, 2021, pp. 11106–11115.
- [75] V. V. Venkitesh, Microsoft Stock- Time Series Analysis, Kaggle, URL: https://www.kaggle.com/datasets/vijayvvenkitesh/microsoft-stock-time-series-analysis (2021).
- [76] Y. Kopsinis, S. McLaughlin, Development of emd-based denoising methods inspired by wavelet thresholding, IEEE Transactions on signal Processing 57 (4) (2009) 1351–1362.
- [77] J. Terrien, C. Marque, B. Karlsson, Automatic detection of mode mixing in empirical mode decomposition using non-stationarity detection: application to selecting imfs of interest and denoising, EURASIP Journal on Advances in Signal Processing 2011 (2011) 1–8.
- [78] A.-O. Boudraa, J.-C. Cexus, Z. Saidi, Emd-based signal noise reduction, International Journal of Signal Processing 1 (1) (2004) 33–37.
- [79] I. Daubechies, The wavelet transform, time-frequency localization and signal analysis, IEEE transactions on information theory 36 (5) (2002) 961–1005.